

**An HIV-1 CRISPR-Cas9 membrane trafficking screen reveals a role for PICALM
intersecting endolysosomes and immunity**

Norma Paola Guízar Amador

Lady Davis Institute at Jewish General Hospital

Department of Microbiology and Immunology

McGill University

July 2023

A thesis submitted to McGill University in partial fulfillment
of the requirements for the degree of Master of Science

© 2023 Norma Paola Guízar Amador

Table of Contents

LIST OF FIGURES	iii
LIST OF TABLES	iv
LIST OF ABBREVIATIONS	v
ABSTRACT	vii
RÉSUMÉ	viii
ACKNOWLEDGEMENTS	ix
AUTHOR CONTRIBUTIONS TO ORIGINAL KNOWLEDGE	xi
CHAPTER 1: LITERATURE REVIEW AND INTRODUCTION	1
1. Human Immunodeficiency Virus	1
1.1. The HIV/AIDS Pandemic: An Overall Perspective	1
1.2. HIV-1 structure and replication cycle	5
1.3. Current treatments	10
1.4. Establishment of reservoirs and latency	12
1.5. Strategies for an HIV-1 cure	13
2. Phosphatidylinositol binding clathrin-assembly protein (PICALM)	14
2.1. PICALM in a nutshell	14
2.2. PICALM in clathrin-mediated endocytosis	15
2.3. PICALM in autophagy	16
2.4. PICALM in Alzheimer’s Disease	18
2.5. PICALM and its interaction with pathogens	18
2.6. PICALM in cellular homeostasis	19
3. Immune checkpoint molecules	19
3.1. ICMs during chronic infection and cancer	21
3.2. PD-1: PD-L1/L2 pathway	22
3.3. Checkpoint blockade	23
3.4. ICMs on T cell differentiation	24
4. Thesis hypothesis and objectives	31
4.1. Rationale	31
4.2. Objectives	32
CHAPTER 2: MATERIALS AND METHODS	33
Cell Culture	33

Generation of Cas9-expressing T2M-bl Cell line.....	33
Arrayed Screening of the Membrane Trafficking Library and viral infectivity assay	34
Cellular Viability Determination	35
CRISPR Editing of Sup-T1 Cells.....	35
Western Immunoblotting	35
HIV-1 NL4.3 and HIV Nef_CRMZY Viral Stocks and Infection.....	36
HIV-1 viral fusion assay	36
Antibodies and fluorescent probes	37
Immunofluorescence.....	37
Microscopy and imaging analyses	38
Flow cytometry staining and acquisition.	39
Construction, validation and usage of the HIV Nef-CRIMZY reporter.	39
Quantification and statistical analysis.....	40
CHAPTER 3: RESULTS	41
CRISPR screen of membrane trafficking genes reveals HIV-1 modulators.....	24
The identified CRISPR screening hits are involved in clathrin-mediated endocytosis and autophagy to alter infectivity	41
PICALM regulates several stages of HIV-1 replication.	43
PICALM KO supports enhanced HIV-1 replication usurping the autophagy machinery	46
Absence of PICALM leads an activated T effector memory phenotype deficient in immune checkpoint PD-1 expression.	49
Absence of PICALM reduces HIV-1 latency	52
CHAPTER 4: DISCUSSION.....	57
CHAPTER 5: SUMMARY AND CONCLUSION	61
CHAPTER 6: BIBLIOGRAPHY	62
CHAPTER 7: SUPPLEMENTARY MATERIAL	75

LIST OF FIGURES

Figure 1 Structure and organization of the HIV-1 genome.....	6
Figure 2. Structure of the HIV-1 particle.....	7
Figure 3. HIV-1 replication cycle	10
Figure 4. Role of PICALM in clathrin mediated endocytosis.....	16
Figure 5. Role of PICALM in autophag	17
Figure 6. T-cell immune checkpoint molecules and related ligands.....	20
Figure 7. Generation of T2M-bl-Cas9.....	26
Figure 8. Viability and viral infectivity of 140 membrane trafficking CRISPR screen KO cells	29
Figure 9. Viral infectivity and production of viral particle of membrane trafficking CRISPR screen knockouts.....	30
Figure 10. Protein interaction network of CRISPR screen hits and stable KO cell lines.....	43
Figure 11. KOs alter virus entry and the expression of HIV-1 Gag and autophagy proteins Lamp1 and LC3B-II	46
Figure 12. PICALM KO increases expression and colocalization of virus and autophagy proteins, can produces more virus, but have diminished infection rates	49
Figure 13. PICALM KO causes increased cell proliferation, deregulates activation and PD-1 pathways, and leads to a T effector memory-like phenotype	51
Figure 14. PICALM KO reduces latent HIV-1 infection	54
Figure 15. PICALM KO cells that favor latency reversal shows reduced PD-1 expression.....	56

LIST OF TABLES

Table 1. Therapeutic agents targeting HIV-1.	11
Table S 1. CRISPR screen target sequences.	75

LIST OF ABBREVIATIONS

AD: Alzheimer's disease	HDACi: histone deacetylase inhibitors
AHI: Acute HIV-1 infection	HDF: host dependency factor
AIDS: acquired immunodeficiency syndrome	HIV: human immunodeficiency virus
ANOVA: analysis of variance	HSV: herpes simplex virus
AP-2: adaptor protein complex 2	IF: immunofluorescence
APP: amyloid precursor protein	IFN: interferon
ART: antiretroviral therapy	IL-2: interleukin 2
ATG: Autophag-related	IN: integrase
Aβ: amyloid β	INSTI: integrase strand-transfer inhibitor
bnAbs: broadly neutralizing antibodies	kb: kilobase pairs
bp: base pairs	kDa: kilodalton
BTLA: B and T lymphocyte-associated	KO: knockout
CA: capsid	LAG-3: lymphocyte activation gene 3 protein
CCPs: clathrin-coated pits	LAMP1: lysosome-associated membrane glycoprotein 1
CCR5: C-C chemokine receptor type 5	LC3: microtubule-associated protein light chain 3
CCVs: clathrin-coated vesicles	LE/Lys: late endosome/lysosome
CD4: cluster of differentiation 4	LRA: latency-reversing agent
CME: clathrin mediated endocytosis	LTR: long terminal repeat
CRISPR: clustered regularly interspaced short palindromic repeats	MA: matrix
crRNA: CRISPR RNA	MAPK8IP2: mitogen-activated protein kinase 8 interacting protein 2
CTLA-4: cytotoxic T lymphocyte antigen-4	MOI: multiplicity of infection
CXCR4: C-X-C chemokine receptor type 4	mRNA: messenger RNA
DMEM: Dulbecco's Modified Eagle's medium	MSM: men who have sex with men
DNA: deoxyribonucleic acid	mTOR: mammalian target of rapamycin
dsDNA: double-stranded DNA	MTORC1: mTOR complex 1
EGFR: epidermal growth factor receptor	NC: nucleocapsid
ELISA: enzyme-linked immunosorbent assay	Nef: negative regulating factor
ER: endoplasmic reticulum	NIH: National Institute of Health
ERC1: ELKS/Rab6-interacting/CAST family member 1 protein	NK: natural killer
ESCRT: endosomal sorting complex required for transport	NNRTI: non-nucleoside reverse transcriptase inhibitor
FBS: fetal bovine serum	NRTI: Nucleoside Reverse Transcriptase Inhibitor
FDA: Food and Drug Administration	NTP: nucleoside triphosphate
FISH: fluorescence <i>in situ</i> hybridization	PAC3IN3: protein kinase C and casein kinase substrate in neurons 3
GAPDH: glyceraldehyde 3-phosphate dehydrogenase	PANTHER: Protein Analysis Through Evolutionary Relationships
GFP: green fluorescent protein	PBS: phosphate-buffered saline
GO: gene ontology	PD-1: programmed cell death 1
gRNA: guide RNA	PD-1: programmed death-1
GTP: guanosine diphosphate	PEI: polyethylenimine
	PFA: paraformaldehyde

PI: protease inhibitor
PI3K: phosphoinositide 3-kinase
PIC: pre-integration complex
PICALM: phosphatidylinositol-binding clathrin assembly protein
PLWH: people living with HIV
PM: plasma membrane
PR: protease
PrEP: pre-exposure prophylaxis
PrEP: pre-exposure prophylaxis
PtdIns3P: phosphatidylinositol-3-phosphate
Rev: Regulator of virion expression
RNA: ribonucleic acid
RNase: ribonuclease
RNP: ribonucleoprotein
RPMI: Roswell Park Memorial Institute medium
RRE: Rev response element
RT: reverse transcriptase
SDS-PAGE: sodium dodecyl sulfate–polyacrylamide gel electrophoresis
sgRNA: synthetic guide RNA
siRNA: small interfering RNA
SIV: simian immunodeficiency virus
SSA: sub-Saharan Africa
ssRNA: single-stranded RNA
STRING: Search Tool for the Retrieval of Interacting Genes
TAR: *trans*-activation response element
Tat: *trans*-activator of transcription
TBST: Tris-buffered saline with 0.1% Tween 20
TfR: transferrin receptor
TIGIT: T-cell immunoglobulin and immunoreceptor tyrosine-based inhibitory motif domain
TIM-3: T-cell immunoglobulin domain and mucin domain protein 3
ULK1: Unc-51-like kinase 1
UNAIDS: United Nations program on HIV/AIDS
VAMP-2: vesicle-associated membrane protein 2
VAPB: vesicle-associated membrane protein-associated protein B
Vif: viral infectivity factor
Vpr: virus protein
VPS4: vacuolar protein sorting-associated protein 4
Vpu: virus protein U
vRNA: viral RNA
VSV-G: *Indiana vesiculovirus* G protein
WHO: World Health Organization
WT: wild type

ABSTRACT

HIV-1 hijacks multiple host cell functions towards its replicative advantage, including host proteins of membrane trafficking dynamics and fusion, directed transport, and endocytic and autophagic pathways. Because these membranous processes are critical to virus replication, their discrete usurped mechanisms become essential to understand for the development of effective antiviral strategies. Despite their strong potential as clinical targets, only a few membrane trafficking proteins have been functionally characterized in relation to HIV-1 replication. To elucidate their roles thus further in HIV-1 replication, we performed a CRISPR-Cas9 screen on 140 of these membrane trafficking proteins. We identify host protein phosphatidylinositol-binding clathrin assembly protein (PICALM) as essential for HIV-1 infection. The absence of PICALM inhibits viral entry, and PICALM knockout (KO) CD4⁺ T cells display modified intracellular trafficking and increased abundance of intracellular Gag, and decreased latency, in addition to modified autophagic pathways, altered T cell memory phenotypes, and differential expression of immune checkpoint PD-1. This work reveals that PICALM modulates viral entry, autophagic flux, and control of virus replication, highlighting its potential as a future target for the control of HIV-1.

RÉSUMÉ

Le VIH-1 détourne plusieurs fonctions de la cellule hôte vers son avantage répliatif, y compris les protéines hôtes de la dynamique et de la fusion du trafic membranaire, du transport dirigé et des voies endocytaires et autophagiques. Parce que ces processus membranaires sont essentiels à la réplication du virus, leurs mécanismes usurpés discrets deviennent essentiels à comprendre pour le développement de stratégies antivirales efficaces. Malgré leur fort potentiel en tant que cibles cliniques, seules quelques protéines de trafic membranaire ont été caractérisées fonctionnellement en relation avec la réplication du VIH-1. Pour élucider davantage leurs rôles dans la réplication du VIH-1, nous avons effectué un criblage CRISPR-Cas9 sur 140 de ces protéines de trafic membranaire. Nous identifions la protéine d'assemblage de la clathrine liant le phosphatidylinositol de la protéine hôte (PICALM) comme étant essentielle à l'infection par le VIH-1. L'absence de PICALM inhibe l'entrée virale, et les lymphocytes T CD4⁺ PICALM knock-out (KO) présentent un trafic intracellulaire modifié et une abondance accrue de Gag intracellulaire, ainsi qu'une latence réduite, en plus de voies autophagiques modifiées, de phénotypes de mémoire des lymphocytes T altérés et d'une expression différentielle du système immunitaire. point de contrôle PD-1. Ce travail révèle que PICALM module l'entrée virale, le flux autophagique et le contrôle de la réplication du virus, soulignant son potentiel en tant que cible future pour le contrôle du VIH-1.

ACKNOWLEDGEMENTS

I would firstly like to express my sincere gratitude to my supervisor Dr. Andrew J. Mouland for the opportunity to work in his research group. All of his support, patience and direction over this years have been essential for completing my degree, even during the challenging times during the pandemic that I believed I was not going to be able to finish. Dr. Mouland was always very supportive and gave me a lot of independence and freedom to do any type of experiment that I considered convenient for my project, and I am profoundly grateful for that.

Thanks should also go to everyone in the Mouland lab, especially Ana Luiza Abdalla, Dr. Anne Monette, and Gabriel Guajardo. More than my labmates I would consider them part of my Montreal family; words cannot express my gratitude for all their guidance, advice in the lab and all of their moral and emotional support, I will always be indebted to them. I would also like to thank my Supervisor Committee members, Dr. Chen Liang and Dr. Benoit Barbeau, for all the stimulating discussions and knowledge provided. I would like to thank Dr. Thomas Murooka and his lab members Xinyun and Oluwaseu for providing the HIV Nef_CRMZY plasmid and for letting our lab show their findings.

I am also extremely grateful to Sergio Alpuche Lazcano for training me when I arrived to the lab, to Christian Young and Mathew Duguay from the Lady Davis Core Facility for their kind technical support, it allowed me to learn a lot. Thank you to the department of Immunology and Microbiology for always providing a very upholding and friendly environment, thank you to the Canadian Institutes of Health Research (CIHR) for financing this project, and thank you to the Mexican Instituto de Financiamiento e Información para la Educación (EDUCAFIN) for granting me funding for two years to study at McGill.

I would like to thank my family, especially my parents and siblings. Their unconditional faith, love and support have been fundamental to finishing my studies. Finally, I would like to thank my friends or my “chosen family”, their belief in me has kept my motivation high during this process.

AUTHOR CONTRIBUTIONS TO ORIGINAL KNOWLEDGE

This thesis presents scholarly work derived from a collaboration between three laboratories: those of Andrew Mouland, Chen Liang and Thomas Murooka. The work described in this thesis was derived from graduate students, Norma Paola Guízar Amador (M.Sc. student), Kristin Davis (former M.Sc. student), Ana Luiza Abdalla (Ph.D student) (students in Thomas' lab). The project was conceived by Dr. Andrew J. Mouland and experiments were designed by all of the authors: Kristin Davis performed the initial CRISPR-Cas9 screen and analyzed data; Norma Paola Guízar Amador generated stable CRISPR cell lines, western blotting experiments, ELISA experiments, flow cytometry analyses, imaging experiments, BlaM assay and analyzed data for secondary hit data; all the imaging data for autophagy flux analyses was generated and analyzed by Dr. Anne Monette and Meijuan Niu; flow cytometry data for latency analysis was generated and analyzed by Ana Luiza Abdalla; Dr. Thomas Murooka and his lab designed and provided the HIV Nef-CRIMZY reporter construct used to assess latency.

Data shown in Figures 7-9 of this thesis were generated by Kristin Davis, M.Sc. and were obtained from work performed during her Master's thesis. Figure 11A-C and Figure 12F-G were generated by Dr. Anne Monette, Figures 14 and 15 were generated by Ana Luiza Abdalla.

All other results presented in other figures are derived from my own original efforts. All figures and data will contribute to a paper that is currently under review titled "An HIV-1 CRISPR-Cas9 membrane trafficking screen reveals a role for PICALM intersecting endolysosomes and immunity" authored by Paola Guizar, Anne Monette, Ana Luiza Abdalla, Kristin Davis, Meijuan Niu, Xinyun Liu, Oluwaseun Ajibola, Thomas T. Murooka, Chen Liang, Andrew J. Mouland ¹. Additionally, I participated in the research project and publication of the paper: Ramos, H., Monette, A., Niu, M., Barrera, A., López-Ulloa, B.,

Fuentes, Y., Guizar, P., Pino, K., DesGroseillers, L., Mouland, A.J., and López-Lastra, M. (2022). The double-stranded RNA-binding protein, Staufen1, is an IRES-transacting factor regulating HIV-1 cap-independent translation initiation. *Nucleic Acids Res* 50, 411-429. [10.1093/nar/gkab1188](https://doi.org/10.1093/nar/gkab1188)².

CHAPTER 1: LITERATURE REVIEW AND INTRODUCTION

1. Human Immunodeficiency Virus

1.1. The HIV/AIDS Pandemic: An Overall Perspective

1.1.1. Origin of the AIDS pandemic and HIV discovery

June 5, 2023 marked 42 years since the first reports of what was later known to be acquired immunodeficiency syndrome (AIDS). Cases of an alleged “gay disease” began to be heard in the United States during the summer of 1981 when homosexual men started falling ill and dying of atypical opportunistic infections³. Those affected became emaciated and usually developed severe pneumonia or a form of cancer called Kaposi’s sarcoma. Fear increased throughout the gay community since most patients showed a rapid downhill course and a death rate of almost 100% despite their doctors attempting to treat every opportunistic infection⁴.

Eventually, in 1983, Barré-Sinoussi and collaborators at the Pasteur Institute in Paris isolated a retrovirus, now named human immunodeficiency virus (HIV) that was recognized as the causative agent of the AIDS pandemic⁵, discovery for which they were awarded the Nobel Prize in Physiology and Medicine later on in 2008⁶. Since its identification, the virus is one of the best-characterized known viruses, and our knowledge about its biology, transmission, and pathogenesis is noticeably vast⁴.

HIV is currently still an incurable infection that is transmitted primarily by sexual mucosal contact; however, the virus is also able to enter the body via eczematous or injured skin or mucosa, unsafe injection of drugs, and perinatal routes. The virus is found in blood, vaginal fluids, breast milk, pre-seminal fluid, and semen, and is disseminated via direct contact of these fluids with the bloodstream or mucosa of another individual⁷.

1.1.2. Evolution and classification

HIV belongs to the genus *Lentivirus*, subfamily *Orthoretrovirinae*, family *Retroviridae*. Lentiviruses cause chronic infections in several mammalian species. HIV is one of the most genetically diverse pathogens as a result of its fast replication rate, and high-recombination and mutation rates since the viral retrotranscriptase has no proofreading activity⁸. The AIDS pandemic was caused by two of these viruses, the human immunodeficiency virus type 1 and 2 (HIV-1 and HIV-2). It is believed that around 1920 to 1940, both viruses arose through multiple cross-species transmissions of simian immunodeficiency viruses (SIVs) from nonhuman primates to humans, and that one of these transmission events in southeastern Cameroon led to the development of HIV-1 groups M, N, O, and P that resulted in the global pandemic. Group M is the main cause of the pandemic and is found in essentially every country in the planet³. HIV-2 and HIV-1 groups N, O, and P have not propagated extensively around the world, mainly because these lineages activate cGAS and TRIM5-mediated antiviral responses, while HIV-1 group M has adapted to block them^{9 10}.

1.1.3. HIV-1 infection (symptomatology)

Symptoms of HIV-1 infection start between 2 and 6 weeks after exposure to the virus. The early or acute infection symptoms are generally mild and self-limited that are almost unnoticed. People can present fever, headaches, myalgia and arthralgia, rashes, pharyngitis and mouth sores, and swollen lymph nodes^{11 12}. Following this stage, the chronic infection is characterized by a continuing viral spreading and immune cell destruction. If it is not treated, HIV-1 turns into AIDS in approximately 8 to 12 years and a diagnosis is made if the CD4⁺ T cell count falls below 200 per microliter. When this happens, the immune system is already extremely weakened and opportunistic infections, neurodegenerative diseases and cancers arise in infected people¹².

1.1.3.1. Acute infection

Acute HIV-1 infection (AHI) constitutes the initial interaction between the virus and the host. Clinically, AHI is mostly asymptomatic or there is a mononucleosis-like illness, while causing detrimental effects on immune function¹³. AHI includes the eclipse phase, when the virus has to endure the defenses of the immune system; the expansion phase during which the virus replicates exponentially and where there is a mass CD4⁺T cell destruction; and the containment phase when the set-point levels of viremia and immune activation are established¹⁴.

Since 80% of adults acquire HIV-1 following exposure at mucosal surfaces, virus replication is firstly limited to the mucosal infection site. The eclipse phase ranges from 5-6 days to several weeks and dissemination of the virus is generally inefficient, HIV-1 infection at mucosal sites is frequently eliminated, and infection is usually established by a single founder virus resulting in a homogenous population in the early infection^{14 15}.

During the expansion phase, HIV-1 replicates exponentially and spreads to the regional lymph nodes and then disseminates to other lymphocyte-rich areas throughout the body, especially the gut-associated lymphoid tissue. Gut mucosal immunity is severely damaged, resulting in increased permeability to microbial products and an altered equilibrium¹⁶. This period is extremely infectious due to high viral loads and an extreme decline of CD4⁺T cells, a general activation of innate and adaptive responses is expected to occur¹⁴.

Following the peak of viral load, viremia decreases later in the containment phase as HIV-1 specific CD8⁺ T cells are induced and CD4⁺ T cells are depleted. At this point, the HIV-1 genome is already established into the host genome constituting the latent reservoir¹³.

1.1.3.2. Chronic infection and AIDS

With the current availability of over 20 medications offered from 5 drug classes, life expectancy of HIV-1 infected individuals have significantly increased and this infection turned into more of a chronic disease rather than a terminal condition, and despite treatments have significantly decreased the prevalence of many HIV-1 and AIDS-associated complications, 20% to 30% of HIV/AIDS treated patients still manifest related cognitive and motor afflictions ¹⁷.

Aged HIV-1 infected patients present a three times higher risk of developing neurocognitive disorders, such as Alzheimer's and Parkinson's disease, than the general population¹⁸; probably by disrupting the blood-brain barrier, facilitating the entrance of the virus in the central nervous system and inducing neuronal damage ¹⁹. Additionally, there is an increased risk of cardiovascular diseases in HIV-1 infected victims due to chronic inflammation, a higher risk of developing kidney disease ^{20,21}, a greater risk of HIV-1 related pulmonary disease ²², and an increased prevalence of gastrointestinal disorder symptoms due to the damage of the mucosal barrier. Additionally, men can suffer from deficient semen quality and pregnancy loss is more common in HIV-1 infected women ²³.

In the absence of therapy, HIV-1 infection results in active viral transcription, immunosuppression and finally in AIDS development. The time to develop apparent symptoms of immunodeficiency ranges from 2 to 25 years or more. A wide range of opportunistic diseases are associated with this syndrome. The infections in HIV-1 immunosuppressed patients present with atypical features, have higher infection loads and are more difficult to treat⁷. The main cancer in AIDS patients is Kaposi's sarcoma (KS) where patients develop multiple-pigmented sarcomas on the skin that gradually spread throughout the body, and it may lead to fatal lesions²⁴. Although KS incidence has been dramatically reduced since the introduction of HIV-1 treatment, in Africa it is still more common than

prostate cancer in the US ²⁵. The prevalence of HIV-related KS in East Africa has not improved in the last 5 years and recently, patients have developed KS-related immune reconstitution inflammatory syndrome represented by the development of new or pre-existing KS within the start of HIV-1 treatment ²⁶.

1.1.4. The unfinished pandemic

Since its sudden emergence, HIV-1 has proven to be a persevering challenge and is known to be one of the most destructive pathogens known to human history²⁷. The Joint United Nations Program on HIV/AIDS (UNAIDS) estimated that 80 million people have become infected with this retrovirus since the beginning of the epidemic, and 36 million lives have been lost due to AIDS-related illnesses, leaving millions of children orphaned and disrupting social stability of the world. Tragically, HIV-1 infection has afflicted the sub-Saharan Africa (SSA) region the hardest, by being home to two-thirds (~69%) of the global HIV-1 infections (UNAIDS).

Currently, approximately 37.9 million people throughout the world are living with HIV-1²⁸. Out of the SSA, key populations, such as people who inject drugs (PWID) and men who have sex with men (MSM) are the predominant groups of HIV-1 infected people. These groups are frequently prone to stigma that affects access to HIV-1 assistance¹⁰. For all of these reasons, HIV-1 research, and the search of new therapeutic targets remains a top priority to find the most fitting approach to cure infection. This will ultimately lead to viral elimination, prevent new infections, and end stigma and discrimination ^{29,30}.

1.2. HIV-1 structure and replication cycle

1.2.1. Genome and virion composition

The HIV-1 genome consists of two identical copies of single-stranded RNA (ssRNA) molecules. Reverse transcription and integration are the defining characteristics of

retroviruses, where the RNA genome is converted into DNA and then integrated into the human genome^{31 32}. The 9.2-9.6 kb DNA genome is bordered by long terminal repeat sequences. The 5' LTR region codes for the promoter for transcription of the viral genes. The structural *gag* gene follows, encoding the matrix (MA, p17), the capsid (CA, p24), the nucleocapsid (NC, p7), and p6, an important protein for the formation of viral particles since it acts as a docking site for cellular and viral factors, including Vpr³³. Later, the *pol* gene codes for important enzymes, including the reverse transcriptase (RT, p51), the integrase (IN, p32), the protease (PR, p12), and the ribonuclease (RNase) H (p15) or RT plus RNase H (p66). Next to it, the *env* reading frame codes for the two viral envelope glycoproteins gp120 (surface protein, SU) and gp41 (transmembrane protein, TM). HIV-1 is characterized by carrying a group of other regulatory and accessory proteins as well, these include Tat (transactivator protein), Rev (Regulator of virion expression), Nef (negative regulating factor), Vpr (virus protein R), Vif (viral infectivity factor), and Vpu (virus protein U) (Figure 1)^{32 34}.

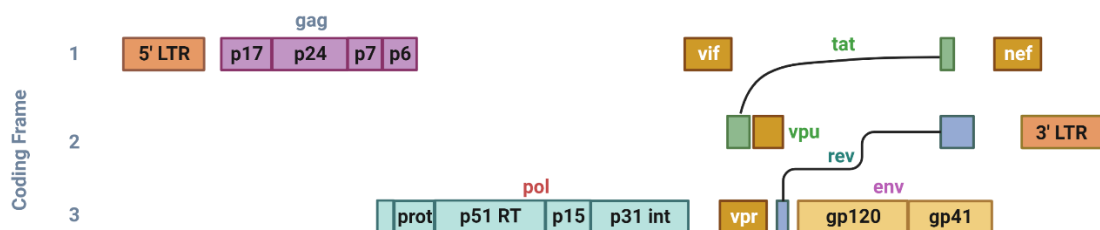


Figure 1 Structure and organization of the HIV-1 genome. The boxes represent open reading frames. The scale is representative of base pairs (bp). LTR=long terminal repeat; gag=group-specific antigen; pol=polymerase; env=envelope. Created with BioRender.com.

HIV-1 virions are a spherical particle with a diameter of ~100 nm and are enveloped by a lipoprotein-rich membrane. The membranes hold glycoprotein heterodimer complexes compiled of gp120 and gp41 glycoproteins bound together. The viral envelope surrounds the

MA, which is anchored to the inside of the viral membrane. Viral membrane and the MA protein include the CA made of polymers of the core antigen (p24). The CA encloses essential elements required for replication, including the two copies of ssRNA coupled with NC protein, RT, and IN (Figure 2) ³⁴.

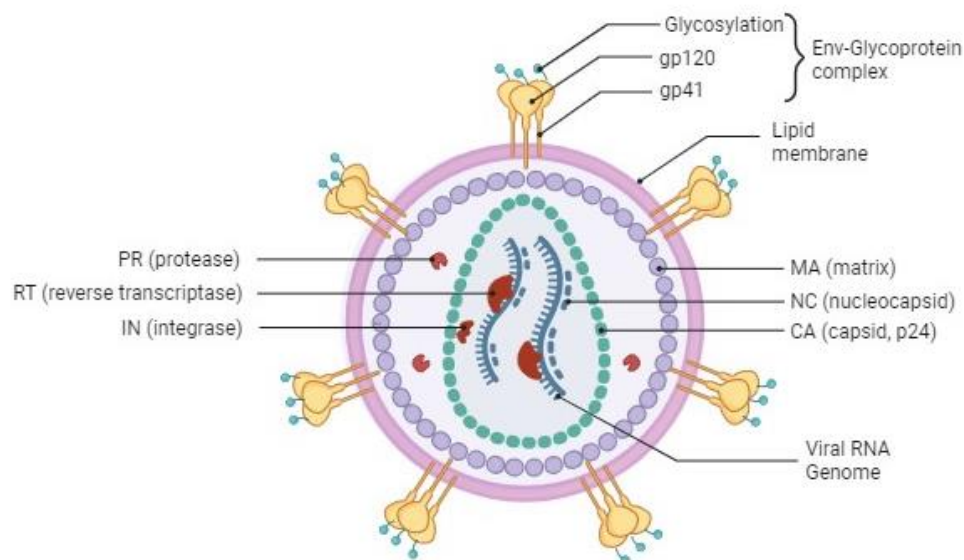


Figure 2. Structure of the HIV-1 particle. Created with BioRender.com.

1.2.2. Replication cycle

HIV-1 targets cells of the immune system expressing the CD4 receptor and the chemokine receptors C-C chemokine receptor type 5 (CCR5) and C-X chemokine receptor type 4 (CXCR4). These include CD4⁺T cells, monocytes and macrophages, and dendritic cells.

1.2.2.1. Viral attachment and entry

The attachment and entry of HIV-1 is denoted as a 30 min to 2 h process of complex and tightly controlled protein-protein interactions ³². HIV-1 surface glycoprotein gp120 first binds to the CD4 molecule on the host cell, gp120 then undergoes a conformational change, exposing a domain in gp120 capable of binding to the CCR5 or CXCR4 chemokine receptor,

allowing a more stable bond that helps gp41 fold into a hairpin conformation that assists in bringing the virus and the cell membrane close enough to form a fusion pore and enable fusion of their membranes and entrance of the virus ³⁵. Directly after membrane fusion, the capsid monomers disassemble from the core and the RNA genome dissociates in a multiple process called uncoating ^{34,36}.

1.2.2.2. Reverse transcription and integration

Reverse transcription is the signature event of retroviruses, this step is where the ssRNA genome becomes a double-stranded DNA (dsDNA) copy and it requires around 6 h ³⁷. Once the viral core is released into the cytoplasm, the RT transcribes the RNA genome into a single-stranded DNA while the RNA strand is degraded by the RNase H. Finally, the dsDNA or proviral DNA is generated by the DNA-dependent DNA polymerase activity of the RT^{32 34}.

The proviral genome is then integrated into the cell nucleus in the form of a pre-integration complex consisting of the viral dsDNA, the IN, Vpr, and matrix proteins. For this purpose, the IN cleaves the 3' ends of the dsDNA to create sticky ends, facilitating its integration into the host genome ³². The matrix proteins, that hold nuclear localization signals, direct the pre-integration complex through nucleopores into the nucleus where IN transfers the dsDNA into the host genome. Integration of the provirus is an irreversible process which allows the virus to escape from the immune system and to persist in the infected cell ³⁸.

1.2.2.3. Transcription and translation of HIV-1

Once the genome is integrated, transcription of viral mRNA is induced by strong promoters in the LTRs, and it is developed when the target cell is in an activated state. The initial transcription process results in the production of short, completely spliced mRNAs (around 2kb long), where regulatory proteins are assembled, including Tat and Rev ³⁹. Tat

binds to the TAR site (Transactivation Response Element) at the 5' end of the HIV-1 RNA and stimulates the transcription of longer RNA transcripts. Rev promotes the production of longer RNA transcripts by inhibiting host regulatory proteins that normally degrade incompletely spliced (around 4kb) and unspliced transcripts (around 9kb). To achieve this, Rev binds to the Rev response element (RRE), located in the *env* region of the incompletely spliced and unspliced transcript^{40,41} and allows nuclear export of viral mRNAs into the cytoplasm for 3' processing and polyadenylation^{42 43}.

After viral RNAs are exported to the cytoplasm, structural proteins of new virions are synthesized. The proteins coded by *pol* and *gag* genes form the nucleus of the maturing HIV-1 particle; while the gene products coded by the *env* gene form the glycoprotein spikes of the viral envelope. The large Env gp160 precursor proteins are synthesized at the endoplasmic reticulum (ER) glycosylated at the Golgi apparatus and assembled into a trimer of gp120-gp41 heterodimers⁴⁴. Gag is produced as a 55kDa precursor protein containing MA, CA, NC, p6 domains, and two spacer peptides, SP1 and SP2; while the 160 kDa GagPol polyprotein precursor containing the PR, RT, and IN is also produced at around 5% of the level of Gag⁴⁰.

1.2.2.4. Viral assembly, release, and maturation

Viral components will form new infectious particles during the assembly and release stages. During these steps, the Env glycoprotein, Gag, and GagPol, together with an array of host factors gather in conjunction with the HIV-1 genome near the cell membrane and new particles separate from the cellular membrane⁴⁵. The host Endosomal Sorting Complexes Required for Transport (ESCRT-1) machinery has been shown to be essential for HIV-1 budding. Viral maturation, a necessary process for the particle to become infectious, takes place after the new virions are released by means of the protease. During maturation, cleavage of Gag and Gag-Pol by HIV-1 protease results in the formation of functional

cleaved components, resulting in all the viral structural proteins (MA, CA, NC, PR, RT, and IN). Protease also cleaves Nef, Vif, and a number of host proteins that help with viral protein generation ³⁸.

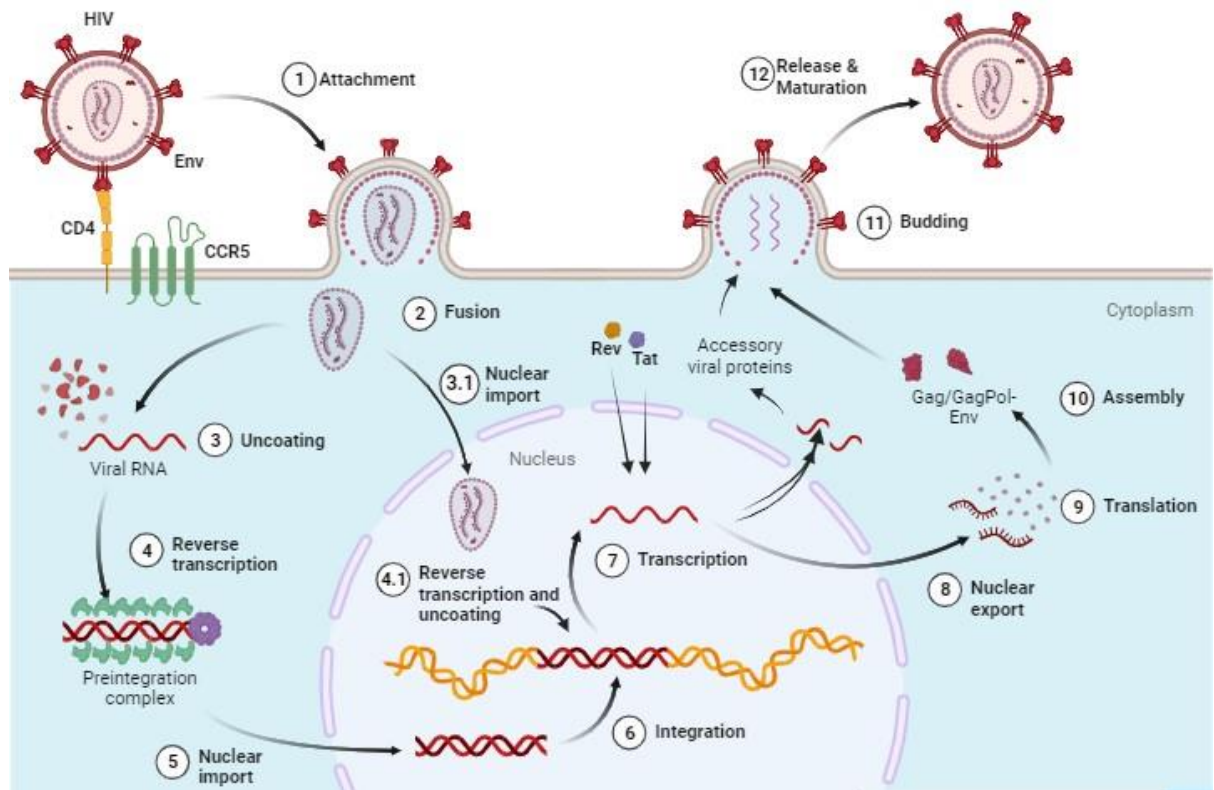


Figure 3. HIV-1 replication cycle. Created with BioRender.com.

1.3. Current treatments

Despite the success of several vaccines in limiting or eradicating infectious diseases, no cure or vaccine has yet been achieved for HIV-1 infection. Several approaches have been studied throughout the years, however, in the present-day, life-long antiretroviral therapy (ART) is the only approach for the treatment and prevention of HIV-1 infection¹⁶. The treatment regimen is composed of three or four drugs, which includes medications such as abacavir, efavirenz, atazanavir, maraviroc, ibalizumab, etc. and is recommended to be initiated in all individuals with HIV-1 regardless of the clinical stage or CD4 cell count to

preserve the patient's immune system, control viral replication, and reduce new transmissions.

The five main classes of HIV-1 ARTs are classified by the viral proteins they target⁴⁶.

The five categories are presented in Table 1.

Table 1. Therapeutic agents targeting HIV-1.

Drug Class	Details and Mechanism of Action	Drug class examples (Commercial name)	Refs.
Nucleoside/nucleotide reverse transcriptase inhibitors (NRTIs)	Competitive inhibitors of the HIV-1 enzyme reverse transcriptase (RT) to block viral replication.	<ul style="list-style-type: none"> • zidovudine (Retrovir) • lamivudine (Epivir) • abacavir sulfate (Ziagen) 	47
Non-nucleoside reverse transcriptase inhibitor (NNRTIs)	Non-competitive inhibitors that stop RT from adding new nucleotides. NRTIs and NNRTIs date back to the 80s and are currently the most used drugs and the backbones of the treatments. They target the catalytic site of HIV-1 RT.	<ul style="list-style-type: none"> • doravirine (Pifeltro) • efavirenz (Sustiva) • etravirine (Intelence) • nevirapine (Viramune, Viramune XR) • rilpivirine (Edurant). 	48,49
Protease inhibitors ⁵⁰	PIs and INIs appeared in the mid-90s and are associated with lower levels of resistance compared to reverse transcriptase-based therapy and act as a competitive inhibitor of the protease to block the cleavage of <i>gag</i> and <i>gagpol</i> precursors.	<ul style="list-style-type: none"> • atazanavir (Reyataz) • darunavir (Prezista) • fosamprenavir (Lexiva) • indinavir (Crixivan) • lopinavir/ritonavir (Kaletra) • nelfinavir (Viracept) • ritonavir (Norvir) 	48
Integrase inhibitors (INIs or INSTIs)	Introduced in 2007, INSTIs inhibit the strand transfer step of viral DNA integration into the cell genome.	<ul style="list-style-type: none"> • atazanavir (Reyataz) • darunavir (Prezista) • fosamprenavir (Lexiva) • indinavir (Crixivan) 	46
Entry inhibitors	Such as CCR5 antagonists that block the interaction of HIV-1 gp120 with the CCR5 receptor and fusion inhibitors that bind to the viral glycoprotein gp41 to inhibit the conformational changes necessary for the fusion.	<ul style="list-style-type: none"> • enfuvirtide (Fuzeon) • fostemsavir (Rukobia) • ibalizumab-uiyk (Trogarzo) • maraviroc (Selzentry) 	49

Additionally, some anti-HIV-1 drugs have been approved for pre-exposure prophylaxis (PrEP) for people that possess a high risk of getting HIV-1, and new compounds and mechanisms are being studied for HIV-1 treatment and prevention ⁵¹.

For the approximately 37.9 million people living with HIV-1 (PLWH), the use of ART suppresses HIV-1 to undetectable levels by keeping HIV-1 replication suppressed. Nevertheless, while ART is truly remarkable for the treatment of HIV-1 infection, it is incapable to eliminate HIV-1 due to the persistence of the latent virus, therefore, if the treatment is interrupted, the virus can be reactivated and lead to AIDS ⁵². Additionally, access to therapy is not universal, it is only accessible to approximately 72% of the PLWH ⁴⁸, some individuals develop drug-resistant strains and the treatment may cause side effects ^{53 54}.

1.4. Establishment of reservoirs and latency

The persistence of latent reservoir of HIV-1 is the major challenge in eradicating infection since ART does not target this population¹⁶. Latently infected cells possess an integrated but transcriptionally silent and immunologically inert HIV-1 provirus that can be reactivated ^{55 56}. Although the specific process is still not completely understood, it is widely accepted that the HIV-1 reservoir is established early in infection, and that CD4⁺T cells of resting memory constitute most of it, however, other cell types and tissues throughout the body can also contribute to this reservoir. The genome is reversely transcribed from RNA into DNA, which is then integrated into the genome of mainly CD4⁺T cells of resting memory ²⁸.

Diverse approaches are being developed for the elimination or control of the latent reservoir ⁵⁵. The leading approaches include strategies like “shock and kill”, that involves the use of latency reversing agents ⁵⁷ to activate the latently infected cells (shock) to then eliminate the virus (kill) through the anti-HIV cytotoxic CD8⁺T cell response along with

ART and an enhanced immune response with broadly neutralizing antibodies (bNAbs) to promote cell apoptosis^{28,55}. Opposite to the “shock and kill” strategy, the “block and lock” approach is meant to permanently silence the virus to keep it from reactivating. In order to achieve this, several angles have been proposed, such as the inhibition of Tat protein expression, the inhibition of HIV-1 integration, the use of small interfering RNA (siRNA) to silence HIV-1 transcription genes, and the use of mammalian target of rapamycin (mTOR) inhibitors^{28,56}.

1.5. Strategies for an HIV-1 cure

Early HIV-1 research was remarkably fruitful, nonetheless, up to this moment, man-made drugs and the brilliant defense provided by our immune system are thus far not enough to cure HIV-1 infection. The remarkably high mutation rate of the virus and latent reservoir are the major aspects behind the failure of all current treatments, preventatives, and vaccine trials³⁸.

Several strategies continue to emerge in the HIV-1 cure field. Some attempts have centered on the “shock and kill” strategy, where some LRAs have even entered clinical trials, including histone deacetylase inhibitors (HDACi). A few favorable results have been achieved and HDACi has shown to induce reverse latency, HIV-1 RNA expression and immune clearance⁵⁸, however, these have not been fully successful yet due to their limited effect on the size of the latent reservoir⁵⁹. Meanwhile, the counterpart of this strategy, the “block and lock” technique has been able to prevent viral reactivation but the effect is only sustained for a short period of time and it would require lifelong adherence, therefore, it can not be considered a cure⁶⁰.

Other novel therapies have come to light, gene therapy is, likewise, at the lead of HIV-1 cure strategies, where clustered regularly interspaced short palindromic repeats

(CRISPR) is a strong candidate for either the deletion of genes expressing the CCR5 and CXCR4 coreceptors or the removal of the proviral genome ⁶¹. Immune checkpoint modulation is another approach since it is known that HIV-1 infection exhausts T cells and immune checkpoint blockade has the potential of annulling that event, consequently causing an increase in the effectiveness of HIV-1 specific T cells as well as the performance of vaccines ⁶².

Several attempts have been made to develop a vaccine against HIV-1 infection, the first phase 1 trial for this disease was since 1987, however, so far, all trials have failed. Nonetheless, other therapies and vaccines continue to be developed and entering phase 1 trials with the hope of producing positive results in the near future. Some of these include the use of a few viruses like cytomegalovirus, Adenovirus 4, and Ankara as vectors to deliver the trimeric form of the protein Env to evoke an immune response. Other approaches include consecutive immunizations with distinct HIV-1 proteins to generate bNAbs, the use of plants to produce bNAbs ⁶³, as well as the use of different adjuvants or nanoparticles and liposomes to increase delivery and immunity ⁶⁴.

2. Phosphatidylinositol binding clathrin-assembly protein (PICALM)

1.1. PICALM in a nutshell

The human *PICALM* gene is located on chromosome 11 and it encodes the protein PICALM (also known as CALM that stands for clathrin assembly lymphoid myeloid leukemia). PICALM is a ubiquitous protein and is expressed in the brain, bone marrow, lymphoid tissues, skin, endocrine tissues, respiratory system, gastrointestinal tract, liver and gallbladder, pancreas, muscle, kidney, urinary bladder, connective tissues, and in female and male tissues, <https://www.proteinatlas.org/ENSG00000073921-PICALM/tissue> (accessed on 1 June 2023).

This protein is primarily known as one of the most critical proteins in clathrin mediated endocytosis (CME) and one of the three most abundant proteins of clathrin-coated vesicles ⁶⁵. However, PICALM also has multiple roles in cellular functions, including macroautophagy (hereafter referred to as “autophagy”), lipid and iron homeostasis ^{66,67}, transferrin uptake, immunity ⁶⁸, and it has also been widely associated with Alzheimer’s disease ⁶⁹⁻⁷⁶.

1.2. PICALM in clathrin-mediated endocytosis

Clathrin-mediated endocytosis is the main endocytic pathway in mammalian cells. It is an essential mechanism to transport several cargo molecules from the plasma membrane to the interior of the cell and it is fundamental for maintaining cellular homeostasis by regulating a wide range of physiological processes, including nutrient uptake, intracellular signaling, PM remodeling, cell adhesion, etc.⁷⁷. CME starts at the PM through the assembly of clathrin-coated pits (CCPs), formed with mainly two components, clathrin polymers called “triskelia” that form polygonal lattices, and clathrin-adaptor proteins, subsequently, the scission process separates the CCPs from the PM to generate clathrin-coated vesicles (CCVs) and ultimately, the resulting vesicle is uncoated and the cargo is delivered to early endosomes to recycle back to the PM, send to the trans-Golgi network, or deliver to lysosomes for degradation. CME requires the action of more than 50 endocytic accessory proteins, including PICALM ⁷⁸.

PICALM and AP-2 are the most abundant clathrin-adaptor proteins, accounting for 30-35% of the adaptors in a CCV, respectively ⁷⁹, and they are considered endocytic pioneers since they are recruited to CCPs at the earliest stages of CME in order to initiate the endocytic process ⁸⁰ (Figure 4). Clathrin-adaptor proteins interact with specific cargoes to start clathrin recruitment and PM deformation to induce CCP growth and stabilization. PICALM is a decisive protein in CCV formation as it promotes membrane curvature and it helps overcome the PM tension to create the invaginations ^{79,81}. Moreover, depletion of PICALM leads to an increase in number of early endosomes, increases the ratio of abortive

CCPs, impairs CCP maturation, produces larger CCPs/CCVs and ultimately reduces endocytic rate^{77,82}.

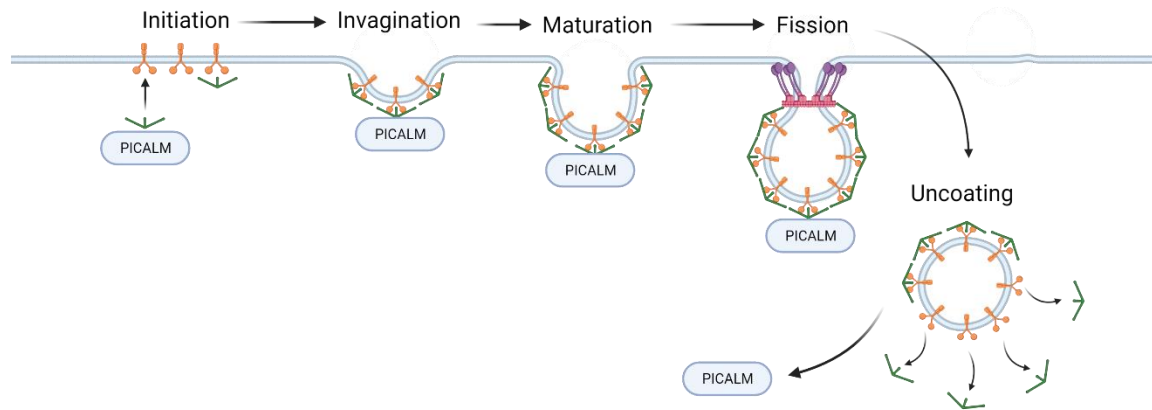


Figure 4. Role of PICALM in clathrin mediated endocytosis. PICALM is a key component in CME as a clathrin-adaptor protein by initiating CCP formation and at later steps, inducing its growth and maturation. Uncoating releases PICALM back to the cytosolic pool. Created with BioRender.com.

1.3. PICALM in autophagy

Autophagy (Greek, “self-eating”) is an evolutionary conserved process where cytoplasmic cargo is sequestered in double-membrane structures termed autophagosomes and then delivered to lysosomes for degradation and recycling, and it is another fundamental cellular pathway for maintaining cellular and organismal homeostasis⁸³. It is necessary for removal of unwanted cargo (e.g., damaged organelles, pathogens, long-lived proteins), adaptation to nutrient-restricted conditions, prevention of genomic disturbance, and cell renovation during differentiation and development⁸⁴. These activities protect the organism against cancer, stress management, infections, neurodegeneration, aging, and inflammation, and it is mediated by about 16-20 core autophagy related (ATG) proteins⁸⁵.

Autophagy is a multiphasic process that is usually portrayed in six steps (Figure 5). The *initiation* step is commanded by the mTOR complex 1 (MTORC1) which dissociates from

ULK1 complex when autophagy is induced⁸⁶. Activated ULK1 complex favors the autophagic cascade by recruiting and phosphorylating the class III phosphoinositide 3-kinase (PI3K) complex I which generates phosphatidylinositol-3-phosphate (PtdIns3P) to promote phagophore *nucleation* and its followed by its engagement with WIPI and ubiquitin-like microtubule-associated protein 1 light chain 3 (LC3) proteins for the *elongation* of the phagophore⁸⁷. The membrane that makes up the phagophore comes from the ER⁸⁸, PM⁸⁹, Golgi apparatus⁹⁰, and mitochondria⁹¹. The phagophore continues to expand, and eventually closes around the cargo and *matures* into a 0.5 to 1.5 μm double-membrane autophagosome. Subsequently, the outer membrane of the autophagosome *fuses* with the lysosomal membrane to form the autolysosome. The contents are then *degraded* by the lysosomal enzymes and finally reused by the cell⁹².

Autophagy and endocytosis intersect at several steps throughout vesicle formation, fusion, and trafficking, therefore, both pathways share components of the molecular machinery⁹³, including PICALM⁹⁴ (Figure 5). PICALM is involved in several steps in autophagy, its knockdown leads to a reduced autophagosome biogenesis, and reduced autophagosome-lysosome fusion⁹⁵, therefore, PICALM depletion results in a general reduction in autophagic flux. Additionally, PICALM is also implicated in the maturation of Cathepsin D, which is a critical lysosomal component⁹⁶.

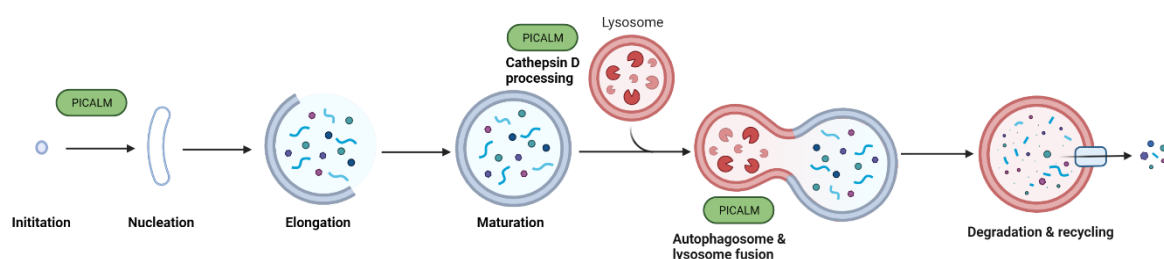


Figure 5. Role of PICALM in autophagy. PICALM also participates in certain steps of the autophagy pathway. PICALM is an important modulator of the de novo formation of the autophagosome, autophagosome-lysosome fusion, and Cathepsin D processing. Created with BioRender.com.

1.4. PICALM in Alzheimer's Disease

Alzheimer's disease (AD) is a progressive neurodegenerative disorder and the major cause of dementia worldwide, accounting for 60%-80% of all dementia diagnoses⁹⁷. Patients present memory disfunctions and increasing cognitive impairments as disease progresses. This disease is characterized by the progressive build up of amyloid β ($A\beta$) plaques, and accumulations of hyperphosphorylated tau as neurofibrillary tangles⁹⁴. Thus far, several genome-wide association studies (GWAS) have identified *PICALM* as a gene with a very strong association with late-onset AD susceptibility⁹⁸⁻¹⁰¹.

PICALM expression is reduced in post-mortem brains of people with tauopathies including AD¹⁰², and its depletion increases tau aggregation and hyperphosphorylation while impairing autophagy flux in transgenic mice¹⁰³. *PICALM* is also known to recognize and transfer amyloid precursor protein (APP) to the LC3-marked autophagic pathway, therefore regulating $A\beta$ clearance¹⁰⁴. Additionally, *PICALM* modulates both tau and $A\beta$ degradation via autophagosome formation and autophagosome fusion in view of an LC3-II accumulation due to a mis-trafficking of lysosomal enzymes and membrane proteins when *PICALM* is deleted, which finally leads to an accumulation of AD associated tau and $A\beta$ ¹⁰⁵. Furthermore, it has been shown that *PICALM* is critical for guiding $A\beta$ to Rab5 and Rab11 to mediate $A\beta$ transcytosis and clearance across the blood-brain barrier¹⁰⁶.

1.5. PICALM and its interaction with pathogens

PICALM is also implicated directly or indirectly in some pathogen's life cycle, it controls the endocytosis of the mannose-6-phosphate receptor used as an element of late endosomes that is disrupted by *Helicobacter pylori* during infection¹⁰⁷ and which is also used for entry and/or intracellular transport of herpes simplex virus (HSV), and *C. pneumoniae*^{108,109}. *PICALM* also binds to a nuclear exportin used by HSV for nuclear egress¹⁰⁹, and it has been

demonstrated that the downregulation of PICALM both *in vitro* and *in vivo* can inhibit enterovirus A71 infection¹¹⁰.

1.6. PICALM in cellular homeostasis

PICALM is necessary for cellular cholesterol homeostasis by regulating the expression of proteins involved in cholesterol biosynthesis and lipoprotein uptake. Knockdown of PICALM leads to a significant increase in LDL receptor expression and to up to a 50% increase in cholesterol biosynthesis gene expression, resulting in higher total cellular cholesterol content⁶⁶. PICALM is also critical in iron homeostasis and cellular growth since it regulates the internalization and localization of some cell surface proteins, such as the transferrin receptor (TfR) and the epidermal growth factor receptor (EGFR). Loss of PICALM in murine embryonic fibroblasts results in perturbed internalization of TfR and EGFR, resulting in impaired iron metabolism, anemia, reduced cellular proliferation and shortened life span¹¹¹
⁶⁷.

Finally, PICALM is also involved in several hematopoietic malignancies, including malignant lymphomas, and acute lymphoblastic and myeloid leukemias. Chromosomal translocations result in the fusion of *PICALM* to the *AF10* transcription factor gene and to the *MLL* histone methyltransferase gene, leading to these malignancies, however, the role of PICALM in this process has not been yet elucidated⁶⁷.

3. Immune checkpoint molecules.

Immune checkpoint molecules (ICMs) are negative regulators of the immune response. Once the immune response has completed its purpose, such as eliminating harmful pathogens, it needs to be tuned down to avoid collateral tissue damage or a response against self-antigens^{112,113}. For this purpose, CD4 and CD8 T cells need to shift into a unique differentiation state known as “exhausted” state, characterized with an altered transcriptional

and epigenetic state that leads them to lose their effector function due to cells losing their proliferative potential, diminished cytokine production, reduced cytotoxic capacity, and an altered metabolic profile^{114 115}.

Although no main regulator of exhaustion has been discovered, one of the major hallmarks of T cell exhaustion is the high and sustained co-expression of ICMs, including the cytotoxic T lymphocyte antigen-4 (CTLA-4), B and T lymphocyte associated (BTLA), T-cell immunoglobulin domain and mucin domain protein 3 (TIM-3), programmed cell death 1 (PD-1), lymphocyte activation gene 3 protein (LAG-3), T-cell immunoglobulin and immunoreceptor tyrosine-based inhibitory motif domain (TIGIT), CD160, 2B4 among others on a variety of T cells which suppress and fine tune T cell activation by dimerizing with their ligands on antigen-presenting cells (Figure 6). These immune checkpoints are responsible for transducing the necessary inhibitory signals to induce T cell exhaustion¹¹⁶.

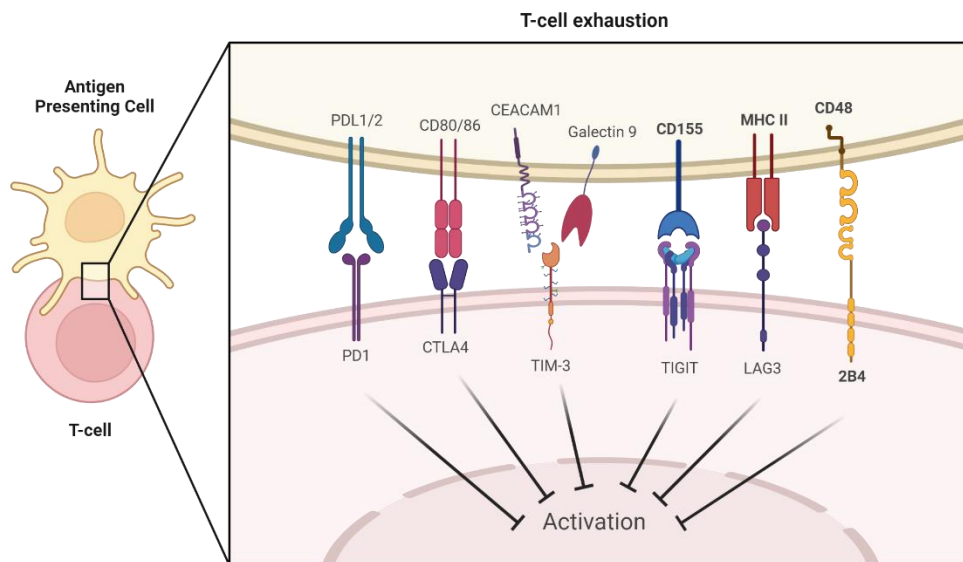


Figure 6. T-cell immune checkpoint molecules and related ligands. Immune checkpoint inhibitors such as PD-1, CTLA-4, LAG3, TIGIT, TIM-3, and 2B4 inhibit T cell effector function following interaction with their related ligands expressed on antigen-presenting cells. Created with BioRender.com.

The interplay of ICMs and their ligands is complex and can happen at distinct T cell activation stages, additionally, ICMs are highly diverse and their mechanisms of action is different between them, for example, they can increase the threshold for T cell activation, attenuate T cell expansion, compete with co-stimulatory receptors, interfere with downstream signals from co-activatory and T cell receptors, and/or upregulate genes that are involved in T cell dysfunction^{117 116}. Generally, the higher the number of ICMs co-expressed, the more extreme the exhaustion¹¹⁷.

1.1. ICMs during chronic infection and cancer

Termination of the immune response is a necessary self-limit process to avoid cellular damage after antigen clearance. However, pathogens and tumors are able to mimic the ICM ligands to paralyze the immune system¹¹⁸. When it comes to chronic infections or cancer and the immune system is unable to clear the foreign antigen, T cells also enter into exhaustion. These exhausted T cells can linger for years generating a loss of effector function and ultimately a poor control of persisting infections and tumors^{119 117}. Studies have found that during HIV-1, HCV, HTLV-1, and several other infections, high amounts and persistent antigen exposure leads to CD8 T cells expressing a considerably higher and sustained expression of multiple ICMs, including PD-1, LAG-3, TIM-3, CTLA4 among others¹²⁰⁻¹²², which also correlates with a progressive virus-specific CD8 T cell exhaustion causing a weakened function and a lowered cytokine production¹²³.

As it is well known, chronic HIV-1 infection is established in most infected people after CD8 T cells partially restrain viral replication¹²⁴. Several studies have confirmed that with persistent antigen exposure and constant inflammatory signals, HIV-specific T cells become exhausted and lose their ability to eliminate infected cells^{120,122,125,126}. PD-1 is the main marker of exhaustion in HIV-1 infection and a high expression of PD-1 is related to

impairment of CD8 T cells and a diminished number of CD4 T cells. Nevertheless, elite controllers and ART treated patients show a low PD-1 expression¹²⁰.

Cancer patients have a high tolerance to antitumor immune responses and also share many molecular features with exhausted T cells during a chronic infection¹²⁷. Ligands of ICMs are highly expressed on many metastatic lesions of cancer patients, and CD8 T cells in the tumor microenvironment also have an increased level of ICMs compared to other CD8 T cells in circulation¹²⁸. Furthermore, a high ICM expression in cancer cells triggers a metabolic reprogramming of both malignant cells and immune cells that impedes a proper immune control. Nutrients are depleted and toxic metabolites are also produced in the tumor microenvironment to inhibit anti-tumor responses¹¹³.

1.2. PD-1: PD-L1/L2 pathway

The PD-1: PD-L1/L2 axis is recognized as the major inhibitory pathway regulating T cell function. PD-1 is a transmembrane protein that is expressed by several types of immune cells, including T cells, B cells, monocytes, dendritic cells, and natural killer cells, and it generates a strong inhibitory signal upon binding to its ligands PD-L1 and PD-L2, resulting in down-regulation of pro-inflammatory T-cell activity¹²⁶. PD-L1 can be found on several immune cells (resting T cells, B cells, dendritic cells, macrophages), and in various non-immune endothelial and epithelial cells, including tissues like placenta, heart, and spleen. In contrast, PD-L2 expression is limited to dendritic cells and macrophages¹¹⁵.

Transcription factors such as nuclear factor of activated T cells (NFAT), interferon regulatory factor 9 (IRF9), and Forkhead box protein O1 (FOXO1) cause the expression of PD-1¹²⁹. After its engagement with its ligands, PD-1 goes through a conformational change and recruits the phosphatase SHP-2, which results in the dephosphorylation and inhibition of the T cell receptor (TCR) and CD28 pathways, leading to the suppression of T cell activation,

proliferation, cytokine production (IL-2, IFN- γ , and TNF- α), altered metabolism and consequent death of T cells. Furthermore, PD-1 increases the expression of transcription factors that suppress the expression of effector genes¹³⁰.

1.3. Checkpoint blockade

Knowledge on the implication of ICMs on T cell exhaustion has recently led to the development of immunotherapies for certain cancers¹³¹. The discovery that exhausted T cells are not terminally impaired led to the blockade of checkpoint proteins with monoclonal antibodies to reverse T cell exhaustion and it has demonstrated to restore and reinvigorate T cell function to eliminate numerous cancers including metastatic melanomas and carcinomas of various organs^{112 132}. The use of ICM-specific antibodies has shown to improve T cell cytotoxicity, proliferation, and cytokine production, therefore, increasing their effector function to reduce tumor load¹³³. Additionally, checkpoint inhibitors have also a great potential of becoming a valuable treatment for infectious diseases since they have demonstrated to improve T cell function of patient cells with chronic viral, bacterial, or parasitic infections¹²⁸.

Humanized monoclonal antibodies targeting ICMs have achieved a high clinical relevance due to their remarkable efficiency. In the present day, three types of checkpoint inhibitors have already been approved for the treatment of melanoma, non small cell lung cancer, and renal and bladder cancers, these include PD-1 inhibitors (Nivolumab, Pembrolizumab, and Cemiplimab), PD-L1 inhibitors (Atezolimumab, Durvalumab, and Avelumab), and CTLA-4 inhibitor (Ipilimumab)¹³⁴. Currently, more than 1,000 clinical trials targeting ICMs are underway (www.clinicaltrials.gov).

1.4. ICMs on T cell differentiation

Even though ICM expression has been primarily related to T cell exhaustion, ICMs are also associated to both, differentiation, and activation status in CD8 T cells. ICM levels change depending on T cell differentiation, for instance, CTLA-4 is up-regulated in Treg cells, BTLA is present at low levels on differentiated cells, and TIM3 is lowly expressed on naïve T cells ¹³⁵. The differentiation subsets of CD8 T cells (naïve, effector, and memory cells) show broad differences in ICM expression, indicating that ICMs could also play a role in memory versus effector cell differentiation ¹¹⁶.

4. CRISPR screen of membrane trafficking genes reveals HIV-1 modulators

CRISPR genetic screens have greatly improved discovery efforts aimed at the uncovering of essential host factors for HIV-1 replication. Some studies have focused on identifying new host dependency factors (HDFs) maintaining viral latency ¹³⁶⁻¹⁴¹, whereas others have been focused on factors assisting virus integration ¹⁴²⁻¹⁴⁴. Despite a growing repertoire of their importance in HIV-1 pathogenesis, a CRISPR screen specifically focused on identifying new HDFs from membrane trafficking pathways has yet to be reported.

To uncover membrane trafficking pathway HDFs that may serve critical roles in HIV-1 replication, we performed an arrayed screen using a library of 140 membrane trafficking genes in CD4⁺ HeLa derived TZMbl-Cas9 cells (**Table S1**). The Protein Analysis Through Evolutionary Relationships (PANTHER) gene ontology (GO) tool was used to perform enrichment analysis of the gene set to classify them into subgroups with diverse molecular functionalities in membrane trafficking, where it mostly identified proteins with catalytic functions (40%; e.g., Rab GTPases), binding functions (39%; e.g., clathrin adaptors), and those involved in cytoskeleton maintenance and actin remodeling (10%) (**Figure 10C**).

The well-established HeLa-derived TZM-bl cell line was chosen as parental cell line for the functional CRISPR screen due to its amenability to transfection, permissibility to

HIV-1 infection, and it's harboring a luciferase cassette driven by a Tat-responsive integrated HIV-1 LTR for quantitative measurement of HIV-1 infectivity in relative light units (RLUs). TZM-bl cells were made to constitutively and stably express the Cas9 endonuclease, herein designated as the TZM-bl-Cas9 cell line used for the CRISPR screen.

To ensure that the Cas9 endonuclease in TZM-bl-Cas9 cells could effectively target and cleave the correct genomic targets, we designed a sgRNA (i.e., sgLTR362) targeting the highly conserved NF- κ B binding site of the HIV-1 LTR in TZM-bl cells, which is required for provirus transcription and expression of the luciferase gene cassette. The sgLTR362 was cloned within the lentiGuide-Puro vector (**Figure 7E**), which was then transduced into TZM-bl-Cas9 cells which were then infected with NL4.3 virus. This resulted in 20-fold decrease ($p \leq 0.0001$) in luciferase expression by TZM-bl-Cas9 cells (**Figure 7F and 7G**), validating both the presence and functionality of the Cas9 protein of these TZM-bl-Cas9 cells.

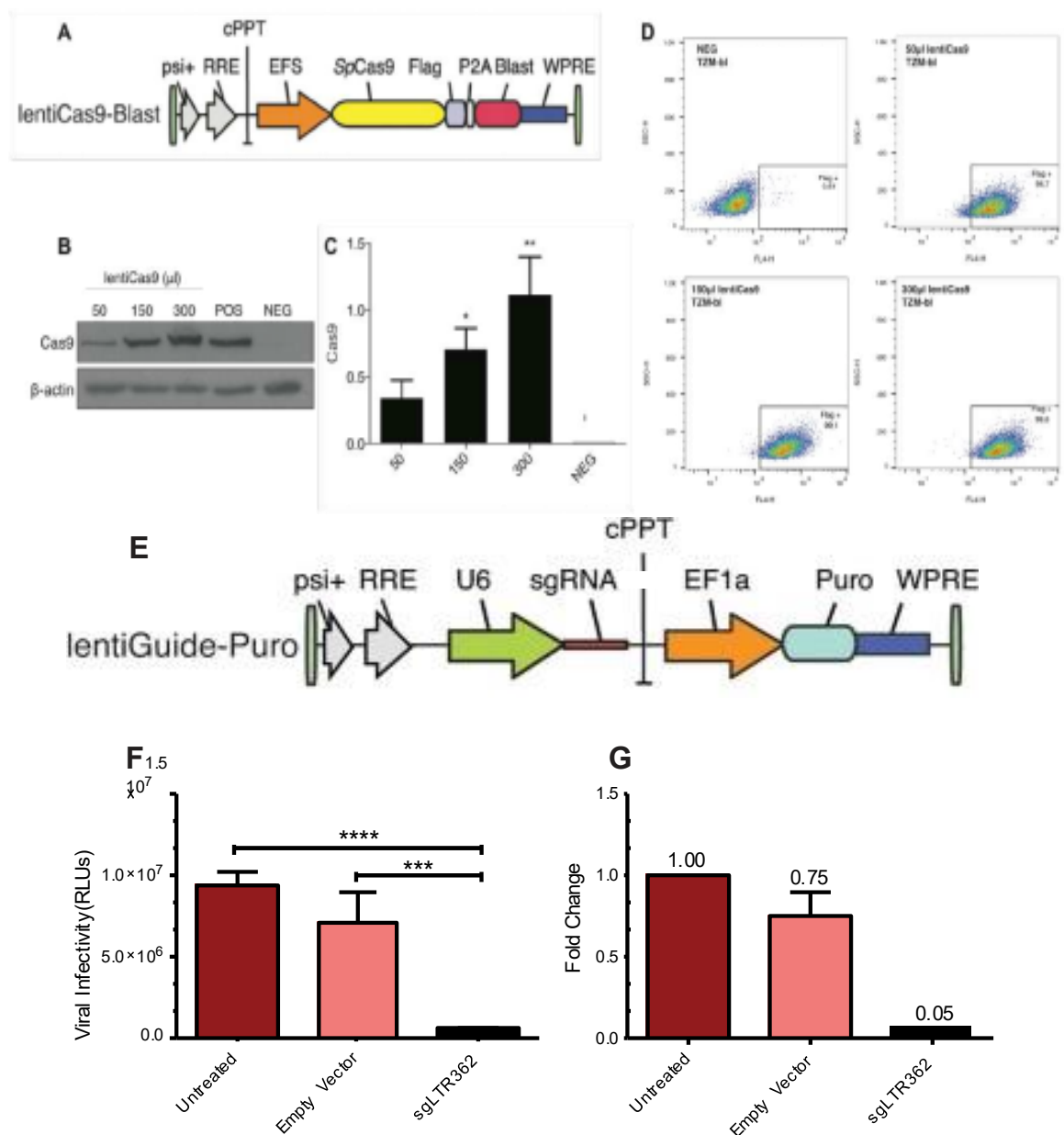


Figure 7. Generation of TZM-bl-Cas9. (A) Schematic representation of the lentiCas9-Blast vector. (B) Western blot of TZM-bl cells transduced with various volumes of lentiCas9-Blast. (C) Levels of Cas9 normalized to loading control. (D) Flow cytometry of C-terminal FLAG-tagged Cas9 endonuclease. Representative of three independent experiments. (E) Schematic representation of the lentiGuide-Puro vector containing a 20-mer sgRNA targeting the LTR362 genomic region. (F) Untreated, empty vector and sgRNA treated cells were challenged with HIV-1 NL4.3 and viral infectivity was measured as luciferase production in relative light units (RLUs). (G) Fold change relative to the untreated control. Representative of three independent experiments. One-Way ANOVA; * $p \leq 0.05$, ** $p \leq 0.01$, *** $p \leq 0.001$, **** $p \leq 0.0001$. Retrieved from ¹⁴⁵.

We performed three independent arrayed CRISPR screens in the TZM-bl-Cas9 cells using the 140 membrane trafficking gene library to uncover genes that may be essential to HIV-1 replication (**Figure 8A; Table S1**). The crRNA library was transfected into the TZM-bl-Cas9 cells the respective tracrRNA, and a non-targeting crRNA (1:1) used as a negative control. TZM-bl-Cas9 cells were assessed for viability three days post crRNA transfection using flow cytometry, with 70% of targets displayed $\geq 75\%$ cellular viability following gene perturbation (**Figure 8B-F**), this relative to an observed $\sim 90\%$ for non-transfected and non-targeting controls crRNA transfected cells. The seven gene targets identified as detrimental to cellular viability (i.e., $< 60\%$) were excluded from later experiments (**Figure 8F**).

CRISPR-Cas9 gene edited cells were infected with purified HIV-1 NL4.3 virus (MOI=1) following viability assessments, and infectivity and virus production was quantified 48 hours later from cell lysates and supernatants using the TZM-bl luciferase and p24 antigen enzyme-linked immunosorbent assays ¹⁴⁶, respectively. To ensure the luciferase assay was compliant with the TZM-bl-Cas9 cells and with the sgRNAs, we compared these to WT TZM-bl cells, and also compared to non-transfected, mock transfected (transfection reagent only), and non-targeting controls, to find that these yields had no significant differences (**Figure 9A-B**). Satisfied with these key control experiments, the three independent pooled sgRNA screens demonstrated that numerous gene KOs caused modified virus infectivity (**Figure 8G, Figure 9C**).

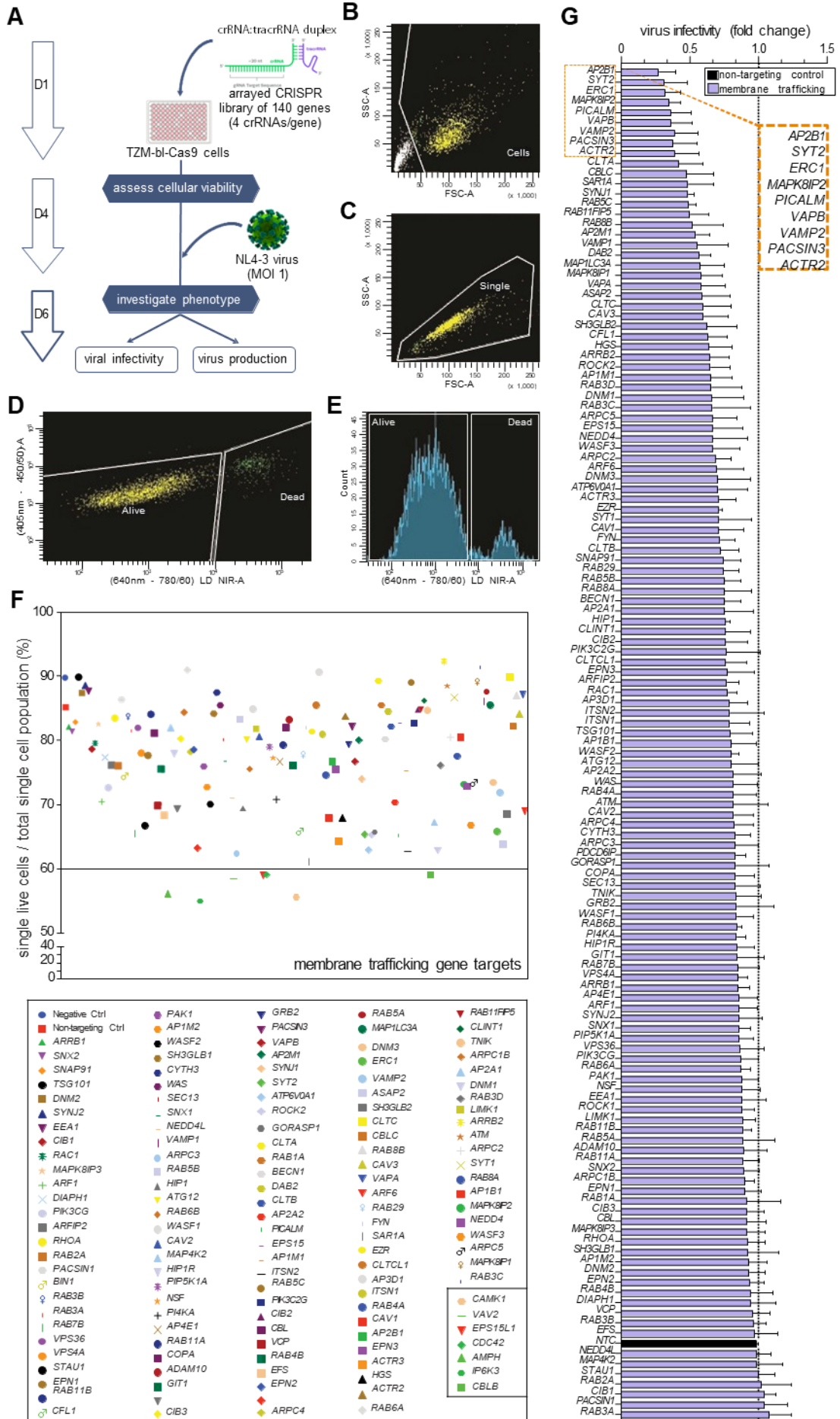


Figure 8. Viability and viral infectivity of 140 membrane trafficking CRISPR screen KO cells. (A) Schematic representation of the arrayed CRISPR screen protocol, where negative control uses a non-targeting crRNA. The 140 gene crRNA library was transfected into TZM-bl-Cas9 cells at a 1:1 ratio with the respective tracrRNA. (B-E) Flow cytometry was used to assess cellular viability of the CRISPR genetically edited cells three days following transfection, with gating strategy involving (B), forward and side scatter (FSC-A vs. SSC-A) to identify cells, followed by (C), forward area versus height (FSC-A vs. FSC-H) to differentiate singlets from doublets, then (D), a live/dead amine-binding kit, also demonstrated here via histogram function (E). (F) Cellular viability of individual CRISPR-edited gene screen KOs is represented as a percentage of single live cells to total single cell population (top), with gene legend (bottom), with KOs having lower than 60% cellular viability boxed at bottom right corner. (G) Representative bar graph demonstrating fold-change in viral infectivity of three independent CRISPR screen knockouts infected with NL4.3 as measured by TZM-bl luciferase assay, with dotted line added as cut-off value relative to effect of non-targeting control (NTC, black bar). Retrieved from ¹⁴⁵.

Throughout three replicate screens, nine of the gene KOs displayed a greater than a 2-fold decrease in infectivity compared to the non-targeting controls. These genes (with associated fold decreases) were *AP2B1* (0.28-fold), *SYT2* (0.32-fold), *ERC1* (0.33-fold), *MAPK8IP2* (0.36-fold), *PICALM* (0.37-fold), *VAPB* (0.37-fold), *VAMP2* (0.38-fold), *PACSIN3* (0.38-fold), and *ACTR2* (0.39-fold). A threshold of 2-fold decrease or higher in viral infectivity levels compared to non-targeting control was chosen based on what is reported as significant and a worthwhile cutoff in the literature ¹⁴⁷. These results suggest that these nine genes are essential to the early stages of HIV-1 replication cycle.

To supplement viral infectivity data, virus production by CRISPR screen KOs were also quantified using p24 ELISA assays on cell-free supernatants. No effects were observed from controls including non-transfected, mock transfected and non-targeting controls (**Figure 9D**), whereas the CRISPR screen KOs did reveal differential virus production (**Figure 9E and 9F**). Interestingly, the *VPS36* (EAP45) gene KO consistently exhibited >2-fold decrease in virus production (**Figure 9F**), implicating a key function for this protein in the later steps of HIV-1 replication, and confirming our earlier work¹⁴⁸. While gene KOs affecting virus production is interesting, we were most interested in pursuing this work by further analyzing gene KOs abrogating infection.

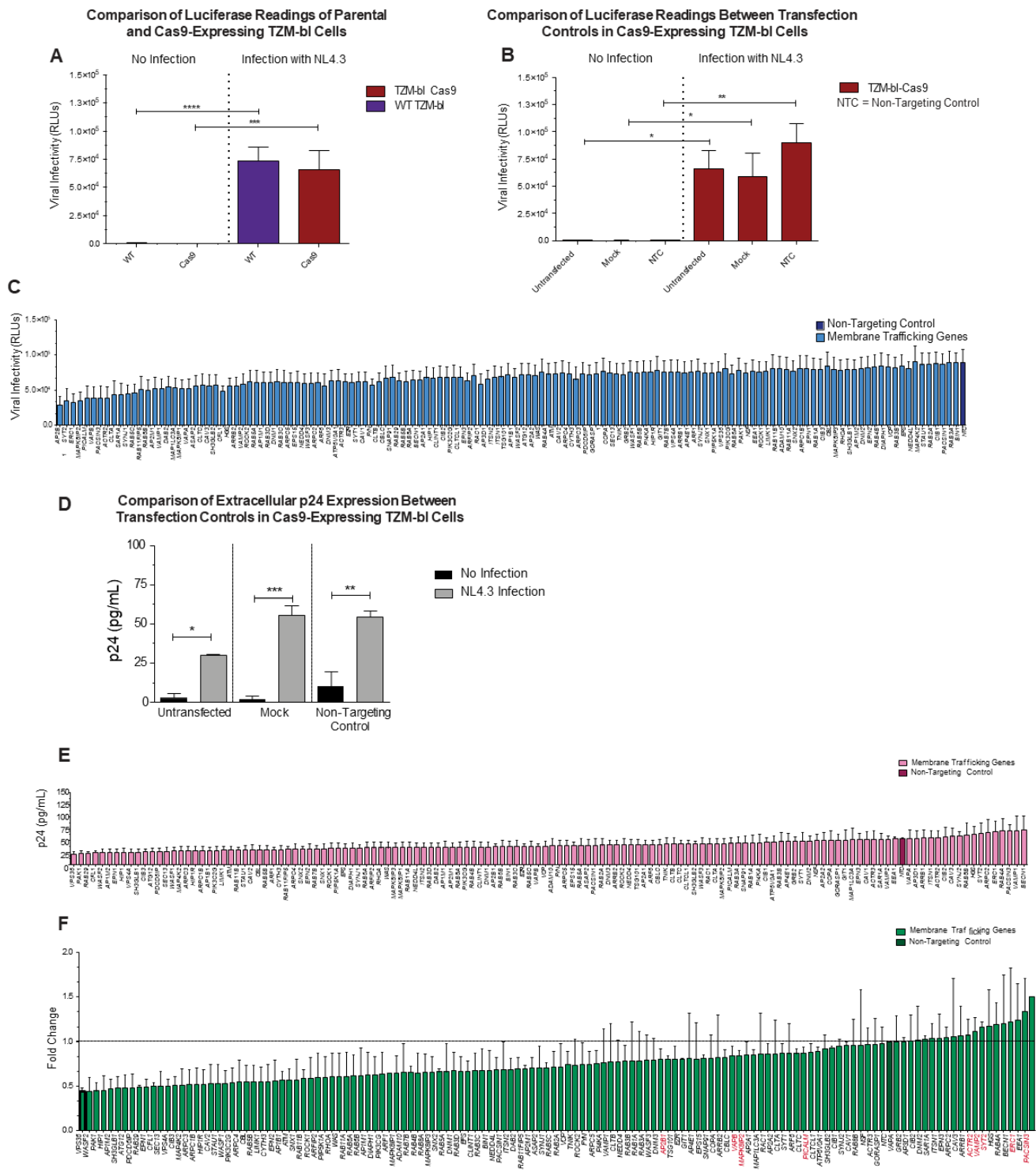


Figure 9. Viral infectivity and production of viral particle of membrane trafficking CRISPR screen knockouts. (A) Wild-type (WT) TZM-bl and TZM-bl-Cas9 were infected with NL4.3 or uninfected, and luciferase activity was measured. (B) TZM-bl-Cas9 were transfected with a non-targeting control crRNA (NTC), with transfection reagent only (mock), or left untransfected and either infected with NL4.3 or not infected, and luciferase activity was measured. (C) Viral infectivity of CRISPR screen knockouts infected with NL4.3 as measured using the TZM-bl luciferase assay. (D) TZM-bl-Cas9 were transfected with a non-targeting control crRNA (NTC), with transfection reagent only

(mock), or left untransfected and either infected with NL4.3 or not infected, and luciferase activity was measured. **(E)** Released virus particles of CRISPR screen knockouts infected with NL4.3 were measured using the extracellular p24 antigen capture assay. **(F)** Plot summarizing the fold change of knockouts compared to the NTC (dark green). In red are highlighted the 9 genes that the knockout reduced viral infectivity. Representative of two independent experiments. The dotted line is representative of the averaged NTC. One-Way ANOVA; * $p \leq 0.05$, ** $p \leq 0.01$ ***, $p \leq 0.001$. Retrieved from ¹⁴⁵.

5. Thesis rationale and objectives

1.1. Rationale

Even though HIV-1 has been around for more than 4 decades and is one of the most studied viruses in human history, there are still crucial loopholes that we need to close in order to get the full picture of the mechanisms that dominate HIV-1 infection with the goal of developing new strategies and therapeutic approaches. Considering that HIV-1 is an obligatory intracellular pathogen, host factors are usurped and are critical for all stages of its replication cycle. At the moment, evidence of interactions between HIV-1 and members of the membrane trafficking pathway exists but the complete network of these host proteins and their precise mechanisms of action assisting HIV-1 replication remains poorly understood. To better understand this network, we decided to apply a CRISPR screen targeting 140 membrane trafficking proteins to discover those that are essential for HIV-1 replication. This screen was previously performed by Kristin Davis, M.Sc. and in this study, we proceeded to then create stable knockout (KO) cell lines of the most promising candidates identified to elucidate the mechanisms by which these proteins impact HIV-1 replication.

1.2. Objectives

- 1.2.1. *Aim 1:* Generate stable knockout cell lines of the most promising candidates identified in the CRISPR-Cas9 screen in Sup-T1 CD4 T cells, which is a relevant cell line for the study of HIV-1 infection.
- 1.2.2. *Aim 2:* Analyze the effects of the different knockouts on HIV-1 infection to characterize and elucidate how these proteins take part of the HIV-1 replication cycle.

CHAPTER 2: MATERIALS AND METHODS

1. Cell Culture

HEK293T and TZM-bl cells were grown in Dulbecco's Modified Eagle's medium (DMEM) (Life Technologies) supplemented with 10% fetal bovine serum (FBS) (Invitrogen) and 1% penicillin and streptomycin (Invitrogen). TZM-bl cells (NIH AIDS Reagent Program, Cat #8129) are a HeLa-derived cell line expressing CD4, CCR5, and CXCR4, and have a luciferase gene cassette driven by the HIV-1 LTR. Human T-Cell Lymphoma Sup-T1 Cells (Sup-T1 cells) (NIH AIDS Reagent Program, Cat# ARP-100) are derived from human T-cell lymphoblast and are grown in Roswell Park Memorial Institute (RPMI) (Life Technologies) medium supplemented with L-glutamine (Sigma-Aldrich), 10% FBS and 1% penicillin and streptomycin. The knockouts were kept with RPMI + Puromycin (2 µg/mL). All cell lines were maintained at 37°C and 5% CO₂. Human CD4⁺ T cell cells were isolated from the PBMC fraction of healthy donors obtained from NetCAD (Canadian Blood Services), expanded in vitro using Dynabeads coated with anti-human CD3/CD28 antibody (1:1, bead:cell ratio, Life Technologies Cat #11131D) in RPMI1640 supplemented with 10% FBS (VWR Seradigm Cat #1500-500), 2 mM GlutaMAX (Gibco Cat #3050-061), 1 mM sodium pyruvate (Corning Cat #25-000-CI) and 10 mM HEPES (Sigma-Aldrich Cat #H4034). All work with human blood has been approved by the University of Manitoba Biomedical Research Ethics Board.

2. Generation of Cas9-expressing TZM-bl Cell line

In relationship to chapter 1 about the CRISPR screen of membrane trafficking genes performed by Krsitin Davis, we used a lentiviral vector to deliver the Cas9 nuclease to the TZM-bl cells. For that, we co-transfected HEK293T cells with the plasmids LentiCas9-Blast

(Figure 7A) (Addgene #52962), *Indiana vesiculovirus* G protein (VSV-G)¹⁴⁹ (AddGene #14888) and psPAX2 (Addgene #12260) using PEI (Polysciences). Viral supernatant were collected at 48 hours post-transfection and used to transduce TZM-bl with polybrene (Sigma-Aldrich). After 48 hours, cells were subjected to the blasticidin selection.

We tested different volumes of lentivirus to determine the best transduction efficiency, and we determined, by WB and Flow cytometry, that 300 uL was the optimum volume (viral titration was not done) to provide a homogenous population of Cas9-positive cells (99.6%) **(Figure 7)** with low cellular toxicity **(Figure 7B and 7C)**.

3. Arrayed Screening of the Membrane Trafficking Library and viral infectivity assay

The crRNA library consists of a panel of 140 human membrane trafficking genes (4 crRNAs per gene and 1 non-targeting control (NTC) crRNA) in an arrayed 96-well plate format for one gene-per-well analysis (Dharmacon™ Edit-R crRNA Library, Cat #GC-005505-01). Each crRNA and the associated tracrRNA were stored in 10mM Tris-HCl buffer pH 7.4 (Dharmacon™) at -20°C. TZM-bl-Cas9 cells were plated in 96 well plates (5×10³ cells/well in serum-free RPMI). The following day, cells were transfected with 20 µL of transfection mix, containing 25nM crRNA and tracrRNA (1:1), DharmaFECT 1 transfection reagent (Dharmacon™) diluted in serum-free RPMI and then, incubated for 24 hours at 37°C with 5% CO₂. After 24 hours, the serum-free RPMI was changed to complete media.

Viral infectivity was evaluated by infecting the transfected-TZM-bl -Cas9 cells, after crRNA/tracrRNA transfection described above, with NL4.3 (MOI 1) and evaluating the luciferase production. Briefly, cells were lysed, frozen at -80 °C for 1 hour, and then mixed with 1X Luciferase substrate (1M KPO₄, 1m MgSO₄, 1M DTT, 100 mM ATP, 10x Luciferin) and activity was measured in relative light units (RLUs) using MicroBeta® TriLux luminescence counter (PerkinElmer).

4. Cellular Viability Determination

Cellular viability was determined at 72 hours post-transfection of the crRNA library using the LIVE/DEAD™ Fixable Near-IR Dead Cell Stain Kit as recommended by the manufacturer (ThermoFisher Scientific, Cat #L10119). Following the viability staining, cells were removed with Trypsin and fixed with PFA 4% for 15 minutes at room temperature. Cells were stored in PBS at 4°C until analysis. Results and cell population statistics were acquired on a BD LSRFortessa™ cell analyzer (BD Biosciences).

5. CRISPR Editing of Sup-T1 Cells

gRNAs were cloned into the lentiCRISPRv2 vector (Addgene plasmid #52961), which expresses a mammalian codon-optimized *S. pyogenes* Cas9 and confers resistance to puromycin. HEK293T cells were co-transfected with LentiCRISPRv2¹⁵⁰, VSV-G, and psPAX2 using JetPRIME (Polyplus), as recommended by the manufacturer. Viral supernatants were harvested and filtered at 48 hours post-transfection and used to infect Sup-T1 cells by spinoculation (1800 rpm, 45 minutes, at room temperature). At 48 hours post-infection, cells were expanded from a single-cell culture and positively selected with 2 µg/mL puromycin (Invivogen) in order to generate monoclonal cell lines.

6. Western Immunoblotting

Cells lysates were collected in NP40 lysis buffer (50 mM Tris pH 7.4, 150 mM NaCl, 0.5 mM EDTA, 0.5% NP40), protein concentration was quantified by Bradford assay (Bio-Rad). Equal amounts of protein (20 µg) were separated by sodium dodecyl sulfate-polyacrylamide gel electrophoresis (SDS-PAGE) and transferred to a nitrocellulose membrane (Bio-Rad). Membranes were blocked (5% milk TBST), incubated with primary

antibody overnight at 4°C, and 1 hour with secondary HRP α -mouse or Rabbit (Rockland Immunochemicals), then developed using Western Lightning Plus-ECL (PerkinElmer) and signal was acquired using ChemiDoc (BioRad). Signal intensities were analyzed by densitometry using ImageJ software (NIH, Bethesda, USA).

7. HIV-1 NL4.3 and HIV Nef_CRMZY Viral Stocks and Infection

NL4.3 and HIV Nef_CRMZY virus particles were produced by transfecting HEK293T cells with the HIV-1 NL4.3 or HIV Nef_CRMZY + VSVg (to increase infectivity) provirus-encoding plasmid pNL4.3 using 1 μ L/ μ g JetPrime. Supernatants were collected 48 hours post-transfection, filtered through a 0.45 μ m pore-sized filter (Pall Corporation). Virus were concentrated by ultra-centrifugation (20,000 rpm for 1 hour at 4°C) and stored at -80°C. The viral titer was quantified using the X-gal staining assay in TZM-bl indicator cells as described previously in the literature ¹⁵¹ and used to determine the volume for the indicated MOI.

Sup-T1 cells expressing CXCR4 ¹⁵² were infected with NL4.3, an X4- (CXCR4) tropic virus ¹⁵³, or HIV Nef_CRMZY by spinoculation (1,800 rpm for 45 minutes at room temperature), and incubated for extra 2.5 hours and, then replenished with complete media. Cell and supernatants were collected at the indicated time points.

8. HIV-1 viral fusion assay

HIV-1 particles containing β -lactamase-Vpr (BlaM-Vpr) chimera proteins were produced by co-transfecting HEK293T cells with HIV-1 NL4.3 provirus-encoding plasmid pNL4.3, and pCMV-BlaM-Vpr DNA ¹⁵⁴ using PEI (Polysciences). Virus was collected after 48 hours and concentrated as described before. SupT1 cell lines were spinoculated with HIV-1 particles containing BlaM-Vpr. After a 2-hour incubation at 37°C, the cells were washed

with CO₂-independent medium (Invitrogen) and incubated with 1X loading solution (CCF2/AM substrate, Invitrogen), for 1 hour protected from light. After washing, cells were fixed with PFA 1% for 30 minutes. The levels of CCF2/AM and its cleaved products were measured by flow cytometry.

9. Antibodies and fluorescent probes

Primary antibodies used were as follows: mouse anti-p24 (IF, 1:250; WB, 1:10,000; NIH AIDS ARRPP); sheep anti-p17 polyclonal serum (IF, 1:250; NIH AIDS ARRPP), LC3B (IF, 1:250; Cell signaling technology, cat# 2775S), mouse anti-Lamp1 (IF, 1: 50; Abcam cat# ab25630), sheep anti-Digoxigenin-AP, Fab fragments (IF, 1:250; Roche #11093274910). For IF, secondary antibodies used were as follows: Donkey anti-Sheep IgG (H+L) Cross-Adsorbed, Alexa Fluor® 488 (1:500; Invitrogen-Thermo Fisher Scientific #A-11015); Donkey anti-Rabbit IgG (H+L) Highly Cross-Adsorbed, Alexa Fluor® 594 (1:500; Invitrogen-Thermo Fisher Scientific #A-21207); Donkey anti-Mouse IgG (H+L) Highly Cross-Adsorbed, Alexa Fluor® 647 (1:500; Invitrogen-Thermo Fisher Scientific #A-31571); Donkey anti-Rabbit IgG (H+L) Highly Cross-Adsorbed, Alexa Fluor® 647 (1:500; Invitrogen-Thermo Fisher Scientific #A-31573); Donkey anti-Mouse IgG (H+L) Highly Cross-Adsorbed, Alexa Fluor® 594 (1:500; Invitrogen-Thermo Fisher Scientific #A-21203). For western blotting, secondary antibodies used were goat anti-mouse or goat anti-rabbit IgG polyclonal antibodies conjugated to horseradish peroxidase¹⁵⁵ (Rockland Immunochemicals).

10. Immunofluorescence

Immunofluorescence (IF) analyses were performed exactly as described previously¹⁵⁶. Briefly, for suspension cells, sterile 18 mm ø No. 1 cover glasses (VWR) were treated with 0.1 % poly-L-lysine solution (Sigma) overnight at 4°C. Cover glasses were dropped into

wells, and 4×10^5 WT or KO cell lines were allowed to settle onto these for 1 hour at 37 °C prior to fixing cells onto cover glasses. For fixing cells onto cover glasses, cells were washed once in D-PBS (Wisent) and fixed with 4% paraformaldehyde for 15 minutes. Fixed cells were then washed with D-PBS, quenched in 0.1 M glycine for 10 minutes, washed with D-PBS, permeabilized in 0.2% Triton X-100 for 5 minutes and washed twice with D-PBS. Cells were briefly washed in PBS before being blocked in 1 X blocking solution¹⁵⁷. Primary antibodies were applied for 1 hour at 37 °C, and then washed for 10 minutes in PBS followed by secondary antibodies for 1 hour. Cells were washed for 20 minutes in PBS before being mounted on glass slides using ProLong Gold Antifade Reagent with DAPI (Life Technologies). Negative isotype-matched antibodies were used to control staining specificity.

11. Microscopy and imaging analyses

Laser confocal microscopy was performed using a Leica DM16000B microscope equipped with a WaveFX spinning disk confocal head (Quorum Technologies) and HCX PL APO / 40X, Oil / 0.75-1.25 NA CS and HCX PL APO / 63X, Oil / 0.60-1.40 NA BL objectives, and images were acquired with a Hamamatsu EM-charge coupled device digital camera. Images were recorded from laser-scanned cell layers with a thickness of 1 μm and were digitized at a resolution of 1024×1024 pixels. For multi-color image capture, AlexaFluor-647, -594, 488, conjugated secondary antibody emissions were sequentially captured with 665-715, 570–620, and 500–550, bandpass filters, followed by 435–485 nm [for 4',6-diamidino-2-phenylindole (DAPI) staining] followed by differential image capture¹⁵⁵ image capture. Raw .liff files were exported by the Volocity software (Perkin Elmer) for import into Imaris software v. 9.6.0 (Bitplane/Oxford Instruments) used for generation of colocalization channels, and .xlsx file exports of quantitative measurements of mean signal

intensity values used for downstream data harmonizing and statistical analyses using Excel (Microsoft) and GraphPad v9 (Prism), respectively.

12. Flow cytometry staining and acquisition.

Cells were collected at the indicated time points. Prior to staining, cells were incubated in Fc blocker (BD Biosciences, catalog #564220) and Fixed Viability Stain 510 (BD Biosciences, catalog #564406) or Zombie NIR (Biolegend, #423106) for 15 min at room temperature, followed by incubation with antibodies (Table S3) for 30 min at room temperature. Cells were then fixed with 1% paraformaldehyde (PFA) for 30 min. For the intracellular staining, cells were permeabilized and fixed with CytoFix/CytoPerm™ kit (BD Bioscience) prior to staining with intracellular markers and after extracellular staining. For the analysis of cell surface vs whole cell, the extracellular staining in the whole cell group was performed after the permeabilization. An average of 100,000 cells were analyzed using a 4-laser LSR Fortessa (BD Biosciences) or using, where indicated, the Spectral Cytometer Sony ID7000 at the Flow Cytometry Core Facility, Lady Davis Research Institute. Single stain controls for each fluorochrome were prepared using Compensation Beads (BD Biosciences, catalog #552843) or UltraComp eBeads™ (ThermoFisher). Data was analyzed using FlowJo V10 (Tree Star).

13. Construction, validation and usage of the HIV Nef-CRIMZY reporter.

The E2-Crimson-EF1a-ZsGreen DNA insert was amplified from the Hi.Fate latency plasmid ¹⁵⁸ using primers 5'-TGC ACG CGT GGA GGG GGC GGT ATG GAT AGC ACT GAG AAC G-3' and 5'-GCT ACC CGG GTC AGG GCA AGG CGG AGC CGG AGG CG-3' by PCR, and inserted into the R5-tropic 'HIV-GFP' proviral vector ¹⁵⁹ using unique restriction enzyme sites XmaI ^{155 R0180S} and MluI ^{155 R0198S}. A flexible 4 amino acid linker

DNA was added between Nef and E2-Crimson. The resulting plasmid, termed ‘HIV Nef-CRIMZY’, was sequenced on both strands before transfection into HEK293T cells. Viral supernatant was collected and concentrated by ultracentrifugation, as previously described¹⁵⁹. Viral stocks were titrated using MAGI.CCR5 and expressed as blue forming units (b.f.u.) per ml.

14. Quantification and statistical analysis

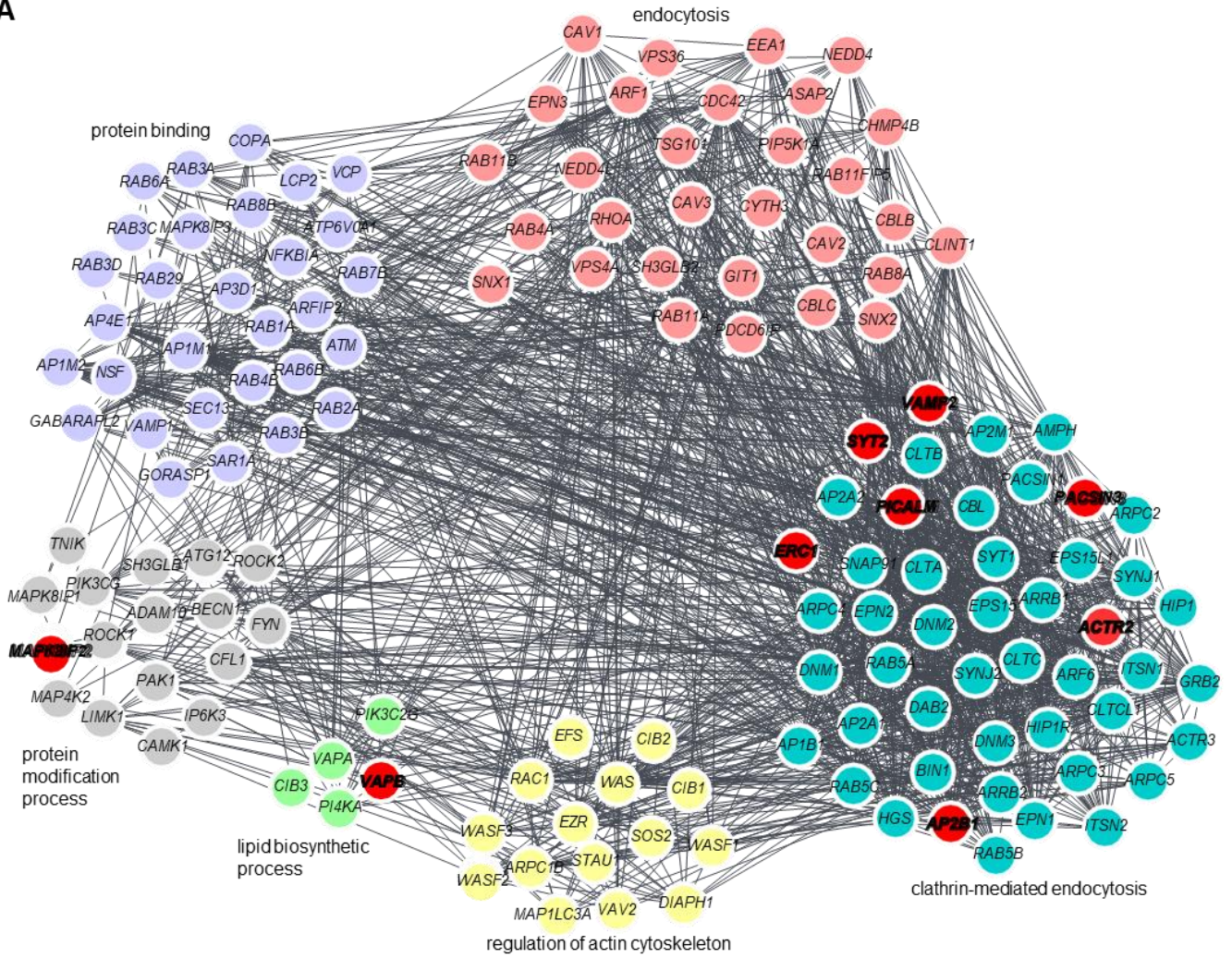
All experiments were performed in triplicate with similar results, unless otherwise indicated in figure legends as n=#. Two independent observers validated phenotypes resulting from all experimental conditions tested. Cellular imaging statistics reported for mean fluorescence (MFI) are from observation of average of n = 130 cells per condition tested. Statistical analyses were performed using Prism V6.01, GraphPad, where one-way ANOVA (with Tukey's post-test) and 95% CI was used for multiple comparisons, and an unpaired 2-tailed student's t test with 95% CI was used to compare two groups. Data are presented as mean \pm SEM or SD, as indicated in figure legends, and P-values of less than 0.05 were considered to indicate a statistically significant difference.

CHAPTER 3: RESULTS

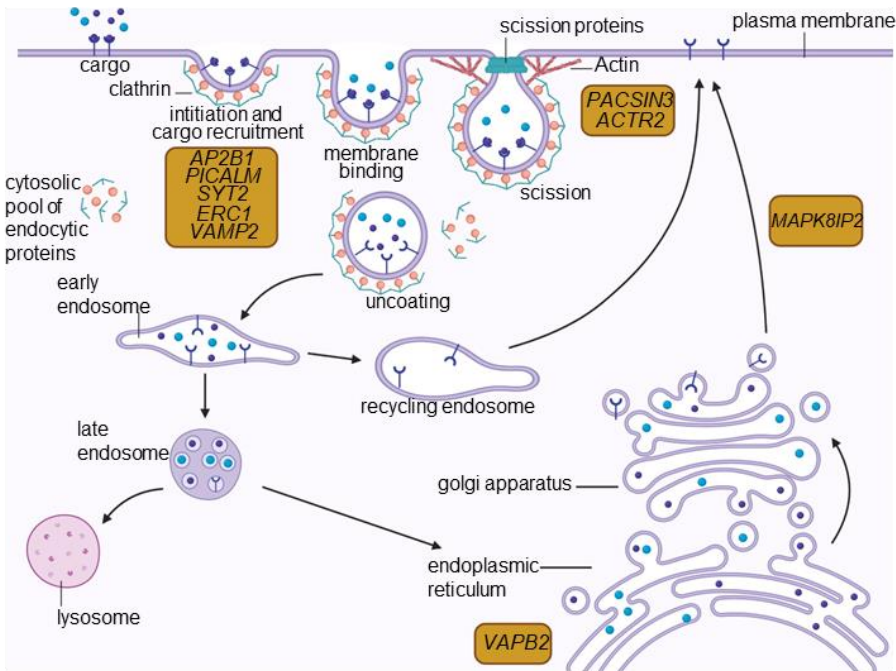
1. The identified CRISPR screening hits are involved in clathrin-mediated endocytosis and autophagy to alter infectivity

Our screen identified nine genes as necessary cofactors for HIV-1 replication. We used the Search Tool for the Retrieval of Interacting Genes (STRING) and Cytoscape software to visualize their interaction networks, revealing that an overwhelming majority of our hits (7/9) are well-known cofactors of clathrin-mediated endocytosis (**Figure 10A**). These findings highlight the importance of clathrin-mediated endocytosis for the HIV-1 replication cycle likely facilitating virus ingress (**Figure 10B**). It is worth mentioning that *CLTA* (i.e., clathrin light chain A), another essential gene in clathrin-mediated endocytosis which knockout also showed a significant lower HIV-1 infectivity (**Figure 8G**) was left out of this study since it has already been shown to be involved in the early stages of HIV-1 replication⁵⁷ and since homozygous *CLTA* KO mice are frequently non-viable¹⁶⁰. Unlike many other enveloped RNA viruses, HIV-1 entry has been shown to be pH-independent, and rather relies on direct hemi-fusion with the plasma membrane for access to the cytoplasm¹⁶¹. Nonetheless, several lines of evidence support that in certain cell types, HIV-1 may also require endocytic support for cellular entry. Indeed, HIV-1 has been shown to engage in vesicular-mediated endocytosis in both macrophages^{162,163} and T cells¹⁶⁴⁻¹⁶⁶. Mechanisms of HIV-1 endocytosis remain highly controversial as it is still unclear which host factors take part in the process. Our KO screen results broaden our knowledge of how clathrin cofactors may contribute to this mechanism, revealing a cluster of seven genes identified that jointly contribute to clathrin-mediated endocytosis (**Figure 10A,B**)⁷⁸. These results imply that HIV-1 may depend on the coordinated actions of all these gene products, such that the depletion of one may significantly interfere with this entire pathway.

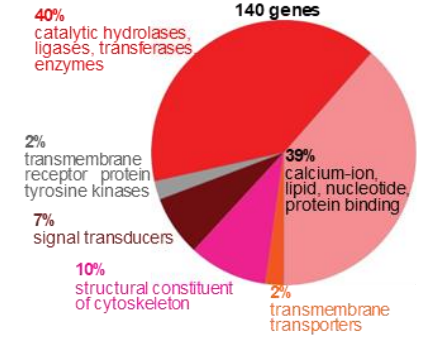
A



B



C



D

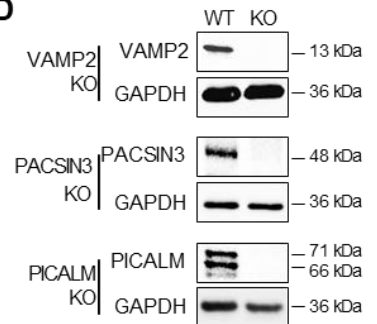


Figure 10. Protein interaction network of CRISPR screen hits and stable KO cell lines. ¹ The network of protein-protein interactions was obtained with the Search Tool for the Retrieval of Interacting Genes (STRING) tool and Cytoscape software. Genes are represented as colorful nodes. Genes clustering in clathrin-mediated endocytosis are denoted in the cyan bubble. **(B)** Candidate genes from KO screen with putative roles in the HIV-1 replication cycle are denoted within yellow rectangles at their established subcellular localization. Created with BioRender.com **(C)** Pie chart representing PANTHER GO subcategories from enrichment analysis of the 140 membrane trafficking genes. **(D)** Western blot depicting successful stable PICALM, VAMP2 and PACSIN3 knockout (KO) cell lines using wild-type (WT) Sup-T1 T cells, as confirmed using specific antibodies. Retrieved from Guizar et al ¹

There is however accumulating evidence that some of these proteins also mediate non-endocytic effects that can have an influence on cellular functions linked to membrane biology, including autophagy ¹⁶⁷, as recapitulated by PANTHER GO tool-mediated enrichment analysis **(Figure 10C)**. It has been observed that the inhibition of clathrin-mediated internalization affects the formation of mature autophagosomes since the plasma membrane¹⁵⁵ directly contributes to the formation of early VAMP2-positive autophagosome precursors¹⁶⁸. In addition, it is well established that as one of the three main proteins of mammalian endocytic clathrin coated vesicles (CCVs) (i.e., clathrin, AP2, and PICALM), PICALM modulates the autophagic degradation of Tau, the protein causatively linked to Alzheimer's disease ^{71,73}. Indeed, the down regulation of PICALM has been observed to affect autophagosome degradation and results in a larger number of autophagosomes as represented by increased LC3B-II expression ⁶⁹.

2. PICALM regulates several stages of HIV-1 replication.

To validate and explore the effects of the CRISPR screen hits in the context of the HIV-1 replication cycle, we genetically altered the nine gene hits in a more biologically relevant CD4⁺ Sup-T1 T lymphoblastic cell line. As the CRISPR-Cas9 mediated KO of *AP2B1*, *ERCI*, *SYT2*, *MAPK8IP2*, *ACTR2* and *VAPB* resulted in non-viable cells, these genes were not pursued further. The CRISPR-Cas9 mediated KO of *VAMP2*, *PACSIN3* and *PICALM* did however successfully generate viable cell lines, as confirmed by Western

blotting (**Figure 10D**). The *VAMP2* and *PACSIN3* proteins were represented by single bands in western blots, while WT Sup-T1 provided two anti-PICALM detectable protein bands. Indeed, while four PICALM isoforms have been identified (i.e., isoforms 1–4: NCBI RefSeq: NP_009097.2, NP_001008660.1, NP_001193875.1 and NP_001193876.1, respectively) ⁷⁶, we could only detect two of these in Sup-T1 cells using western blotting (**Figure 10D**), with the top 71 kDa band representing isoform 1 and the lower 66 kDa band represents isoform 2 ¹⁶⁹, and both isoforms successfully knocked out by the CRISPR sgRNAs.

To confirm the effect of the KO in virus expression, we performed immunofluorescence (IF) for HIV-1 Gag and fluorescence in situ hybridization ¹⁵⁵ permitting visualization the full-length vRNA ¹⁷⁰ in WT HIV-1 NL4-3 infected *VAMP2*, *PACSIN3* and *PICALM* KOs. In parallel, we noticed that those proteins play a role in regulating membrane trafficking ^{66,106,171,172} and autophagy ¹⁰⁵ (**Figure 10B**), then we stained for Lamp-1 and LC3B-II as well (**Figure 11A-C**).

At the initial steps of autophagosome formation, the microtubule associated protein 1 light chain 3 (MAP1LC3; LC3B-I) is cleaved and lipidated to generate LC3B-II ¹⁷³, which initiates autophagy with autophagosome formation. Previous work has demonstrated increased expression of LC3B-II in HIV-1-infected primary CD4⁺ T cells ^{174,175}. However, HIV-1 has been shown to inhibit autophagosome maturation (i.e., fusion) with lysosomes to prevent the targeting and degradation of viral proteins via autophagy ¹⁷⁶⁻¹⁷⁸.

The staining for LC3B-II and Lamp-1 is used to evaluate autophagy and the treatment of coverslips with saponin removes the LC3B-I (cytosolic), allowing evaluation of only LC3B-II membranes-bound. Therefore, the increase in MFI for LC3B-II suggest autophagosome formation and the co-localization with Lamp-1 suggest autophagosome-lysosome fusion. We observed that while all three KOs had effect on the expression of endosomal proteins (e.g., increased Lamp1 and Lamp-LC3B-II colocalization by *PACSIN3*

KO), the *PICALM* KO cells had the most interesting phenotype. We saw increased LC3B-II expression ($p < 0.0001$) and Gag expression ($p < 0.0001$) and increase in their co-localization, in addition to reduced co-localization of Lamp-1 and LC3B-II (**Figure 11A-C**). These data together suggest that *PICALM* could potentially play a role in regulating autophagy during HIV-1 infection.

We further confirmed that only *PICALM* KO had increased Gag expression by WB, and p24 in the supernatant by ELISA (**Figure 11D-F**). From these experiments we found that *PICALM* KO cells had the most striking effects on HIV-1 infection and replication kinetics, thus becoming the focus of the rest of this study.

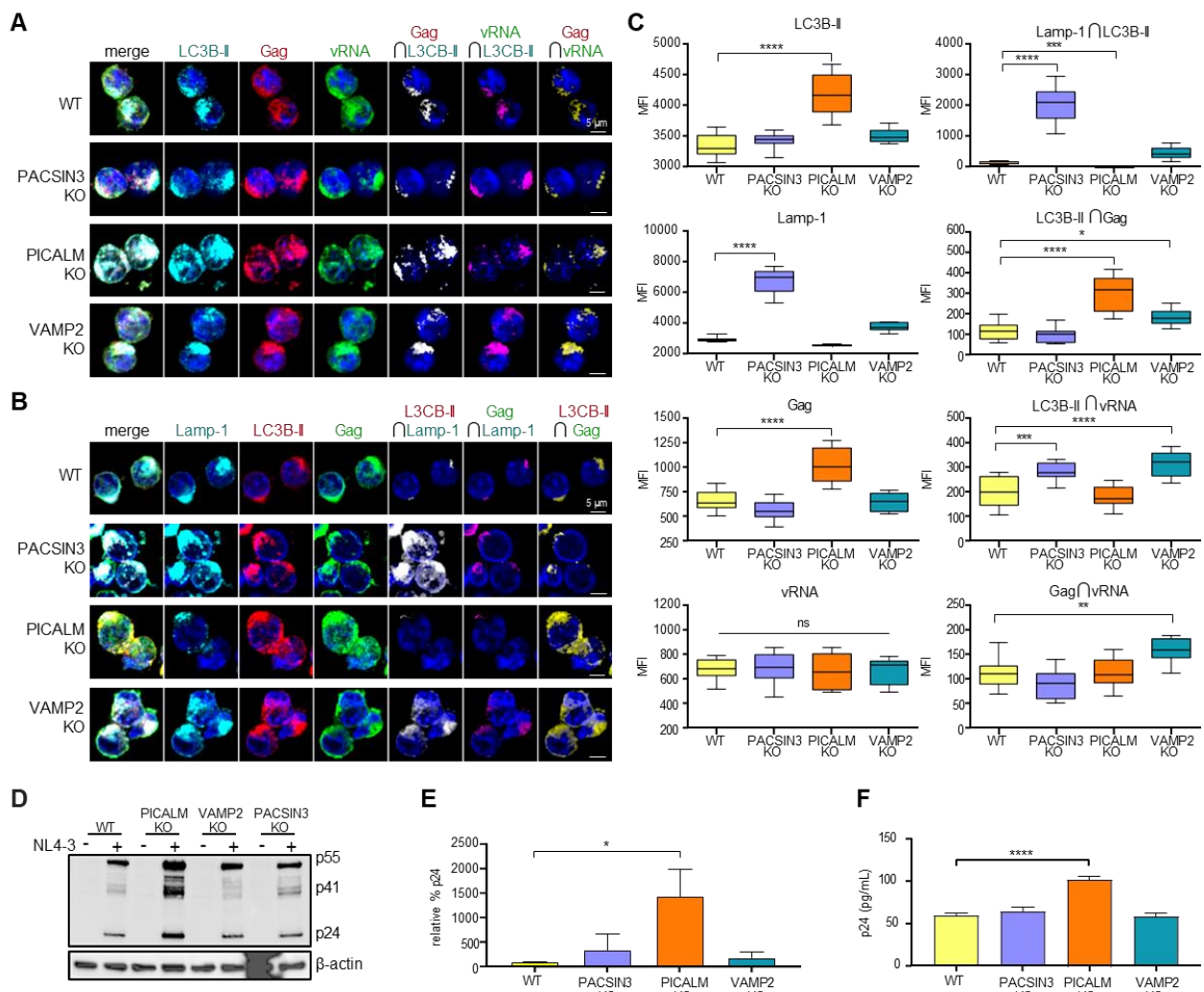


Figure 11. KO alter virus entry and the expression of HIV-1 Gag and autophagy proteins Lamp1 and LC3B-II. (A-B) KO cell lines were infected with WT NL4-3 provirus (MOI=5; n=3) for 48 hrs. Cells were treated with 0.1% saponin to deplete LC3B-I from cells. Cells were collected for FISH analysis for the HIV-1 vRNA and immunofluorescence for HIV-1 Gag protein and host proteins LC3B-II and Lamp1. (C) Corresponding box plots demonstrate that PACSIN3 KO caused increased Lamp1 and its colocalization with LC3B-II. LC3B-II colocalization with the vRNA is also increased in PACSIN3 KO. PICALM KO caused increased LC3B-II expression, increased Gag expression, along with increased LC3B-II colocalization with Gag. VAMP2 KO caused increased Lamp1, and increased colocalization between LC3B-II and Gag, LC3B-II and the vRNA, and Gag and the vRNA. LC3B-II colocalization with Lamp1 in the PICALM KO is shown but it is juxtaposed with the x-axis since it is particularly low. (D) Lysates were collected and immunoblotted for Gag p55 and p24. (E) Bar graph from data in (D). In parallel, culture supernatant was collected and (F) virus were determined by ELISA p24. One-Way ANOVA; * $p \leq 0.05$, ** $p \leq 0.01$ ***, $p \leq 0.001$, **** $p \leq 0.0001$. Error bars from bar graphs indicate standard deviation (SD). MFI, mean fluorescence intensity; %, percent; rel., relative; UI, uninfected; Inf., infected. Ω , colocalization (i.e., intersection); KO, knock out; μm , micrometer. Retrieved from Guizar et al ¹.

3. PICALM KO supports enhanced HIV-1 replication usurping the autophagy machinery

We initially identified PICALM as a protein important for the infectivity of HIV-1 (Figure 8G) in the model of Cas9-TZM-bl infected cells, and further observed a possible role in regulating autophagy (Figure 11A-C), which could be related to the regulation in HIV-1 expression in SupT1 (Figure 11D-F). Thus, we queried if the SupT1 PICALM KO could modulate virus uptake by inhibiting HIV-1 fusion and infection. For this purpose, HIV-1 fusion with the PICALM KO cells was examined using the gold-standard β -lactamase (BlaM) activity assay that quantifies viral fusion ¹⁷⁹. It provided evidence that the PICALM KO had reduced virus fusion tantamount to inactivated (Inact.) virus (Figure 12A-B), but with no concomitant perturbation of cell surface expression of CD4 and CXCR4 in KO relative to WT cells (Figure 12C-D), despite lowered CD4 expression by HIV-1 infection serving as an internal control for infection. These results support a role for clathrin-mediated endocytosis in productive HIV-1 entry, as shown previously in investigations demonstrating that HIV-1 co-opts clathrin adaptors to mediate entry into cells through CD4/co-receptor-mediated endocytosis ^{164,180,181}.

We observed previously that PICALM KO had an increase in LC3B-II expression by IF and reduced co-localization with Lamp-1 (**Figure 12A-C**). Therefore, we speculated that PICALM KO might have a direct effect on autophagy, and consequently on HIV-1 infection. As autophagy kinetics can vary across cell lines, Bafilomycin A1 (BAF A1; BAF) is commonly used to evaluate autophagy flux because it inhibits the H⁺ vATPase to blunt autophagosome-lysosome acidification, thereby abrogating the degradation of the content, allowing identification by IF¹⁵⁵. In general, the co-localization of LC3B-II and LAMP1 suggests autophagosome-lysosome fusion typically leading to the degradation of autophagic targets. In the context of BafA1 treatment, the increased co-localization of Lamp-1 and LC3B-II suggest that autophagy flux is intact.

Thus, to evaluate further the role of PICALM in autophagy flux, we infected WT and PICALM KO cells, as described before, and before harvesting, cells were treated with BafA1 for 2 hours. We evaluated LC3B-II and LAMP1 and we observed significant changes in the expression levels of autophagy proteins in PICALM KO cells. First, we observed, as shown previously, that the expression of LC3B-II is increased in PICALM-infected cells relative to WT levels (**Figure 12F, H**). In parallel, the expression of Lamp1 was reduced (**Figure 12B, G**), leading to a reduced co-localization of Lamp-1 and LC3B-II ($p < 0.0005$) (**Figure 12F-I**), which suggest that autophagy levels flux is impaired. However, the treatment with Bafilomycin A1 revealed the opposite, the co-localization increased in PICALM KO compared to WT Baf A1 treated (**Figure 12F-I**), suggesting that autophagy flux in PICALM KO is even higher than WT cells. The increased autophagy flux would lead to a fast degradation of the contents in lysosomes, explaining why initially the levels of Lamp1 are reduced in PICALM KO. In summary, this data suggests that PICALM KO cells have an increased autophagy flux related to WT. In addition to the increased co-localization of Gag

and LC3B-II and increased overall Gag, these data provide a mechanistically link of viral replication and autophagy in CD4⁺T cells.

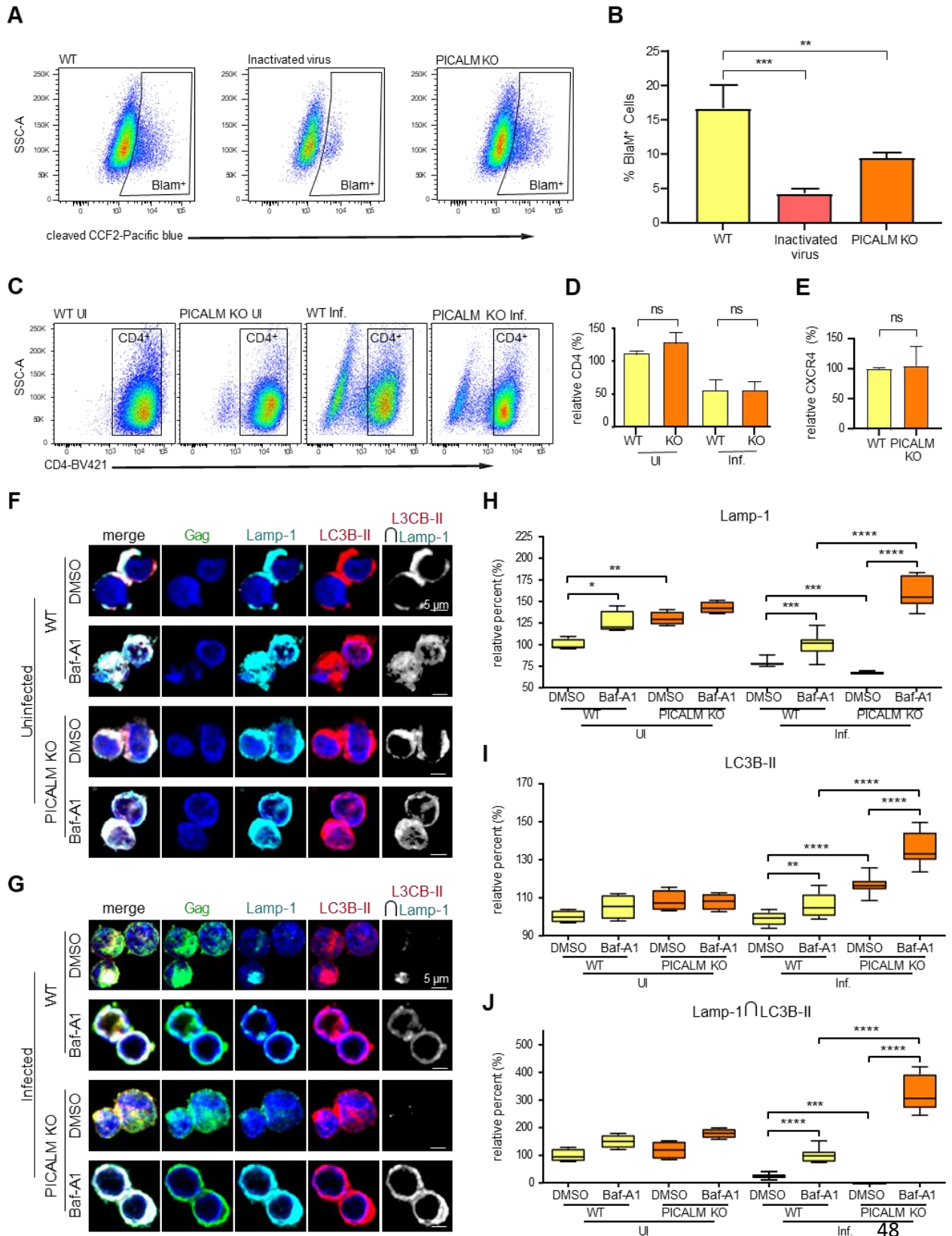


Figure 12. PICALM KO increases expression and colocalization of virus and autophagy proteins, can produces more virus, but have diminished infection rates. (A-B) WT and PICALM KO cell lines were infected with WT NL4-3 or -heat-inactivated virus containing BlaM-Vpr (MOI=1) for 2 hours and virus fusion was evaluated by the expression of cleaved CCF2 (acquired in Pacific blue channel, LSR Fortessa BD biosciences). (A) Representative dot plots and (B) bar graphs of % of cells + for cleaved CCF2 (BlaM +). (C-D) WT and PICALM KO cells were infected with NL4.3 for 48 hours and CD4-BV421 expression were analyzed by Flow cytometry. (E) Data representative of uninfected WT and PICALM KO stained for CXCR4 BB700.¹⁵⁵ WT and PICALM KO were infected with NL4.3 for 48 hours (MOI 5, n=3), and 2 hours before harvesting, treated with BafA1 (100 nM), then collected for IF, coverslips were treated with 0.1% Saponin to deplete free cytoplasmic LC3BI, then stained for Gag (AF488), Lamp-1 (AF647), LC3B (AF594) and DAPI. (F-G) Representative images and plotted data showing (H) Lamp-1, (I) LC3B-II expression, and (J) Lamp-1 and LC3B-II co-localization. Relative values (%) were calculated by setting WT values to 100%. ¹⁴⁶μm, micrometer; KO, knock out; ∩, colocalization (intersection); UI, uninfected; Inf., infected. ∩, colocalization (i.e., intersection). *, p < 0.05; **, p < 0.01; ***, p < 0.001; ****; 1-way ANOVA, Tukey post-test. Retrieved from Guizar et al ¹.

4. Absence of PICALM leads an activated T effector memory phenotype deficient in PD-1 cell surface protein expression.

We consistently observed that PICALM KO cells appeared healthier and larger with a higher proliferative capacity compared to other KOs and WT cells. To validate these observations, we used flow cytometry to analyze the expression of proliferation marker Ki67, which was found to be increased in PICALM KO cells relative to WT cells, and which could be rescued to WT levels by transfecting cells with a PICALM expression construct (**Figure 13A**). Since Ki67 also represents an activation marker ¹⁸², we decided to investigate whether PICALM KO cells also displayed increases in other activation markers ¹⁸³. Indeed, early activation marker CD69 was also increased in PICALM KO cells independent of HIV-1 infection (**Figure 13B**). PD-1 is also another molecule that is rapidly co-expressed and upregulated in conjunction with CD69 ¹⁸⁴, but it was surprisingly found to be markedly decreased in both infected and uninfected PICALM KO cells (**Figure 13C**), as validated by a different anti-PD-1 antibody (**Figure 13D**). Due to the linkage between interferon-gamma (IFN-γ) and the PD-1/PD(L)-1 axis, we next analyzed PD-1 observing that it was increased in

PICALM KO cells (**Figure 13E**), as supported by reports indicating that it can lower PD-1 expression¹⁸⁵.

Next, because of PICALM's roles in endosomal pathways, we were curious to see if decreased PD-1 was due to defects in endosome recycling. We thus analyzed the distribution of PD-1 and other key molecules both at the cell surface and within cells by staining both permeabilized and non-permeabilized cells. Indeed, while PD-1 expression is decreased on PICALM KO cell surfaces, its expression levels are relatively unchanged within whole cells (**Figure 13F**). While CD4⁺CD25⁺ T regulatory cells (Tregs) are a population known to retain intracellular PD-1, we could rule this out from observations that PICALM KO cells had significantly diminished CD25 expression, despite an increased surface expression of this molecule as expected by HIV-1 infection (**Figure 13G**).

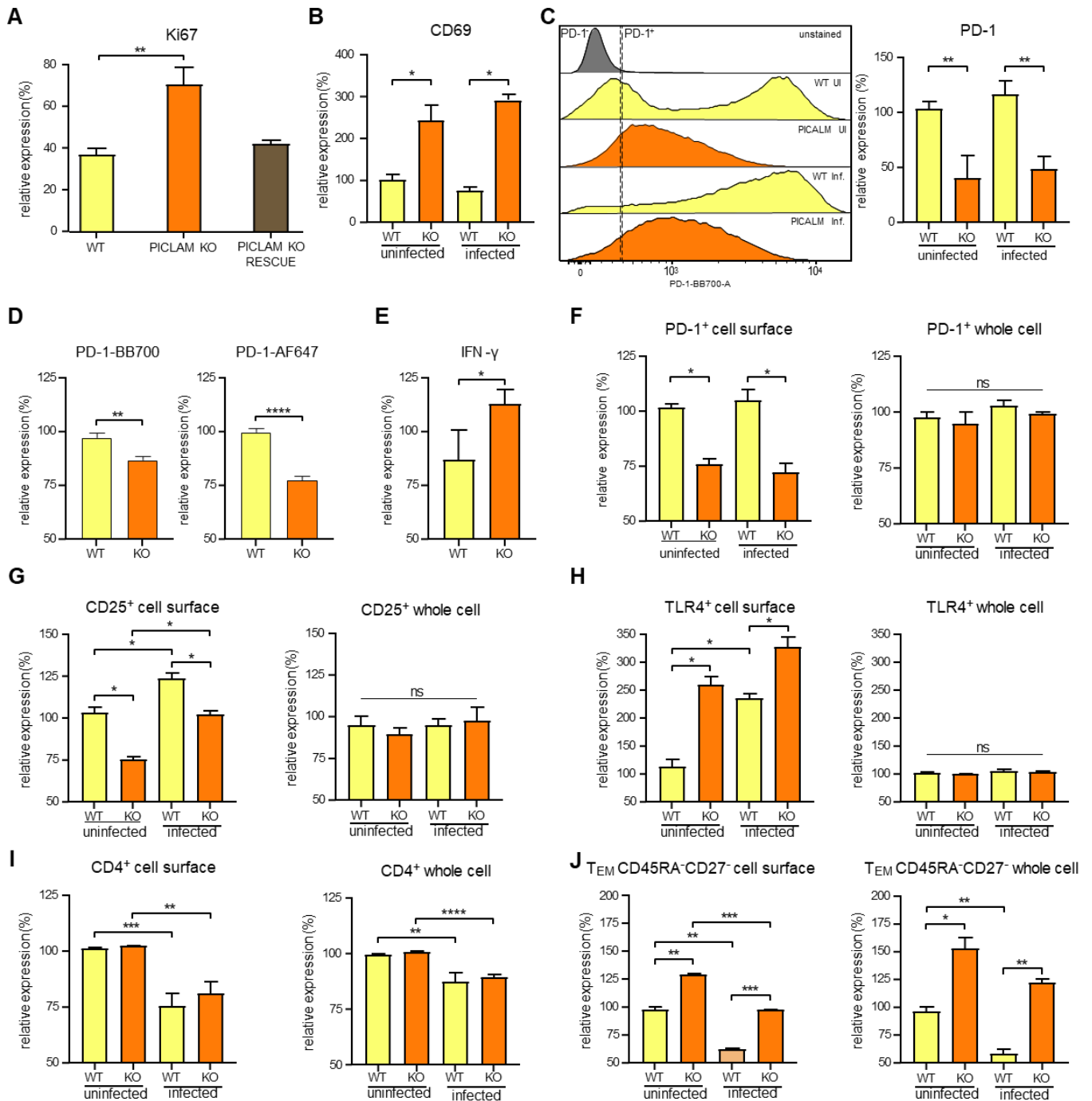


Figure 13. PICALM KO causes increased cell proliferation, deregulates activation and PD-1 pathways, and leads to a T effector memory-like phenotype. (A) WT, PICALM KO T cells and PICALM KO T cells transfected with a PICALM protein expressing ‘rescue’ plasmid. Flow cytometry was used to assess cell surface expression of Ki67, demonstrating that PICALM cells have increased propensity to proliferate. (B-C) WT and PICALM KO T cells were infected with WT NL4-3 virus (MOI=5) for 48 hrs. Cells were analyzed for cell surface expression of PD-1 and CD69 expression flow cytometry, demonstrating that PICALM KO reduces expression of PD-1, and increases that of CD69, independently of virus infection. (D) Flow cytometry was used to assess cell surface expression of PD-1 of PICALM KO cells using two different antibodies, validating that PICALM KO decreases PD-1

expression. (E) Flow cytometry was used to assess expression of INF- γ of PICALM KO, demonstrating that PICALM KO increases INF- γ expression. (F-J) WT and PICALM KO T cells were infected with WT NL4-3 virus (MOI=5) for 48 hrs. Cells were analyzed for both cell surface expression and overall cellular expression of numerous immunological biomarkers using a cell permeabilization staining flow cytometry protocol. Bar graphs demonstrate that PICALM modulated expression of both PD-1 (F), CD25 (G), and TLR4 (H) is cell surface dependent. (I) CD4 was also analyzed by this assay, demonstrating that both cell surface and whole cell CD4 are downregulated by HIV-1 infection, but that CD4 levels are unaffected by PICALM KO in either case. (J) Analysis of CD45RA and CD27 provides evidence that PICALM KO induces cells polarization to a CD45RA⁻CD27⁻ T_{EM}-like phenotype. *, p < 0.05; **, p < 0.01; ***, p < 0.001; ****, p < 0.0001; 1-way ANOVA, Tukey post-test. Retrieved from Guizar et al ¹.

To reexamine the possibility that the PICALM KO modulates cell surface PD-1 through a defect in endocytosis, we examined the TLR4 receptor, known to be a substrate for via clathrin-mediated endocytosis ¹⁸⁶, and whose internalization and signaling can be abolished by direct inhibition of clathrin-dependent pathways ¹⁸⁷. Indeed, we did observe that TLR4 is maintained at the cell surface in PICALM KO cells (**Figure 13H**), whereas CD4 is unaffected by the PICALM KO (**Figure 13I**). Finally, to determine whether PICALM KO induces pleiotropic effects blocking cell differentiation and polarization, we analyzed common cell surface CD45 and CD27 markers, demonstrating that the PICALM KO polarized CD4⁺ T cells towards a CD45RA⁻CD27⁻ T_{EM}-like phenotype ¹⁸⁸ (**Figure 13J**). Together, these results suggest that PICALM KO cells may have impeded endocytic pathways maintaining a functional, activated, and proliferating T_{EM} memory-like phenotype.

5. Absence of PICALM reduces HIV-1 latency

PICALM KO led to increased Gag expression and virus production (**Figures 11 and 12**), while these cells also exhibited increased activation and proliferation markers. Considering that a PD-1 blockade potentiates HIV-1 latency reversal ¹⁸⁹, we wondered whether decreased levels of PD-1 in PICALM KO would induce a reduction in latency thereby promoting Gag expression and virus production. For this determination, we used a

full-length dual fluorescent HIV-1 reporter system capable of quantifying both productively and latently infected cells longitudinally. This reporter contains a Nef-Crimson fusion protein under the control of the HIV-1 LTR promoter, and ZsGreen1 under the control of the mammalian EF1a promoter (called HIV Nef-CRIMZY; **Figure 14A**). To validate the ability of the HIV Nef-CRIMZY to identify latently infected cells, primary CD4⁺ T cells were prepared and then activated and expanded in culture for seven days and then infected with HIV Nef-CRIMZY viruses at an MOI of 0.1 in 3D collagen gels¹⁹⁰. These cells were analyzed five days later using flow cytometry for productive or latent infection. Populations of either productively infected cells (Nef-Crimson^{hi}ZsGreen1^{hi}) or latently infected cells (Nef-Crimson^{neg}ZsGreen1^{hi}) were clearly distinguishable. Importantly, both Env and Nef proteins are functional, as extensive CD4 downregulation is observed in productively infected (p24^{hi}), but not in latently infected (p24^{neg}), T cells (**Figure 14B**). Indeed, infecting cells with this reporter provided evidence that PICALM KO SupT1 CD4⁺ T cells could persistently limit the percentage of cells latently infected (Crimson⁻ZsGreen⁺) over several days (i.e., days 1 to 15) (**Figure 14C-D**). These data suggest that the PICALM KO induces a cellular phenotype that favors replication over latency by reducing clathrin-mediated endocytosis of particular cellular markers.

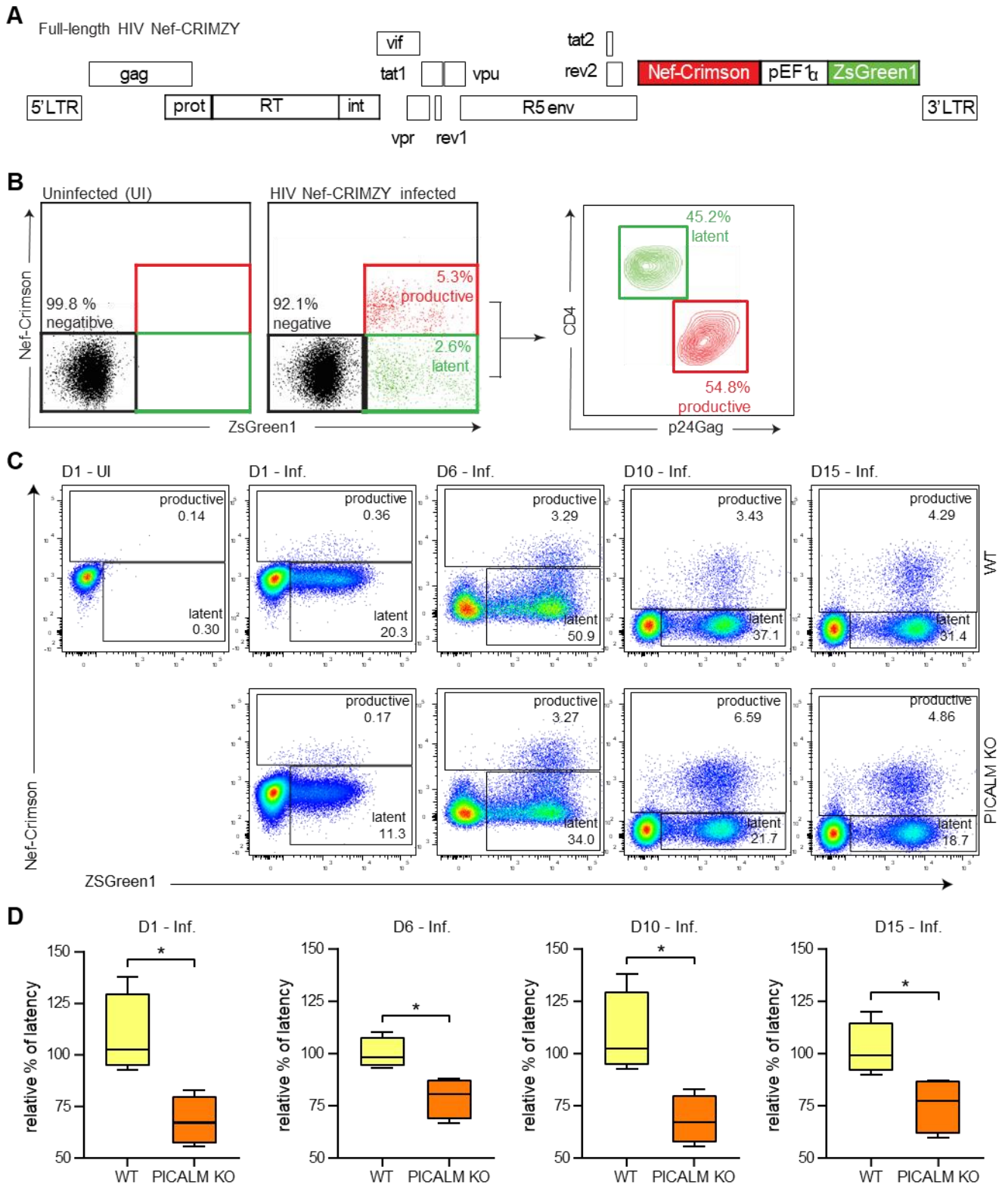


Figure 14. PICALM KO reduces latent HIV-1 infection. (A) Schematic of the HIV Nef-CRIMZY reporter construct used to assess latency, containing the WT NL4-3 HIV-1 genome, with an in-frame fusion of HIV-1 Nef and the Crimson reporter protein for productive infection readout, followed by the ZsGreen reporter under the control of the EF1 α promoter for a latent infection readout. Human CD4⁺T cells were isolated from PBMC, activated with

Dynabeads CD3/CD28 antibody and infected with HIV Nef_CRMZY with MOI 0.1 for 5 days. **(B)** Representative dot plots of flow cytometry analyses demonstrating that the co-expression of crimson and ZsGreen quantifies productive infection, with concomitant CD4 downregulation and increased Gag expression, as compared to latent infection by only ZsGreen1 expression where CD4 is increased in expression and Gag is decreased in expression. **(C)** SupT1 WT and PICALM KO cells were infected with HIV Nef-CRIMZY viruses produced in HEK293T cells (MOI 1) and were evaluated for Crimson and ZSGreen1 expression at days 1, 6, 10 and 15 post-infection (PI) using flow cytometry gated on cell viability using fixable viability staining (FVS)-780. **(D)** Corresponding box plots demonstrating that PICALM KO induces a reduction in latency. Relative values (%) were calculated by setting WT values to 100%, $p < 0.05$; unpaired two-tailed T-test; %, percent; UI, uninfected; Inf., infected; D, day. Retrieved from Guizar et al ¹.

Because the largest difference in latency (Crimson⁻ZsGreen⁺) between PICALM KO and WT cells was at 6 days (post-infection, we therefore assessed the phenotype of these cells using the Sony ID7000 Spectral Cell Analyzer. Here again, we observed that PICALM KO reduced PD-1 expression (**Figure 15B**) and characteristic of a T_{EM}-like phenotype (**Figure 15C, 6D**). Also, in these experiments we again observed that PICALM KO blunts PD-1 by HIV-1 infection (**Figure 15E**). Finally, PICALM KO induced T_{EM}-like cells that are enriched in the latently infected cell populations (**Figure 15F**), providing evidence that PICALM may have an effect in controlling latency via T_{EM} controlling PD-1 expression.

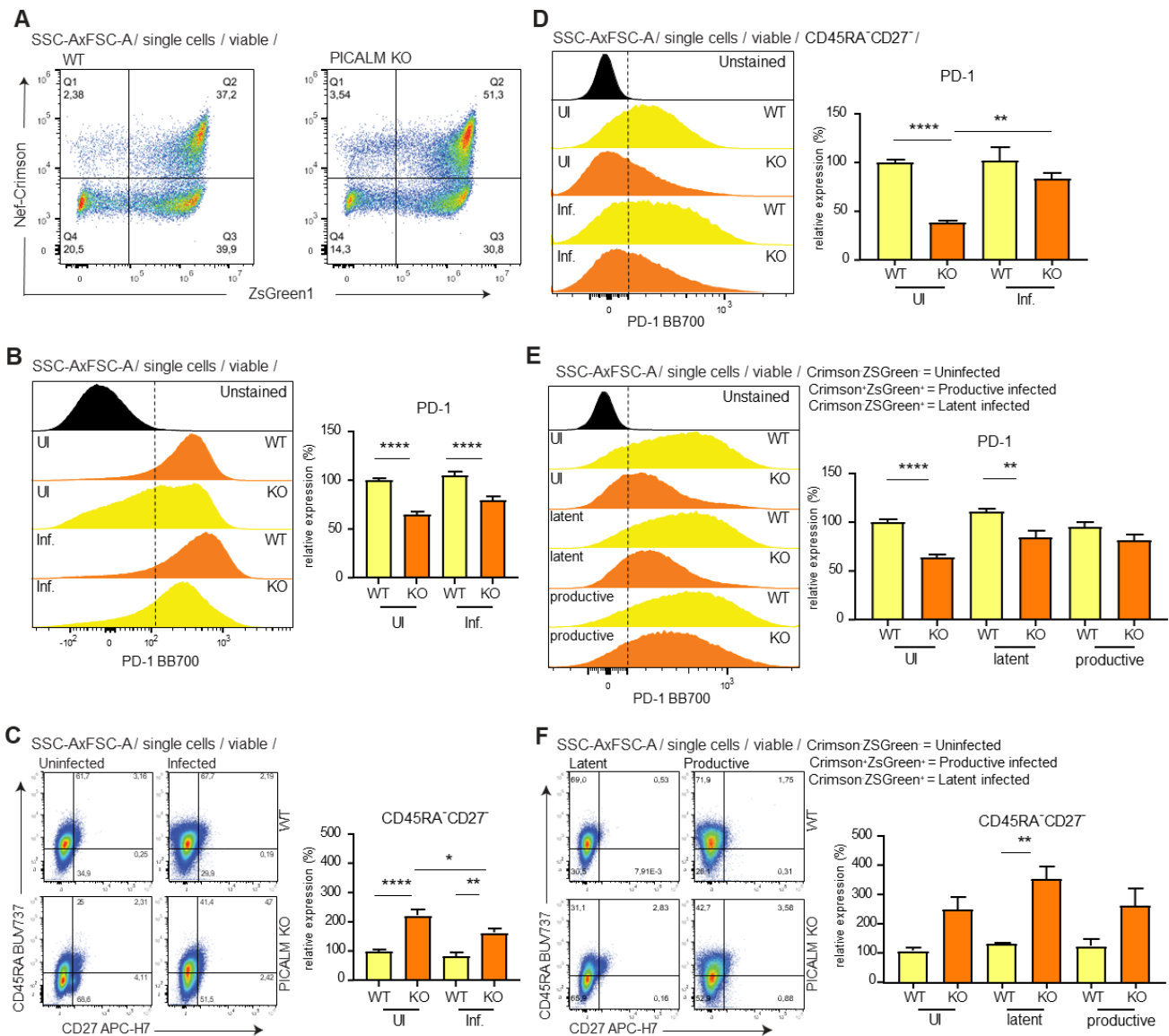


Figure 15. PICALM KO cells that favor latency reversal shows reduced PD-1 expression. SupT1 WT and PICALM KO were infected with HIV Nef-CRIMZY virus and were harvested at day 6 post-infection. (A) Productively and latently infected cells were analyzed by the expression of Crimson and ZsGreen1, demonstrating that PICALM KO cells had decreased number of latently infected cells. The overall expression of (B) PD-1 and (C) CD45RA and CD27 was analyzed to determine that PICALM KO cells display decreased PD-1 expression (% of PD-1+ cells) and increased T_{EM} -like phenotypes. (D) Gating on T_{EM} -like cells (CD45RA⁻CD27⁺) demonstrate that these have decreased relative PD-1 expression, which is increased by infection. (E) Gating on uninfected (Crimson⁻ZsGreen1⁻), latently (Crimson⁻ZsGreen1⁺), or productively (Crimson⁺ZsGreen1⁺) infected subpopulations demonstrates that the PICALM KO latent population has the most significant difference in PD-1 expression levels, and that these have the most significant increase in the T_{EM} -like phenotype (F). Dashed lines in the histograms represent where the gate for PD-1 was placed. Relative values (%) were calculated by setting WT values to 100%. Graphs show mean \pm SEM. Statistical Analysis were performed using ANOVA one-way, with Tukey post-test. $p < 0,05$, $< **0.001$, $< ***0.0001$. Retrieved from Guizar et al ¹.

CHAPTER 4: DISCUSSION

To successfully infect and replicate, HIV-1 must hijack host cellular proteins from several different cellular pathways including the endocytic and autophagy/lysosomal degradation pathway^{176-178,191,192}. The precise mechanisms by which it does this remain unclear. In this study, we demonstrate that PICALM, a component of both clathrin-mediated endocytosis and autophagy pathways⁶⁹ plays an important role in HIV-1 entry into host CD4⁺ T cells, and that it is also an important protein in the host response against HIV-1 infection via distinct mechanisms. PICALM's absence also leads to the accumulation of HIV-1 viral Gag protein in infected cells and modifies the T-cell immune response by decreasing immune checkpoint PD-1 expression, activation marker CD25, and by eliciting a CD45RA⁻CD27⁻ T_{EM}-like phenotype to these cells.

An interesting finding of our study is that PICALM seems to be a key regulator of HIV-1 entry into CD4⁺ T cells. As observed in our BlaM assays (**Figure 12A-B**), the PICALM KO cells resist viral entry, and it was shown to be independent of CD4 or CXCR4 HIV-1 receptor and co-receptors expression (**Figure 12C-D**). Altogether, these results support the idea of an alternative entry of HIV-1 and are supported by previous reports that demonstrate that HIV-1 entry into CD4⁺ T cells can occur via clathrin-mediated endocytosis^{181,193}.

Infection of PICALM KO Sup-T1 T cells displayed an accumulation of LC3B-II puncta, but these had diminished colocalization with LAMP1 positive organelles, while the BAF treatment highly increased their co-localization in PICALM KO cells, suggesting an increase in autophagic flux in these KO cells (**Figure 12E-I**). Indeed, it has been previously observed that PICALM regulates autophagosome-lysosome fusion via the soluble NSF attachment protein receptor (SNARE) Vesicle Associated Membrane Protein 8 (VAMP8)^{69,71,75}. Additionally, we have observed that infected PICALM KO cells exhibit increased Gag

expression and virus production (**Figures 11A-F**). These observations first appeared counterintuitive: that PICALM KO cells exhibited both higher Gag production and increased autophagic flux. However, although high levels of co-localization of LC3B-II and LAMP-1 were observed in PICALM KO cells, endosomal acidification and autophagy can still be inhibited due to the presence of Nef^{194,195}. Autophagy has not been demonstrated to play a role in Gag expression in CD4 T⁺ cells. However, our data suggest this to be the case in PICALM KO cells, considering our observation of increased co-localization between Gag with LC3B-II (**Figure 11A-C**). Thus, the absence of PICALM allows HIV-1 to use autophagosomal membranes as scaffolds for virion assembly, rather than being degraded by them. Together this leads us to believe that HIV-1's ability to exploit the autophagy machinery towards its replication is inhibited by PICALM in CD4⁺ T cells.

We have also demonstrated that PICALM KO cells have dysregulated PD-1 cell surface expression resulting in a T_{EM}-like phenotype (**Figure 13C**). A high PD-1 expression is generally associated with T cell exhaustion during cancer and chronic viral infections, while its blockade has shown to increase T cell activation and proliferation. Therefore, inhibitors of this immune checkpoint have been proven to help in both viral control and the treatment of more than 20 types of cancer^{120,196-198}. Recent studies have however demonstrated that the PD-1 pathway also plays a fundamental role in shaping effector and memory T cell responses^{199,200}.

Indeed, one surprising finding of our study was that while PICALM KO cells had lowered cell surface PD-1, that also displayed elevated proliferation and activation profiles (**Figure 14A-B, 14G**). Contrary to what was expected, while the cells presented reduced viral entry, there was still a higher viral production in latter time points (**Figure 11D-F**), which could be due to the decreased PD-1 expression¹²¹. In addition, PICALM KO cells exhibited a pronounced T_{EM}-like phenotype²⁰¹ (**Figure 14J**). These observations lead to important

considerations since the timing of a PD-1 blockade will determine memory T cell responses during chronic viral infection ^{122,200}. PICALM KO cells also express higher levels of IFN γ , normally produced by T_{EM} cells ²⁰², and increased levels of CD69, as observed in our work (**Figure 13B**), a marker for persistence of CD4⁺ T cell memory ²⁰³. The internalization and degradation of PD-1 can be blocked by the inhibition of clathrin-mediated endocytosis ²⁰⁴ and PD-1 palmitoylation promotes recycling endosome and prevent its lysosome-dependent degradation ²⁰⁵. Our observations that PICALM KO reduces cell surface PD-1 but not whole cell PD-1 expression (**Figure 13C, 13F**), in addition to the published data supporting that PICALM is found in numerous vesicles including clathrin-coated vesicles, early endosomes, and sorting endosomes, suggests that PICALM may indeed be involved in the presentation and/or recycling of PD-1 from the cell surface ^{71,206}.

Finally, using a latency model cell reporter system, PICALM KO cells could persistently antagonize the establishment of HIV-1 latency (**Figure 14**), and this is in line with earlier reports demonstrating that PD-1 contributes to the establishment and maintenance of HIV-1 latency ²⁰⁷, and that PD-1 blockade potentiates HIV-1 latency reversal in CD4⁺ T cells ¹⁸⁹ and in HIV-1-positive cancer patients ²⁰⁸. The lowering of latent cell populations is a desirable goal to eliminate viral reservoirs ²⁰⁹, and our findings that this may be under the control of endocytic PICALM expression is exciting, as targeting PICALM would act to reduce both infection and latency. Here we show that PICALM might play a role in the maintenance of latency, presumably by controlling PD-1 expression at the cell surface. While our results suggest that the knockout of PICALM reduces both latency and levels of PD-1, we observed that the expression of viral proteins is enough to counteract the downregulation of PD-1 by the KO, but not the WT. This suggests that in the WT, the PICALM pathway may intersect with HIV-1 to avoid the HIV-1 induced PD-1 expression (**Figure 15E**). It is known that latently infected cells are largely T_{EM} CD4⁺ T cells (Morcilla,

et al., 2021), a finding that is reflected in our result in PICALM KO cells. In addition, in contrary to the overall population (Figure 6B), the levels of PD-1 increase in infected PICALM KO T_{EM}-like cells, suggesting that PICALM is not the only regulator of PD-1 expression and to reverse latency in T_{EM} cells, and that the role of PICALM in the physiology of cells could be phenotype-related in the context of HIV-1 infection.

In summary, the endocytosis-related protein PICALM appears to have an important role in viral infection, supporting the role of clathrin-mediated endocytosis in HIV-1 entry/fusion. Additionally, PICALM KO cells reveal a link between endocytosis and other pathways, including pro-inflammatory responses, and autophagy; highlighting that components of the molecular apparatus of clathrin-mediated endocytosis also mediate non-endocytosis effects that influence HIV-1 replication. Finally, our data suggest that the targeting of PICALM is positive for CD4⁺ T cell health, increasing their proliferation and preserving their activation status and T_{EM}-like phenotypes while reducing PD-1 expression and latency. Considering that Sup-T1 is a CD4⁺/CXCR4⁺/CCR5⁻ cell line derived from a T-cell lymphoblastic lymphoma ²¹⁰, it would be interesting to knockout PICALM in differentiated CD4⁺ T primary cells to confirm the observations that we make in this study. Further investigations in the precise mechanisms are warranted as this protein may represent a key interesting target that can benefit HIV-1 and cancer patients alike.

CHAPTER 5: SUMMARY AND CONCLUSION

In this work, we discovered that CRISPR-mediated PICALM knockout leads to impaired HIV-1 entry in CD4⁺ SupT1 cells, providing evidence that entry of HIV-1 into T cells occurs via clathrin-mediated endocytosis. However, PICALM deletion did not only affect clathrin-mediated endocytosis, PICALM KO cells also had modified autophagic flux resulting in increased HIV-1 Gag expression, decreased viral latency, an increased T effector memory (T_{EM})-like phenotype and diminished immune activation profiles in response to HIV-1 infection, indicating PICALM may mediate non-endocytic events that also influence HIV-1 infection dynamics. Nevertheless, further studies will be needed to fully understand and validate these mechanisms in primary T cells.

CHAPTER 6: BIBLIOGRAPHY

1. Paola Guizar, A.M., Ana Luiza Abdalla, Kristin Davis, Meijuan Niu, Xinyun Liu, Oluwaseun Ajibola, Thomas T. Murooka, Chen Liang, Andrew J. Mouland (2023). An HIV-1 CRISPR-Cas9 membrane trafficking screen reveals a role for PICALM intersecting endolysosomes and immunity. *iScience In second revision*.
2. Ramos, H., Monette, A., Niu, M., Barrera, A., López-Ulloa, B., Fuentes, Y., Guizar, P., Pino, K., DesGroseillers, L., Mouland, A.J., and López-Lastra, M. (2022). The double-stranded RNA-binding protein, Staufen1, is an IRES-transacting factor regulating HIV-1 cap-independent translation initiation. *Nucleic Acids Res* 50, 411-429. 10.1093/nar/gkab1188.
3. Sharp, P.M., and Hahn, B.H. (2011). Origins of HIV and the AIDS pandemic. *Cold Spring Harb Perspect Med* 1, a006841. 10.1101/cshperspect.a006841.
4. Agarwal-Jans, S. (2020). Timeline: HIV. *Cell* 183, 550. 10.1016/j.cell.2020.09.004.
5. Barré-Sinoussi, F., Chermann, J.C., Rey, F., Nugeyre, M.T., Chamaret, S., Gruest, J., Dautuet, C., Axler-Blin, C., Vézinet-Brun, F., Rouzioux, C., et al. (1983). Isolation of a T-lymphotropic retrovirus from a patient at risk for acquired immune deficiency syndrome (AIDS). *Science* 220, 868-871. 10.1126/science.6189183.
6. Lever, A.M., and Berkhout, B. (2008). 2008 Nobel prize in medicine for discoverers of HIV. *Retrovirology* 5, 91. 10.1186/1742-4690-5-91.
7. Lucas, S., and Nelson, A.M. (2015). HIV and the spectrum of human disease. *J Pathol* 235, 229-241. 10.1002/path.4449.
8. Bbosa, N., Kaleebu, P., and Ssemwanga, D. (2019). HIV subtype diversity worldwide. *Curr Opin HIV AIDS* 14, 153-160. 10.1097/coh.0000000000000534.
9. Zuliani-Alvarez, L., Govasli, M.L., Rasaiyaah, J., Monit, C., Perry, S.O., Sumner, R.P., McAlpine-Scott, S., Dickson, C., Rifat Faysal, K.M., Hilditch, L., et al. (2022). Evasion of cGAS and TRIM5 defines pandemic HIV. *Nature Microbiology* 7, 1762-1776. 10.1038/s41564-022-01247-0.
10. Solomon, S.S., Solomon, S., McFall, A.M., Srikrishnan, A.K., Anand, S., Verma, V., Vasudevan, C.K., Balakrishnan, P., Ogburn, E.L., Moulton, L.H., et al. (2019). Integrated HIV testing, prevention, and treatment intervention for key populations in India: a cluster-randomised trial. *Lancet HIV* 6, e283-e296. 10.1016/s2352-3018(19)30034-7.
11. Vergis, E.N., and Mellors, J.W. (2000). Natural history of HIV-1 infection. *Infect Dis Clin North Am* 14, 809-825, v-vi. 10.1016/s0891-5520(05)70135-5.
12. John M Coffin, S.H.H., and Harold E Varmus. (1997). *Retroviruses* (Cold Spring Harbor Laboratory Press).
13. Boutwell, C.L., Rolland, M.M., Herbeck, J.T., Mullins, J.I., and Allen, T.M. (2010). Viral evolution and escape during acute HIV-1 infection. *J Infect Dis* 202 *Suppl* 2, S309-314. 10.1086/655653.
14. Borrow, P. (2011). Innate immunity in acute HIV-1 infection. *Curr Opin HIV AIDS* 6, 353-363. 10.1097/COH.0b013e3283495996.
15. Nijmeijer, B.M., and Geijtenbeek, T.B.H. (2019). Negative and Positive Selection Pressure During Sexual Transmission of Transmitted Founder HIV-1. *Front Immunol* 10, 1599. 10.3389/fimmu.2019.01599.
16. Huerta, L. (2020). Editorial: Anti-infective 2020: HIV-From pathogenesis to treatment. *Curr Opin Pharmacol* 54, x-xii. 10.1016/j.coph.2020.12.001.
17. Harrison, T.B., and Smith, B. (2011). Neuromuscular manifestations of HIV/AIDS. *J Clin Neuromuscul Dis* 13, 68-84. 10.1097/CND.0b013e318221256f.
18. Tiwari, S., Atluri, V., Kaushik, A., Yndart, A., and Nair, M. (2019). Alzheimer's disease: pathogenesis, diagnostics, and therapeutics. *Int J Nanomedicine* 14, 5541-5554. 10.2147/ijn.S200490.

19. Dehner, L.F., Spitz, M., and Pereira, J.S. (2016). Parkinsonism in HIV infected patients during antiretroviral therapy - data from a Brazilian tertiary hospital. *Braz J Infect Dis* 20, 499-501. 10.1016/j.bjid.2016.05.008.
20. Naicker, S., Rahmanian, S., and Kopp, J.B. (2015). HIV and chronic kidney disease. *Clin Nephrol* 83, 32-38. 10.5414/cnp83s032.
21. Rosenberg, A.Z., Naicker, S., Winkler, C.A., and Kopp, J.B. (2015). HIV-associated nephropathies: epidemiology, pathology, mechanisms and treatment. *Nature Reviews Nephrology* 11, 150-160. 10.1038/nrneph.2015.9.
22. Cribbs, S.K., Crothers, K., and Morris, A. (2020). Pathogenesis of HIV-Related Lung Disease: Immunity, Infection, and Inflammation. *Physiol Rev* 100, 603-632. 10.1152/physrev.00039.2018.
23. Roychoudhury, S., Das, A., Sengupta, P., Dutta, S., Roychoudhury, S., Choudhury, A.P., Ahmed, A.B.F., Bhattacharjee, S., and Slama, P. (2020). Viral Pandemics of the Last Four Decades: Pathophysiology, Health Impacts and Perspectives. *Int J Environ Res Public Health* 17. 10.3390/ijerph17249411.
24. Verma, M. (2015). Epigenetic regulation of HIV, AIDS, and AIDS-related malignancies. *Methods Mol Biol* 1238, 381-403. 10.1007/978-1-4939-1804-1_21.
25. Papalini, C., Brescini, L., Curci, L., Bastianelli, S., Barchiesi, F., Giacometti, A., and Francisci, D. (2023). Kaposi Sarcoma in People Living with HIV: Is it Water under the Bridge? *Mediterr J Hematol Infect Dis* 15, e2023027. 10.4084/mjhid.2023.027.
26. Saberian, C., and Campbell, B.R. (2023). Rapidly Disseminated Kaposi's Sarcoma Despite Initiation of Antiretroviral Therapy. *Cureus* 15, e39627. 10.7759/cureus.39627.
27. Greene, W.C. (2007). A history of AIDS: looking back to see ahead. *Eur J Immunol* 37 Suppl 1, S94-102. 10.1002/eji.200737441.
28. Chen, J., Zhou, T., Zhang, Y., Luo, S., Chen, H., Chen, D., Li, C., and Li, W. (2022). The reservoir of latent HIV. *Front Cell Infect Microbiol* 12, 945956. 10.3389/fcimb.2022.945956.
29. Bonney, E.Y., Lamptey, H., and Kyei, G.B. (2023). HIV cure: an acceptability scientific agenda. *Curr Opin HIV AIDS* 18, 12-17. 10.1097/coh.0000000000000771.
30. Maina, E.K., Adan, A.A., Mureithi, H., Muriuki, J., and Lwembe, R.M. (2021). A Review of Current Strategies Towards the Elimination of Latent HIV-1 and Subsequent HIV-1 Cure. *Curr HIV Res* 19, 14-26. 10.2174/1570162x18999200819172009.
31. Hu, W.S., and Hughes, S.H. (2012). HIV-1 reverse transcription. *Cold Spring Harb Perspect Med* 2. 10.1101/cshperspect.a006882.
32. Blut, A. (2016). Human Immunodeficiency Virus (HIV). *Transfus Med Hemother* 43, 203-222. 10.1159/000445852.
33. Solbak, S.M., Reksten, T.R., Hahn, F., Wray, V., Henklein, P., Henklein, P., Halskau, Ø., Schubert, U., and Fossen, T. (2013). HIV-1 p6 - a structured to flexible multifunctional membrane-interacting protein. *Biochim Biophys Acta* 1828, 816-823. 10.1016/j.bbamem.2012.11.010.
34. Fanales-Belasio, E., Raimondo, M., Suligoj, B., and Buttò, S. (2010). HIV virology and pathogenetic mechanisms of infection: a brief overview. *Ann Ist Super Sanita* 46, 5-14. 10.4415/ann_10_01_02.
35. Xiao, T., Cai, Y., and Chen, B. (2021). HIV-1 Entry and Membrane Fusion Inhibitors. *Viruses* 13. 10.3390/v13050735.
36. Ambrose, Z., and Aiken, C. (2014). HIV-1 uncoating: connection to nuclear entry and regulation by host proteins. *Virology* 454-455, 371-379. 10.1016/j.virol.2014.02.004.
37. Mohammadi, P., Desfarges, S., Bartha, I., Joos, B., Zangger, N., Muñoz, M., Günthard, H.F., Beerenwinkel, N., Telenti, A., and Ciuffi, A. (2013). 24 hours in the life of HIV-1 in a T cell line. *PLoS Pathog* 9, e1003161. 10.1371/journal.ppat.1003161.
38. Johnson, M.M., Jones, C.E., and Clark, D.N. (2022). The Effect of Treatment-Associated Mutations on HIV Replication and Transmission Cycles. *Viruses* 15. 10.3390/v15010107.

39. Shcherbatova, O., Grebennikov, D., Sazonov, I., Meyerhans, A., and Bocharov, G. (2020). Modeling of the HIV-1 Life Cycle in Productively Infected Cells to Predict Novel Therapeutic Targets. *Pathogens* 9. 10.3390/pathogens9040255.
40. Ferguson, M.R., Rojo, D.R., von Lindern, J.J., and O'Brien, W.A. (2002). HIV-1 replication cycle. *Clin Lab Med* 22, 611-635. 10.1016/s0272-2712(02)00015-x.
41. Sherpa, C., Rausch, J.W., Le Grice, S.F., Hammarskjold, M.L., and Rekosh, D. (2015). The HIV-1 Rev response element (RRE) adopts alternative conformations that promote different rates of virus replication. *Nucleic Acids Res* 43, 4676-4686. 10.1093/nar/gkv313.
42. Deeks, S.G., Overbaugh, J., Phillips, A., and Buchbinder, S. (2015). HIV infection. *Nature Reviews Disease Primers* 1, 1-22. 10.1038/nrdp.2015.35.
43. Malim, M.H., Hauber, J., Le, S.Y., Maizel, J.V., and Cullen, B.R. (1989). The HIV-1 rev transactivator acts through a structured target sequence to activate nuclear export of unspliced viral mRNA. *Nature* 338, 254-257. 10.1038/338254a0.
44. Cooley, L.A., and Lewin, S.R. (2003). HIV-1 cell entry and advances in viral entry inhibitor therapy. *J Clin Virol* 26, 121-132. 10.1016/s1386-6532(02)00111-7.
45. Gomez, C., and Hope, T.J. (2005). The ins and outs of HIV replication. *Cell Microbiol* 7, 621-626. 10.1111/j.1462-5822.2005.00516.x.
46. Scarsi, K.K., Havens, J.P., Podany, A.T., Avedissian, S.N., and Fletcher, C.V. (2020). HIV-1 Integrase Inhibitors: A Comparative Review of Efficacy and Safety. *Drugs* 80, 1649-1676. 10.1007/s40265-020-01379-9.
47. Holec, A.D., Mandal, S., Prathipati, P.K., and Destache, C.J. (2017). Nucleotide Reverse Transcriptase Inhibitors: A Thorough Review, Present Status and Future Perspective as HIV Therapeutics. *Curr HIV Res* 15, 411-421. 10.2174/1570162x15666171120110145.
48. Li, G., Wang, Y., and De Clercq, E. (2022). Approved HIV reverse transcriptase inhibitors in the past decade. *Acta Pharm Sin B* 12, 1567-1590. 10.1016/j.apsb.2021.11.009.
49. Pau, A.K., and George, J.M. (2014). Antiretroviral therapy: current drugs. *Infect Dis Clin North Am* 28, 371-402. 10.1016/j.idc.2014.06.001.
50. Liao, H.-K., Gu, Y., Diaz, A., Marlett, J., Takahashi, Y., Li, M., Suzuki, K., Xu, R., Hishida, T., Chang, C.-J., et al. (2015). Use of the CRISPR/Cas9 system as an intracellular defense against HIV-1 infection in human cells. *Nature Communications* 6, 1-10. 10.1038/ncomms7413.
51. Eakle, R., Venter, F., and Rees, H. (2018). Pre-exposure prophylaxis (PrEP) in an era of stalled HIV prevention: Can it change the game? *Retrovirology* 15, 29. 10.1186/s12977-018-0408-3.
52. Bandera, A., Gori, A., Clerici, M., and Sironi, M. (2019). Phylogenies in ART: HIV reservoirs, HIV latency and drug resistance. *Curr Opin Pharmacol* 48, 24-32. 10.1016/j.coph.2019.03.003.
53. Noy, A. (2019). Optimizing treatment of HIV-associated lymphoma. *Blood* 134, 1385-1394. 10.1182/blood-2018-01-791400.
54. Blassel, L., Zhukova, A., Villabona-Arenas, C.J., Atkins, K.E., Hué, S., and Gascuel, O. (2021). Drug resistance mutations in HIV: new bioinformatics approaches and challenges. *Curr Opin Virol* 51, 56-64. 10.1016/j.coviro.2021.09.009.
55. Sarabia, I., and Bosque, A. (2019). HIV-1 Latency and Latency Reversal: Does Subtype Matter? *Viruses* 11. 10.3390/v11121104.
56. Dahabieh, M.S., Battivelli, E., and Verdin, E. (2015). Understanding HIV latency: the road to an HIV cure. *Annu Rev Med* 66, 407-421. 10.1146/annurev-med-092112-152941.
57. Jäger, S., Cimermancic, P., Gulbahce, N., Johnson, J.R., McGovern, K.E., Clarke, S.C., Shales, M., Mercenne, G., Pache, L., Li, K., et al. (2012). Global landscape of HIV-human protein complexes. *Nature* 481, 365-370. 10.1038/nature10719.
58. Archin, N.M., Kirchherr, J.L., Sung, J.A., Clutton, G., Sholtis, K., Xu, Y., Allard, B., Stuelke, E., Kashuba, A.D., Kuruc, J.D., et al. (2017). Interval dosing with the HDAC inhibitor vorinostat effectively reverses HIV latency. *J Clin Invest* 127, 3126-3135. 10.1172/jci92684.

59. Tsai, P., Wu, G., Baker, C.E., Thayer, W.O., Spagnuolo, R.A., Sanchez, R., Barrett, S., Howell, B., Margolis, D., Hazuda, D.J., et al. (2016). In vivo analysis of the effect of panobinostat on cell-associated HIV RNA and DNA levels and latent HIV infection. *Retrovirology* 13, 36. 10.1186/s12977-016-0268-7.
60. Kessing, C.F., Nixon, C.C., Li, C., Tsai, P., Takata, H., Mousseau, G., Ho, P.T., Honeycutt, J.B., Fallahi, M., Trautmann, L., et al. (2017). In Vivo Suppression of HIV Rebound by Didehydro-Cortistatin A, a "Block-and-Lock" Strategy for HIV-1 Treatment. *Cell Rep* 21, 600-611. 10.1016/j.celrep.2017.09.080.
61. Atkins, A.J., Allen, A.G., Dampier, W., Haddad, E.K., Nonnemacher, M.R., and Wigdahl, B. (2021). HIV-1 cure strategies: why CRISPR? *Expert Opin Biol Ther* 21, 781-793. 10.1080/14712598.2021.1865302.
62. Wykes, M.N., and Lewin, S.R. (2018). Immune checkpoint blockade in infectious diseases. *Nat Rev Immunol* 18, 91-104. 10.1038/nri.2017.112.
63. Tremouillaux-Guiller, J., Moustafa, K., Hefferon, K., Gaobotse, G., and Makhzoum, A. (2020). Plant-made HIV vaccines and potential candidates. *Curr Opin Biotechnol* 61, 209-216. 10.1016/j.copbio.2020.01.004.
64. HIV vaccines go to trial. (2019). *Nature Medicine* 25, 703-703. 10.1038/s41591-019-0460-0.
65. Miller, S.E., Mathiasen, S., Bright, N.A., Pierre, F., Kelly, B.T., Kladt, N., Schauss, A., Merrifield, C.J., Stamou, D., Höning, S., and Owen, D.J. (2015). CALM regulates clathrin-coated vesicle size and maturation by directly sensing and driving membrane curvature. *Dev Cell* 33, 163-175. 10.1016/j.devcel.2015.03.002.
66. Mercer, J.L., Argus, J.P., Crabtree, D.M., Keenan, M.M., Wilks, M.Q., Chi, J.-T.A., Bensinger, S.J., Lavau, C.P., and Wechsler, D.S. (2015). Modulation of PICALM Levels Perturbs Cellular Cholesterol Homeostasis. *PLOS ONE* 10, e0129776. 10.1371/journal.pone.0129776.
67. Scotland, P.B., Heath, J.L., Conway, A.E., Porter, N.B., Armstrong, M.B., Walker, J.A., Klebig, M.L., Lavau, C.P., and Wechsler, D.S. (2012). The PICALM protein plays a key role in iron homeostasis and cell proliferation. *PloS One* 7, e44252. 10.1371/journal.pone.0044252.
68. Mertins, P., Przybylski, D., Yosef, N., Qiao, J., Clauser, K., Raychowdhury, R., Eisenhaure, T.M., Maritzen, T., Haucke, V., Satoh, T., et al. (2017). An Integrative Framework Reveals Signaling-to-Transcription Events in Toll-like Receptor Signaling. *Cell Rep* 19, 2853-2866. 10.1016/j.celrep.2017.06.016.
69. Moreau, K., Fleming, A., Imarisio, S., Lopez Ramirez, A., Mercer, J.L., Jimenez-Sanchez, M., Bento, C.F., Puri, C., Zavodszky, E., Siddiqi, F., et al. (2014). PICALM modulates autophagy activity and tau accumulation. *Nat Commun* 5, 4998. 10.1038/ncomms5998.
70. Van Acker, Z.P., Bretou, M., and Annaert, W. (2019). Endo-lysosomal dysregulations and late-onset Alzheimer's disease: impact of genetic risk factors. *Mol Neurodegener* 14, 20. 10.1186/s13024-019-0323-7.
71. Zhao, Z., Sagare, A.P., Ma, Q., Halliday, M.R., Kong, P., Kisler, K., Winkler, E.A., Ramanathan, A., Kanekiyo, T., Bu, G., et al. (2015). Central role for PICALM in amyloid- β blood-brain barrier transcytosis and clearance. *Nat Neurosci* 18, 978-987. 10.1038/nn.4025.
72. Chae, C.W., Lee, H.J., Choi, G.E., Jung, Y.H., Kim, J.S., Lim, J.R., Kim, S.Y., Hwang, I.K., Seong, J.K., and Han, H.J. (2020). High glucose-mediated PICALM and mTORC1 modulate processing of amyloid precursor protein via endosomal abnormalities. *Br J Pharmacol* 177, 3828-3847. 10.1111/bph.15131.
73. Narayan, P., Sienski, G., Bonner, J.M., Lin, Y.T., Seo, J., Baru, V., Haque, A., Milo, B., Akay, L.A., Graziosi, A., et al. (2020). PICALM Rescues Endocytic Defects Caused by the Alzheimer's Disease Risk Factor APOE4. *Cell Rep* 33, 108224. 10.1016/j.celrep.2020.108224.
74. Hattersley, K.J., Carosi, J.M., Hein, L.K., Bensalem, J., and Sargeant, T.J. (2021). PICALM regulates cathepsin D processing and lysosomal function. *Biochem Biophys Res Commun* 570, 103-109. 10.1016/j.bbrc.2021.07.024.

75. Ando, K., Tomimura, K., Sazdovitch, V., Suain, V., Yilmaz, Z., Authelet, M., Ndjim, M., Vergara, C., Belkouch, M., Potier, M.C., et al. (2016). Level of PICALM, a key component of clathrin-mediated endocytosis, is correlated with levels of phosphotau and autophagy-related proteins and is associated with tau inclusions in AD, PSP and Pick disease. *Neurobiol Dis* *94*, 32-43. 10.1016/j.nbd.2016.05.017.
76. Thomas, R.S., Henson, A., Gerrish, A., Jones, L., Williams, J., and Kidd, E.J. (2016). Decreasing the expression of PICALM reduces endocytosis and the activity of β -secretase: implications for Alzheimer's disease. *BMC Neurosci* *17*, 50. 10.1186/s12868-016-0288-1.
77. Mettlen, M., Chen, P.-H., Srinivasan, S., Danuser, G., and Schmid, S.L. (2018). Regulation of Clathrin-Mediated Endocytosis. *Annual review of biochemistry* *87*, 871-896. 10.1146/annurev-biochem-062917-012644.
78. Kaksonen, M., and Roux, A. (2018). Mechanisms of clathrin-mediated endocytosis. *Nature Reviews Molecular Cell Biology* *19*, 313-326. 10.1038/nrm.2017.132.
79. Miller, Sharon E., Mathiasen, S., Bright, Nicholas A., Pierre, F., Kelly, Bernard T., Kladt, N., Schauss, A., Merrifield, Christien J., Stamou, D., Höning, S., and Owen, David J. (2015). CALM Regulates Clathrin-Coated Vesicle Size and Maturation by Directly Sensing and Driving Membrane Curvature. *Developmental Cell* *33*, 163-175. 10.1016/j.devcel.2015.03.002.
80. Popova, N.V., Deyev, I.E., and Petrenko, A.G. (2013). Clathrin-mediated endocytosis and adaptor proteins. *Acta Naturae* *5*, 62-73.
81. Willy, N.M., Colombo, F., Huber, S., Smith, A.C., Norton, E.G., Kural, C., and Cocucci, E. (2021). CALM supports clathrin-coated vesicle completion upon membrane tension increase. *Proc Natl Acad Sci U S A* *118*. 10.1073/pnas.2010438118.
82. Scott, B.L., Sochacki, K.A., Low-Nam, S.T., Bailey, E.M., Luu, Q., Hor, A., Dickey, A.M., Smith, S., Kerkvliet, J.G., Taraska, J.W., and Hoppe, A.D. (2018). Membrane bending occurs at all stages of clathrin-coat assembly and defines endocytic dynamics. *Nat Commun* *9*, 419. 10.1038/s41467-018-02818-8.
83. Green, D.R., and Levine, B. (2014). To Be or Not to Be?: How Selective Autophagy and Cell Death Govern Cell Fate. *Cell* *157*, 65-75. 10.1016/j.cell.2014.02.049.
84. D'Arcy, M.S. (2019). Cell death: a review of the major forms of apoptosis, necrosis and autophagy. *Cell Biol Int* *43*, 582-592. 10.1002/cbin.11137.
85. Levine, B., and Kroemer, G. (2019). Biological Functions of Autophagy Genes: A Disease Perspective. *Cell* *176*, 11-42. 10.1016/j.cell.2018.09.048.
86. Klionsky, D.J., Petroni, G., Amaravadi, R.K., Baehrecke, E.H., Ballabio, A., Boya, P., Bravo-San Pedro, J.M., Cadwell, K., Cecconi, F., Choi, A.M.K., et al. (2021). Autophagy in major human diseases. *Embo j* *40*, e108863. 10.15252/embj.2021108863.
87. Parzych, K.R., and Klionsky, D.J. (2014). An Overview of Autophagy: Morphology, Mechanism, and Regulation. *Antioxidants & Redox Signaling* *20*, 460-473. 10.1089/ars.2013.5371.
88. Hayashi-Nishino, M., Fujita, N., Noda, T., Yamaguchi, A., Yoshimori, T., and Yamamoto, A. (2009). A subdomain of the endoplasmic reticulum forms a cradle for autophagosome formation. *Nature Cell Biology* *11*, 1433-1437. 10.1038/ncb1991.
89. Ravikumar, B., Moreau, K., Jahreiss, L., and Puri, C. (2011). Plasma membrane contributes to the formation of pre- autophagosomal structures. *23*.
90. Takahashi, Y., Meyerkord, C.L., Hori, T., Runkle, K., Fox, T.E., Kester, M., Loughran, T.P., and Wang, H.G. (2011). Bif-1 regulates Atg9 trafficking by mediating the fission of Golgi membranes during autophagy. *Autophagy* *7*, 61-73. 10.4161/auto.7.1.14015.
91. Hailey, D.W., Rambold, A.S., Satpute-Krishnan, P., Mitra, K., Sougrat, R., Kim, P.K., and Lippincott-Schwartz, J. (2010). Mitochondria supply membranes for autophagosome biogenesis during starvation. *Cell* *141*, 656-667. 10.1016/j.cell.2010.04.009.
92. Nakatogawa, H. (2020). Mechanisms governing autophagosome biogenesis. *Nature Reviews Molecular Cell Biology* *21*, 439-458. 10.1038/s41580-020-0241-0.

93. Birgisdottir, Å.B., and Johansen, T. (2020). Autophagy and endocytosis – interconnections and interdependencies. *Journal of Cell Science* 133. 10.1242/jcs.228114.
94. Ando, K., Nagaraj, S., Küçükali, F., de Fisenne, M.A., Kosa, A.C., Doeraene, E., Lopez Gutierrez, L., Brion, J.P., and Leroy, K. (2022). PICALM and Alzheimer's Disease: An Update and Perspectives. *Cells* 11. 10.3390/cells11243994.
95. Menzies, F.M., Fleming, A., and Rubinsztein, D.C. (2015). Compromised autophagy and neurodegenerative diseases. *Nature Reviews Neuroscience* 16, 345-357. 10.1038/nrn3961.
96. Hattersley, K.J., Carosi, J.M., Hein, L.K., Bensalem, J., and Sargeant, T.J. (2021). PICALM regulates cathepsin D processing and lysosomal function. *Biochemical and Biophysical Research Communications* 570, 103-109. 10.1016/j.bbrc.2021.07.024.
97. Rostagno, A.A. (2022). Pathogenesis of Alzheimer's Disease. *Int J Mol Sci* 24. 10.3390/ijms24010107.
98. Lambert, J.-C., Ibrahim-Verbaas, C.A., Harold, D., Naj, A.C., Sims, R., Bellenguez, C., Jun, G., DeStefano, A.L., Bis, J.C., Beecham, G.W., et al. (2013). Meta-analysis of 74,046 individuals identifies 11 new susceptibility loci for Alzheimer's disease. *Nature Genetics* 45, 1452-1458. 10.1038/ng.2802.
99. Seshadri, S., Fitzpatrick, A.L., Ikram, M.A., DeStefano, A.L., Gudnason, V., Boada, M., Bis, J.C., Smith, A.V., Carassquillo, M.M., Lambert, J.C., et al. (2010). Genome-wide analysis of genetic loci associated with Alzheimer disease. *Jama* 303, 1832-1840. 10.1001/jama.2010.574.
100. Harold, D., Abraham, R., Hollingworth, P., Sims, R., Gerrish, A., Hamshere, M.L., Pahwa, J.S., Moskva, V., Dowzell, K., Williams, A., et al. (2009). Genome-wide association study identifies variants at CLU and PICALM associated with Alzheimer's disease. *Nature Genetics* 41, 1088-1093. 10.1038/ng.440.
101. Katsumata, Y., Shade, L.M., Hohman, T.J., Schneider, J.A., Bennett, D.A., Farfel, J.M., Kukull, W.A., Fardo, D.W., and Nelson, P.T. (2022). Multiple gene variants linked to Alzheimer's-type clinical dementia via GWAS are also associated with non-Alzheimer's neuropathologic entities. *Neurobiol Dis* 174, 105880. 10.1016/j.nbd.2022.105880.
102. Ando, K., Brion, J.P., Stygelbout, V., Suain, V., Authelet, M., Dedecker, R., Chanut, A., Lacor, P., Lavaur, J., Sazdovitch, V., et al. (2013). Clathrin adaptor CALM/PICALM is associated with neurofibrillary tangles and is cleaved in Alzheimer's brains. *Acta Neuropathol* 125, 861-878. 10.1007/s00401-013-1111-z.
103. Ando, K., De Decker, R., Vergara, C., Yilmaz, Z., Mansour, S., Suain, V., Slegers, K., de Fisenne, M.-A., Houben, S., Potier, M.-C., et al. (2020). Picalm reduction exacerbates tau pathology in a murine tauopathy model. *Acta Neuropathologica* 139, 773-789. 10.1007/s00401-020-02125-x.
104. Tian, Y., Chang, J.C., Fan, E.Y., Flajolet, M., and Greengard, P. (2013). Adaptor complex AP2/PICALM, through interaction with LC3, targets Alzheimer's APP-CTF for terminal degradation via autophagy. *Proceedings of the National Academy of Sciences* 110, 17071-17076. 10.1073/pnas.1315110110.
105. Moreau, K., Fleming, A., Imarisio, S., Lopez Ramirez, A., Mercer, J.L., Jimenez-Sanchez, M., Bento, C.F., Puri, C., Zavodszky, E., Siddiqi, F., et al. (2014). PICALM modulates autophagy activity and tau accumulation. *Nature Communications* 5, 4998. 10.1038/ncomms5998.
106. Zhao, Z., Sagare, A.P., Ma, Q., Halliday, M.R., Kong, P., Kisler, K., Winkler, E.A., Ramanathan, A., Kanekiyo, T., Bu, G., et al. (2015). Central role for PICALM in amyloid- β blood-brain barrier transcytosis and clearance. *Nature neuroscience* 18, 978-987. 10.1038/nn.4025.
107. Molinari, M., Galli, C., Norais, N., Telford, J.L., Rappuoli, R., Luzio, J.P., and Montecucco, C. (1997). Vacuoles Induced by *Helicobacter pylori* Toxin Contain Both Late Endosomal and Lysosomal Markers*. *Journal of Biological Chemistry* 272, 25339-25344. <https://doi.org/10.1074/jbc.272.40.25339>.
108. Carter, C. (2011). Alzheimer's Disease: APP, Gamma Secretase, APOE, CLU, CR1, PICALM, ABCA7, BIN1, CD2AP, CD33, EPHA1, and MS4A2, and Their Relationships with Herpes

- Simplex, C. Pneumoniae, Other Suspect Pathogens, and the Immune System. *Int J Alzheimers Dis* 2011, 501862. 10.4061/2011/501862.
109. Carter, C.J. (2010). APP, APOE, complement receptor 1, clusterin and PICALM and their involvement in the herpes simplex life cycle. *Neurosci Lett* 483, 96-100. 10.1016/j.neulet.2010.07.066.
 110. Wu, J., Gu, J., Shen, L., Fang, D., Zou, X., Cao, Y., Wang, S., and Mao, L. (2019). Exosomal MicroRNA-155 Inhibits Enterovirus A71 Infection by Targeting PICALM. *International Journal of Biological Sciences* 15, 2925-2935. 10.7150/ijbs.36388.
 111. Suzuki, M., Tanaka, H., Tanimura, A., Tanabe, K., Oe, N., Rai, S., Kon, S., Fukumoto, M., Takei, K., Abe, T., et al. (2012). The clathrin assembly protein PICALM is required for erythroid maturation and transferrin internalization in mice. *PLoS One* 7, e31854. 10.1371/journal.pone.0031854.
 112. Kaufmann, S.H.E. (2019). Immunology's Coming of Age. *Front Immunol* 10, 684. 10.3389/fimmu.2019.00684.
 113. Lim, S., Phillips, J.B., Madeira da Silva, L., Zhou, M., Fodstad, O., Owen, L.B., and Tan, M. (2017). Interplay between Immune Checkpoint Proteins and Cellular Metabolism. *Cancer Res* 77, 1245-1249. 10.1158/0008-5472.Can-16-1647.
 114. Belk, J.A., Daniel, B., and Satpathy, A.T. (2022). Epigenetic regulation of T cell exhaustion. *Nat Immunol* 23, 848-860. 10.1038/s41590-022-01224-z.
 115. Miko, E., Meggyes, M., Doba, K., Barakonyi, A., and Szereday, L. (2019). Immune Checkpoint Molecules in Reproductive Immunology. *Front Immunol* 10, 846. 10.3389/fimmu.2019.00846.
 116. Fuertes Marraco, S.A., Neubert, N.J., Verdeil, G., and Speiser, D.E. (2015). Inhibitory Receptors Beyond T Cell Exhaustion. *Front Immunol* 6, 310. 10.3389/fimmu.2015.00310.
 117. Wherry, E.J., and Kurachi, M. (2015). Molecular and cellular insights into T cell exhaustion. *Nat Rev Immunol* 15, 486-499. 10.1038/nri3862.
 118. Cai, X., Zhan, H., Ye, Y., Yang, J., Zhang, M., Li, J., and Zhuang, Y. (2021). Current Progress and Future Perspectives of Immune Checkpoint in Cancer and Infectious Diseases. *Frontiers in Genetics* 12. 10.3389/fgene.2021.785153.
 119. Wherry, E.J. (2011). T cell exhaustion. *Nat Immunol* 12, 492-499. 10.1038/ni.2035.
 120. Day, C.L., Kaufmann, D.E., Kiepiela, P., Brown, J.A., Moodley, E.S., Reddy, S., Mackey, E.W., Miller, J.D., Leslie, A.J., DePierres, C., et al. (2006). PD-1 expression on HIV-specific T cells is associated with T-cell exhaustion and disease progression. *Nature* 443, 350-354. 10.1038/nature05115.
 121. Schönrich, G., and Raftery, M.J. (2019). The PD-1/PD-L1 Axis and Virus Infections: A Delicate Balance. *Frontiers in Cellular and Infection Microbiology* 9, 207. 10.3389/fcimb.2019.00207.
 122. Zhang, J.Y., Zhang, Z., Wang, X., Fu, J.L., Yao, J., Jiao, Y., Chen, L., Zhang, H., Wei, J., Jin, L., et al. (2007). PD-1 up-regulation is correlated with HIV-specific memory CD8+ T-cell exhaustion in typical progressors but not in long-term nonprogressors. *Blood* 109, 4671-4678. 10.1182/blood-2006-09-044826.
 123. Kurachi, M. (2019). CD8(+) T cell exhaustion. *Semin Immunopathol* 41, 327-337. 10.1007/s00281-019-00744-5.
 124. Cohen, M.S., Shaw, G.M., McMichael, A.J., and Haynes, B.F. (2011). Acute HIV-1 Infection. *N Engl J Med* 364, 1943-1954. 10.1056/NEJMra1011874.
 125. Buggert, M., Frederiksen, J., Lund, O., Betts, M.R., Biague, A., Nielsen, M., Tauriainen, J., Norrgren, H., Medstrand, P., Karlsson, A.C., et al. (2016). CD4+ T cells with an activated and exhausted phenotype distinguish immunodeficiency during aviremic HIV-2 infection. *AIDS* 30, 2415-2426. 10.1097/QAD.0000000000001223.
 126. Fenwick, C., Joo, V., Jacquier, P., Noto, A., Banga, R., Perreau, M., and Pantaleo, G. (2019). T-cell exhaustion in HIV infection. *Immunol Rev* 292, 149-163. 10.1111/imr.12823.

127. Pisibon, C., Ouertani, A., Bertolotto, C., Ballotti, R., and Cheli, Y. (2021). Immune Checkpoints in Cancers: From Signaling to the Clinic. *Cancers (Basel)* *13*. 10.3390/cancers13184573.
128. Dyck, L., and Mills, K.H.G. (2017). Immune checkpoints and their inhibition in cancer and infectious diseases. *Eur J Immunol* *47*, 765-779. 10.1002/eji.201646875.
129. Morad, G., Helmink, B.A., Sharma, P., and Wargo, J.A. (2021). Hallmarks of response, resistance, and toxicity to immune checkpoint blockade. *Cell* *184*, 5309-5337. 10.1016/j.cell.2021.09.020.
130. Ai, L., Xu, A., and Xu, J. (2020). Roles of PD-1/PD-L1 Pathway: Signaling, Cancer, and Beyond. *Adv Exp Med Biol* *1248*, 33-59. 10.1007/978-981-15-3266-5_3.
131. Baxevanis, C.N. (2023). Immune Checkpoint Inhibitors in Cancer Therapy-How Can We Improve Clinical Benefits? *Cancers (Basel)* *15*. 10.3390/cancers15030881.
132. Jiang, Y., Li, Y., and Zhu, B. (2015). T-cell exhaustion in the tumor microenvironment. *Cell Death & Disease* *6*, e1792-e1792. 10.1038/cddis.2015.162.
133. Robert, C. (2020). A decade of immune-checkpoint inhibitors in cancer therapy. *Nat Commun* *11*, 3801. 10.1038/s41467-020-17670-y.
134. Shiravand, Y., Khodadadi, F., Kashani, S.M.A., Hosseini-Fard, S.R., Hosseini, S., Sadeghirad, H., Ladwa, R., O'Byrne, K., and Kulasinghe, A. (2022). Immune Checkpoint Inhibitors in Cancer Therapy. *Curr Oncol* *29*, 3044-3060. 10.3390/curroncol29050247.
135. Baitsch, L., Legat, A., Barba, L., Fuertes Marraco, S.A., Rivals, J.P., Baumgaertner, P., Christiansen-Jucht, C., Bouzourene, H., Rimoldi, D., Pircher, H., et al. (2012). Extended co-expression of inhibitory receptors by human CD8 T-cells depending on differentiation, antigen-specificity and anatomical localization. *PLoS One* *7*, e30852. 10.1371/journal.pone.0030852.
136. Jin, S., Liao, Q., Chen, J., Zhang, L., He, Q., Zhu, H., Zhang, X., and Xu, J. (2018). TSC1 and DEPDC5 regulate HIV-1 latency through the mTOR signaling pathway. *Emerg Microbes Infect* *7*, 138. 10.1038/s41426-018-0139-5.
137. Li, Z., Wu, J., Chavez, L., Hoh, R., Deeks, S.G., Pillai, S.K., and Zhou, Q. (2019). Reiterative Enrichment and Authentication of CRISPRi Targets (REACT) identifies the proteasome as a key contributor to HIV-1 latency. *PLoS Pathog* *15*, e1007498. 10.1371/journal.ppat.1007498.
138. Huang, H., Kong, W., Jean, M., Fiches, G., Zhou, D., Hayashi, T., Que, J., Santoso, N., and Zhu, J. (2019). A CRISPR/Cas9 screen identifies the histone demethylase MINA53 as a novel HIV-1 latency-promoting gene (LPG). *Nucleic Acids Res* *47*, 7333-7347. 10.1093/nar/gkz493.
139. Rathore, A., Iketani, S., Wang, P., Jia, M., Sahi, V., and Ho, D.D. (2020). CRISPR-based gene knockout screens reveal deubiquitinases involved in HIV-1 latency in two Jurkat cell models. *Sci Rep* *10*, 5350. 10.1038/s41598-020-62375-3.
140. Krasnopolsky, S., Kuzmina, A., and Taube, R. (2020). Genome-wide CRISPR knockout screen identifies ZNF304 as a silencer of HIV transcription that promotes viral latency. *PLoS Pathog* *16*, e1008834. 10.1371/journal.ppat.1008834.
141. Yang, X., Wang, Y., Lu, P., Shen, Y., Zhao, X., Zhu, Y., Jiang, Z., Yang, H., Pan, H., Zhao, L., et al. (2020). PEBP1 suppresses HIV transcription and induces latency by inactivating MAPK/NF- κ B signaling. *EMBO Rep* *21*, e49305. 10.15252/embr.201949305.
142. Park, R.J., Wang, T., Koundakjian, D., Hultquist, J.F., Lamothe-Molina, P., Monel, B., Schumann, K., Yu, H., Krupczak, K.M., Garcia-Beltran, W., et al. (2017). A genome-wide CRISPR screen identifies a restricted set of HIV host dependency factors. *Nat Genet* *49*, 193-203. 10.1038/ng.3741.
143. Hultquist, J.F., Schumann, K., Woo, J.M., Manganaro, L., McGregor, M.J., Doudna, J., Simon, V., Krogan, N.J., and Marson, A. (2016). A Cas9 Ribonucleoprotein Platform for Functional Genetic Studies of HIV-Host Interactions in Primary Human T Cells. *Cell Rep* *17*, 1438-1452. 10.1016/j.celrep.2016.09.080.

144. Liu, Z., Chen, S., Jin, X., Wang, Q., Yang, K., Li, C., Xiao, Q., Hou, P., Liu, S., Wu, S., et al. (2017). Genome editing of the HIV co-receptors CCR5 and CXCR4 by CRISPR-Cas9 protects CD4(+) T cells from HIV-1 infection. *Cell Biosci* 7, 47. 10.1186/s13578-017-0174-2.
145. Davis, K. (2019). CRISPR-Cas9 Analysis of the HIV-Host Interaction

Network. McGill University.

146. Li, W., Englund, E., Widner, H., Mattsson, B., van Westen, D., Lätt, J., Rehnroona, S., Brundin, P., Björklund, A., Lindvall, O., and Li, J.-Y. (2016). Extensive graft-derived dopaminergic innervation is maintained 24 years after transplantation in the degenerating parkinsonian brain. *Proceedings of the National Academy of Sciences* 113, 6544-6549. 10.1073/pnas.1605245113.
147. McCarthy, D.J., and Smyth, G.K. (2009). Testing significance relative to a fold-change threshold is a TREAT. *Bioinformatics* 25, 765-771. 10.1093/bioinformatics/btp053.
148. Ghoujal, B., Milev, M.P., Ajamian, L., Abel, K., and Mouland, A.J. (2012). ESCRT-II's involvement in HIV-1 genomic RNA trafficking and assembly. *Biol Cell* 104, 706-721. 10.1111/boc.201200021.
149. Stewart, S.A., Dykxhoorn, D.M., Palliser, D., Mizuno, H., Yu, E.Y., An, D.S., Sabatini, D.M., Chen, I.S., Hahn, W.C., Sharp, P.A., et al. (2003). Lentivirus-delivered stable gene silencing by RNAi in primary cells. *Rna* 9, 493-501. 10.1261/rna.2192803.
150. Sanjana, N.E., Shalem, O., and Zhang, F. (2014). Improved vectors and genome-wide libraries for CRISPR screening. *Nat Methods* 11, 783-784. 10.1038/nmeth.3047.
151. Comparison of three quantification methods for the TZM-bl pseudovirus assay for screening of anti-HIV-1 agents | Elsevier Enhanced Reader.
152. Binda, C.S., Klaver, B., Berkhout, B., and Das, A.T. (2020). CRISPR-Cas9 Dual-gRNA Attack Causes Mutation, Excision and Inversion of the HIV-1 Proviral DNA. *Viruses* 12. 10.3390/v12030330.
153. Berkowitz, R.D., Beckerman, K.P., Schall, T.J., and McCune, J.M. (1998). CXCR4 and CCR5 expression delineates targets for HIV-1 disruption of T cell differentiation. *J Immunol* 161, 3702-3710.
154. Cavrois, M., de Noronha, C., and Greene, W.C. (2002). A sensitive and specific enzyme-based assay detecting HIV-1 virion fusion in primary T lymphocytes. *Nature Biotechnology* 20, 1151-1154. 10.1038/nbt745.
155. Klionsky, D.J., Abdel-Aziz, A.K., Abdelfatah, S., Abdellatif, M., Abdoli, A., Abel, S., Abeliovich, H., Abildgaard, M.H., Abudu, Y.P., Acevedo-Arozena, A., et al. (2021). Guidelines for the use and interpretation of assays for monitoring autophagy (4th edition)(1). *Autophagy* 17, 1-382. 10.1080/15548627.2020.1797280.
156. Vyboh, K., Ajamian, L., and Mouland, A.J. (2012). Detection of viral RNA by fluorescence in situ hybridization (FISH). *Journal of Visualized Experiments: JoVE*, e4002. 10.3791/4002.
157. Chen, H.-J., Anagnostou, G., Chai, A., Withers, J., Morris, A., Adhikaree, J., Pennetta, G., and de Belleruche, J.S. (2010). Characterization of the Properties of a Novel Mutation in VAPB in Familial Amyotrophic Lateral Sclerosis. *The Journal of Biological Chemistry* 285, 40266-40281. 10.1074/jbc.M110.161398.
158. Ratnapriya, S., Harris, M., Chov, A., Herbert, Z.T., Vrbanac, V., Deruaz, M., Achuthan, V., Engelman, A.N., Sodroski, J., and Herschhorn, A. (2021). Intra- and extra-cellular environments contribute to the fate of HIV-1 infection. *Cell Rep* 36, 109622. 10.1016/j.celrep.2021.109622.
159. Murooka, T.T., Deruaz, M., Marangoni, F., Vrbanac, V.D., Seung, E., von Andrian, U.H., Tager, A.M., Luster, A.D., and Mempel, T.R. (2012). HIV-infected T cells are migratory vehicles for viral dissemination. *Nature* 490, 283-287. 10.1038/nature11398.
160. Wu, S., Majeed, S.R., Evans, T.M., Camus, M.D., Wong, N.M., Schollmeier, Y., Park, M., Muppidi, J.R., Reboldi, A., Parham, P., et al. (2016). Clathrin light chains' role in selective

- endocytosis influences antibody isotype switching. *Proc Natl Acad Sci U S A* *113*, 9816-9821. 10.1073/pnas.1611189113.
161. Ashkenazi, A., Viard, M., Wexler-Cohen, Y., Blumenthal, R., and Shai, Y. (2011). Viral envelope protein folding and membrane hemifusion are enhanced by the conserved loop region of HIV-1 gp41. *Faseb j* *25*, 2156-2166. 10.1096/fj.10-175752.
 162. Maréchal, V., Prevost, M.C., Petit, C., Perret, E., Heard, J.M., and Schwartz, O. (2001). Human immunodeficiency virus type 1 entry into macrophages mediated by macropinocytosis. *J Virol* *75*, 11166-11177. 10.1128/jvi.75.22.11166-11177.2001.
 163. Carter, G.C., Bernstone, L., Baskaran, D., and James, W. (2011). HIV-1 infects macrophages by exploiting an endocytic route dependent on dynamin, Rac1 and Pak1. *Virology* *409*, 234-250. 10.1016/j.virol.2010.10.018.
 164. Pauza, C.D., and Price, T.M. (1988). Human immunodeficiency virus infection of T cells and monocytes proceeds via receptor-mediated endocytosis. *J Cell Biol* *107*, 959-968. 10.1083/jcb.107.3.959.
 165. de la Vega, M., Marin, M., Kondo, N., Miyauchi, K., Kim, Y., Epand, R.F., Epand, R.M., and Melikyan, G.B. (2011). Inhibition of HIV-1 endocytosis allows lipid mixing at the plasma membrane, but not complete fusion. *Retrovirology* *8*, 99. 10.1186/1742-4690-8-99.
 166. Kondo, N., Marin, M., Kim, J.H., Desai, T.M., and Melikyan, G.B. (2015). Distinct requirements for HIV-cell fusion and HIV-mediated cell-cell fusion. *J Biol Chem* *290*, 6558-6573. 10.1074/jbc.M114.623181.
 167. Galluzzi, L., and Green, D.R. (2019). Autophagy-Independent Functions of the Autophagy Machinery. *Cell* *177*, 1682-1699. 10.1016/j.cell.2019.05.026.
 168. Ravikumar, B., Moreau, K., Jahreiss, L., Puri, C., and Rubinsztein, D.C. (2010). Plasma membrane contributes to the formation of pre-autophagosomal structures. *Nat Cell Biol* *12*, 747-757. 10.1038/ncb2078.
 169. Alsaqati, M., Thomas, R.S., and Kidd, E.J. (2018). Proteins Involved in Endocytosis Are Upregulated by Ageing in the Normal Human Brain: Implications for the Development of Alzheimer's Disease. *J Gerontol A Biol Sci Med Sci* *73*, 289-298. 10.1093/gerona/glx135.
 170. Vyboh, K., Ajamian, L., and Moulard, A.J. (2012). Detection of viral RNA by fluorescence in situ hybridization (FISH). *J Vis Exp*, e4002. 10.3791/4002.
 171. Wang, C., Tu, J., Zhang, S., Cai, B., Liu, Z., Hou, S., Zhong, Q., Hu, X., Liu, W., Li, G., et al. (2020). Different regions of synaptic vesicle membrane regulate VAMP2 conformation for the SNARE assembly. *Nature Communications* *11*, 1531. 10.1038/s41467-020-15270-4.
 172. Dumont, V., and Lehtonen, S. (2022). PACSIN proteins in vivo: Roles in development and physiology. *Acta Physiol (Oxf)* *234*, e13783. 10.1111/apha.13783.
 173. Nath, S., Dancourt, J., Shteyn, V., Puente, G., Fong, W.M., Nag, S., Bewersdorf, J., Yamamoto, A., Antony, B., and Melia, T.J. (2014). Lipidation of the LC3/GABARAP family of autophagy proteins relies on a membrane-curvature-sensing domain in Atg3. *Nat Cell Biol* *16*, 415-424. 10.1038/ncb2940.
 174. Nardacci, R., Amendola, A., Ciccocanti, F., Corazzari, M., Esposito, V., Vlassi, C., Taibi, C., Fimia, G.M., Del Nonno, F., Ippolito, G., et al. (2014). Autophagy plays an important role in the containment of HIV-1 in nonprogressor-infected patients. *Autophagy* *10*, 1167-1178. 10.4161/auto.28678.
 175. Laforge, M., Limou, S., Harper, F., Casartelli, N., Rodrigues, V., Silvestre, R., Haloui, H., Zagury, J.F., Senik, A., and Estaquier, J. (2013). DRAM triggers lysosomal membrane permeabilization and cell death in CD4(+) T cells infected with HIV. *PLoS Pathog* *9*, e1003328. 10.1371/journal.ppat.1003328.
 176. Killian, M.S. (2012). Dual role of autophagy in HIV-1 replication and pathogenesis. *AIDS Res Ther* *9*, 16. 10.1186/1742-6405-9-16.
 177. Leymarie, O., Lepont, L., and Berlioz-Torrent, C. (2017). Canonical and Non-Canonical Autophagy in HIV-1 Replication Cycle. *Viruses* *9*. 10.3390/v9100270.

178. Santerre, M., Arjona, S.P., Allen, C.N., Callen, S., Buch, S., and Sawaya, B.E. (2021). HIV-1 Vpr protein impairs lysosome clearance causing SNCA/alpha-synuclein accumulation in neurons. *Autophagy* *17*, 1768-1782. 10.1080/15548627.2021.1915641.
179. Cavrois, M., De Noronha, C., and Greene, W.C. (2002). A sensitive and specific enzyme-based assay detecting HIV-1 virion fusion in primary T lymphocytes. *Nat Biotechnol* *20*, 1151-1154. 10.1038/nbt745.
180. Daecke, J., Fackler, O.T., Dittmar, M.T., and Kräusslich, H.G. (2005). Involvement of clathrin-mediated endocytosis in human immunodeficiency virus type 1 entry. *J Virol* *79*, 1581-1594. 10.1128/jvi.79.3.1581-1594.2005.
181. Miyauchi, K., Kim, Y., Latinovic, O., Morozov, V., and Melikyan, G.B. (2009). HIV enters cells via endocytosis and dynamin-dependent fusion with endosomes. *Cell* *137*, 433-444. 10.1016/j.cell.2009.02.046.
182. Motamedi, M., Xu, L., and Elahi, S. (2016). Correlation of transferrin receptor (CD71) with Ki67 expression on stimulated human and mouse T cells: The kinetics of expression of T cell activation markers. *J Immunol Methods* *437*, 43-52. 10.1016/j.jim.2016.08.002.
183. Moran, A.E., Polesso, F., and Weinberg, A.D. (2016). Immunotherapy Expands and Maintains the Function of High-Affinity Tumor-Infiltrating CD8 T Cells In Situ. *J Immunol* *197*, 2509-2521. 10.4049/jimmunol.1502659.
184. Ahn, E., Araki, K., Hashimoto, M., Li, W., Riley, J.L., Cheung, J., Sharpe, A.H., Freeman, G.J., Irving, B.A., and Ahmed, R. (2018). Role of PD-1 during effector CD8 T cell differentiation. *Proc Natl Acad Sci U S A* *115*, 4749-4754. 10.1073/pnas.1718217115.
185. Ding, G., Shen, T., Yan, C., Zhang, M., Wu, Z., and Cao, L. (2019). IFN-gamma down-regulates the PD-1 expression and assist nivolumab in PD-1-blockade effect on CD8+ T-lymphocytes in pancreatic cancer. *BMC Cancer* *19*, 1053. 10.1186/s12885-019-6145-8.
186. Husebye, H., Halaas, O., Stenmark, H., Tunheim, G., Sandanger, O., Bogen, B., Brech, A., Latz, E., and Espevik, T. (2006). Endocytic pathways regulate Toll-like receptor 4 signaling and link innate and adaptive immunity. *EMBO J* *25*, 683-692. 10.1038/sj.emboj.7600991.
187. Pascual-Lucas, M., Fernandez-Lizarbe, S., Montesinos, J., and Guerri, C. (2014). LPS or ethanol triggers clathrin- and rafts/caveolae-dependent endocytosis of TLR4 in cortical astrocytes. *J Neurochem* *129*, 448-462. 10.1111/jnc.12639.
188. Di Mitri, D., Azevedo, R.I., Henson, S.M., Libri, V., Riddell, N.E., Macaulay, R., Kipling, D., Soares, M.V., Battistini, L., and Akbar, A.N. (2011). Reversible senescence in human CD4+CD45RA+CD27- memory T cells. *J Immunol* *187*, 2093-2100. 10.4049/jimmunol.1100978.
189. Fromentin, R., DaFonseca, S., Costiniuk, C.T., El-Far, M., Procopio, F.A., Hecht, F.M., Hoh, R., Deeks, S.G., Hazuda, D.J., Lewin, S.R., et al. (2019). PD-1 blockade potentiates HIV latency reversal ex vivo in CD4(+) T cells from ART-suppressed individuals. *Nat Commun* *10*, 814. 10.1038/s41467-019-08798-7.
190. Lopez, P., Ajibola, O., Pagliuzza, A., Zayats, R., Koh, W.H., Herschhorn, A., Chomont, N., and Murooka, T.T. (2022). T cell migration potentiates HIV infection by enhancing viral fusion and integration. *Cell Rep* *38*, 110406. 10.1016/j.celrep.2022.110406.
191. Januário, Y.C., and daSilva, L.L.P. (2020). Hijacking of endocytosis by HIV-1 Nef is becoming crystal clear. *Nat Struct Mol Biol* *27*, 773-775. 10.1038/s41594-020-0486-5.
192. Pereira, E.A., and daSilva, L.L. (2016). HIV-1 Nef: Taking Control of Protein Trafficking. *Traffic* *17*, 976-996. 10.1111/tra.12412.
193. Marin, M., Kushnareva, Y., Mason, C.S., Chanda, S.K., and Melikyan, G.B. (2019). HIV-1 Fusion with CD4+ T cells Is Promoted by Proteins Involved in Endocytosis and Intracellular Membrane Trafficking. *Viruses* *11*. 10.3390/v11020100.
194. Campbell, G.R., Rawat, P., Bruckman, R.S., and Spector, S.A. (2015). Human Immunodeficiency Virus Type 1 Nef Inhibits Autophagy through Transcription Factor EB Sequestration. *PLoS Pathog* *11*, e1005018. 10.1371/journal.ppat.1005018.

195. Castro-Gonzalez, S., Shi, Y., Colomer-Lluch, M., Song, Y., Mowery, K., Almodovar, S., Bansal, A., Kirchhoff, F., Sparrer, K., Liang, C., and Serra-Moreno, R. (2021). HIV-1 Nef counteracts autophagy restriction by enhancing the association between BECN1 and its inhibitor BCL2 in a PRKN-dependent manner. *Autophagy* 17, 553-577. 10.1080/15548627.2020.1725401.
196. Schönrich, G., and Raftery, M.J. (2019). The PD-1/PD-L1 Axis and Virus Infections: A Delicate Balance. *Front Cell Infect Microbiol* 9, 207. 10.3389/fcimb.2019.00207.
197. Balança, C.C., Salvioni, A., Scarlata, C.M., Michelas, M., Martinez-Gomez, C., Gomez-Roca, C., Sarradin, V., Tosolini, M., Valle, C., Pont, F., et al. (2021). PD-1 blockade restores helper activity of tumor-infiltrating, exhausted PD-1hiCD39+ CD4 T cells. *JCI Insight* 6. 10.1172/jci.insight.142513.
198. Goods, B.A., Hernandez, A.L., Lowther, D.E., Lucca, L.E., Lerner, B.A., Gunel, M., Raddassi, K., Coric, V., Hafler, D.A., and Love, J.C. (2017). Functional differences between PD-1+ and PD-1- CD4+ effector T cells in healthy donors and patients with glioblastoma multiforme. *PLoS One* 12, e0181538. 10.1371/journal.pone.0181538.
199. Wang, Y., Chung, Y.R., Eitzinger, S., Palacio, N., Gregory, S., Bhattacharyya, M., and Penaloza-MacMaster, P. (2019). TLR4 signaling improves PD-1 blockade therapy during chronic viral infection. *PLoS Pathog* 15, e1007583. 10.1371/journal.ppat.1007583.
200. Pauken, K.E., Godec, J., Odorizzi, P.M., Brown, K.E., Yates, K.B., Ngiow, S.F., Burke, K.P., Maleri, S., Grande, S.M., Francisco, L.M., et al. (2020). The PD-1 Pathway Regulates Development and Function of Memory CD8(+) T Cells following Respiratory Viral Infection. *Cell Rep* 31, 107827. 10.1016/j.celrep.2020.107827.
201. Fernandez, T.D., Torres, M.J., Lopez, S., Antunez, C., Gomez, E., Del Prado, M.F., Canto, G., Blanca, M., and Mayorga, C. (2010). Role of effector cells (CCR7(-)CD27(-)) and effector-memory cells (CCR7(-)CD27(+)) in drug-induced maculopapular exanthema. *Int J Immunopathol Pharmacol* 23, 437-447. 10.1177/039463201002300206.
202. Fritsch, R.D., Shen, X., Sims, G.P., Hathcock, K.S., Hodes, R.J., and Lipsky, P.E. (2005). Stepwise differentiation of CD4 memory T cells defined by expression of CCR7 and CD27. *J Immunol* 175, 6489-6497. 10.4049/jimmunol.175.10.6489.
203. Schoenberger, S.P. (2012). CD69 guides CD4+ T cells to the seat of memory. *Proc Natl Acad Sci U S A* 109, 8358-8359. 10.1073/pnas.1204616109.
204. Saad, E., Oroya, A., and Rudd, C. (2020). Anti-PD-1 induces the endocytosis of the co-receptor from the surface of T-cells: Nivolumab is more effective than Pembrolizumab. *held in Philadelphia, (Cancer Res)*, pp. 6528.
205. Yao, H., Li, C., He, F., Song, T., Brosseau, J.P., Wang, H., Lu, H., Fang, C., Shi, H., Lan, J., et al. (2021). A peptidic inhibitor for PD-1 palmitoylation targets its expression and functions. *RSC Chem Biol* 2, 192-205. 10.1039/d0cb00157k.
206. Nelson, A.R., Sagare, A.P., and Zlokovic, B.V. (2016). Chapter 9 - Blood-Brain Barrier Transport of Alzheimer's Amyloid β -Peptide. In *Developing Therapeutics for Alzheimer's Disease*, M.S. Wolfe, ed. (Academic Press), pp. 251-270. <https://doi.org/10.1016/B978-0-12-802173-6.00009-5>.
207. Evans, V.A., van der Sluis, R.M., Solomon, A., Dantanarayana, A., McNeil, C., Garsia, R., Palmer, S., Fromentin, R., Chomont, N., Sékaly, R.P., et al. (2018). Programmed cell death-1 contributes to the establishment and maintenance of HIV-1 latency. *Aids* 32, 1491-1497. 10.1097/qad.0000000000001849.
208. Uldrick, T.S., Adams, S.V., Fromentin, R., Roche, M., Fling, S.P., Gonçalves, P.H., Lurain, K., Ramaswami, R., Wang, C.J., Gorelick, R.J., et al. (2022). Pembrolizumab induces HIV latency reversal in people living with HIV and cancer on antiretroviral therapy. *Sci Transl Med* 14, eab13836. 10.1126/scitranslmed.abl3836.
209. Baron, M., Soulié, C., Lavolé, A., Assoumou, L., Abbar, B., Fouquet, B., Rousseau, A., Veyri, M., Samri, A., Makinson, A., et al. (2022). Impact of Anti PD-1 Immunotherapy on HIV

- Reservoir and Anti-Viral Immune Responses in People Living with HIV and Cancer. *Cells* **11**. 10.3390/cells11061015.
210. Yuan, Y., Jacobs, C., Garcia, I.L., Pereira, P.M., Lawrence, S.P., Laine, R.F., Marsh, M., and Henriques, R. (2021). Single-molecule super-resolution imaging of T-cell plasma membrane CD4 redistribution upon HIV-1 binding. *bioRxiv*, 2021.2001.2005.425371. 10.1101/2021.01.05.425371.

CHAPTER 7: SUPPLEMENTARY MATERIAL

Table S 1. CRISPR screen target sequences.

Gene Symbol	Target Sequence	Genomic Location	PAM
<i>ACTR2</i>	GCTCTTCCCTGGGCGGACGA	hg38 chr2:65227891-65227913	TGG
<i>ACTR2</i>	GTGGTGTGCGACAACGGCAC	hg38 chr2:65227934-65227956	CGG
<i>ACTR2</i>	GGCTGTCCATCGTCCGCCCA	hg38 -chr2:65227897-65227919	GGG
<i>ACTR2</i>	GGATGACATGAAACACCTGT	hg38 chr2:65246610-65246632	GGG
<i>ACTR3</i>	AGAACGGACGTTGACCGGTA	hg38 chr2:113934323-113934345	CGG
<i>ACTR3</i>	TAATAGTGGCCAATCCGCCA	hg38 chr2:113927339-113927361	TGG
<i>ACTR3</i>	TCCACTGTCTATTACCGTAC	hg38 -chr2:113934337-113934359	CGG
<i>ACTR3</i>	TCTTGACCTCAAGACAAGT	hg38 chr2:113934300-113934322	AGG
<i>ADAM10</i>	GGATTCATCCAGACTCGTGG	hg38 -chr15:58679210-58679232	TGG
<i>ADAM10</i>	GGCAACTTTGGATTACTACT	hg38 chr15:58599618-58599640	TGG
<i>ADAM10</i>	ATCTCGGTCTGTGAAGACAT	hg38 chr15:58640823-58640845	AGG
<i>ADAM10</i>	AAGTGTCCCTCTTCATTCGT	hg38 chr15:58682283-58682305	AGG
<i>AMPH</i>	ATTAGTGGCTTACCGTCCAT	hg38 chr7:38432176-38432198	AGG
<i>AMPH</i>	ACTGATTTGGTACAGCCGGT	hg38 -chr7:38429837-38429859	AGG
<i>AMPH</i>	CCTCGGTCACCTTCACAGGT	hg38 -chr7:38462970-38462992	AGG
<i>AMPH</i>	CATCCAAGGAGCGCCAGGT	hg38 -chr7:38465462-38465484	AGG
<i>AP1B1</i>	TTGTGGGCGAGTACGCGGAA	hg38 -chr22:29349281-29349303	CGG
<i>AP1B1</i>	GTTGTTCTTCACGGCCACCT	hg38 chr22:29331516-29331538	AGG
<i>AP1B1</i>	GTTCTTGAGGATGGTCTCGT	hg38 chr22:29328824-29328846	AGG
<i>AP1B1</i>	GATGTCCTTGATGACCACGA	hg38 chr22:29350055-29350077	TGG
<i>AP1M1</i>	CCACGTGCCACGGTAGTTC	hg38 -chr19:16203470-16203492	CGG
<i>AP1M1</i>	GTCCTGCGCAGCGAGATCGT	hg38 chr19:16226439-16226461	GGG
<i>AP1M1</i>	TTGTCTTCGGCCTCCACACT	hg38 -chr19:16233532-16233554	AGG
<i>AP1M1</i>	GAGTCTGTCAACCTCTTGGT	hg38 chr19:16209160-16209182	AGG
<i>AP1M2</i>	GTCCTTCTGAGCGAAATCGT	hg38 -chr19:10581352-10581374	CGG
<i>AP1M2</i>	ATTGATCAGCCGCAACTACA	hg38 -chr19:10584046-10584068	AGG
<i>AP1M2</i>	ATCCCAGAGACGGTGAAGTA	hg38 chr19:10574908-10574930	GGG
<i>AP1M2</i>	TTGATCAGCCGCAACTACAA	hg38 -chr19:10584045-10584067	GGG
<i>AP2A1</i>	TCACGTAGTCGCCCGCAATG	hg38 -chr19:49800045-49800067	CGG
<i>AP2A1</i>	CTGCACTGCATCGCCAACGT	hg38 chr19:49782645-49782667	GGG
<i>AP2A1</i>	GTTCCGGGCCTGCAACCAGCT	hg38 chr19:49799343-49799365	GGG
<i>AP2A1</i>	GTGCGTCTTGACGGCTTCAT	hg38 -chr19:49799446-49799468	GGG
<i>AP2A2</i>	ACCCGGCTACGAGGACCTTA	hg38 -chr11:972235-972257	GGG
<i>AP2A2</i>	TACCCGGCTACGAGGACCTT	hg38 -chr11:972236-972258	AGG
<i>AP2A2</i>	CCTGGCTGAGAAGTACGCGG	hg38 chr11:992520-992542	TGG
<i>AP2A2</i>	CTGCACTGCATCGCCAGCGT	hg38 chr11:972176-972198	GGG
<i>AP2B1</i>	GAGCCTCCCGATCATCTTTA	hg38 -chr17:35624561-35624583	GGG
<i>AP2B1</i>	GGTGGTGGCTAATGCCGTAG	hg38 chr17:35624396-35624418	CGG
<i>AP2B1</i>	TAATCCTTTGATTGAGCCT	hg38 chr17:35608156-35608178	TGG
<i>AP2B1</i>	TTGCAGTGGTAGTGCCAACA	hg38 -chr17:35657617-35657639	GGG
<i>AP2M1</i>	AAATGTTGGACCGCTTAACG	hg38 -chr3:184178950-184178972	TGG
<i>AP2M1</i>	GAGAGGGTATCAAGTATCGT	hg38 chr3:184180907-184180929	CGG

<i>AP2M1</i>	GCATGCCTGAATGCAAGTTT	hg38 chr3:184181142-184181164	GGG
<i>AP2M1</i>	TACCCACAGAATTCCGAGAC	hg38 chr3:184180186-184180208	AGG
<i>AP3D1</i>	TTGCCCAGCCGCGGTTCCAA	hg38 chr19:2129126-2129148	AGG
<i>AP3D1</i>	ATGTCCTCGTCGCTCTCCGT	hg38 chr19:2115265-2115287	GGG
<i>AP3D1</i>	CTGGATGGTGAACACATACT	hg38 chr19:2110187-2110209	GGG
<i>AP3D1</i>	TTCACATACTGATCTGACAT	hg38 chr19:2115391-2115413	AGG
<i>AP4E1</i>	GTGCGCCTGAGATGTCAATT	hg38 -chr15:50958619-50958641	TGG
<i>AP4E1</i>	GGTCACAGCAGCAATTAACC	hg38 -chr15:50958598-50958620	AGG
<i>AP4E1</i>	GCCCTCACCTCCAAGCACGT	hg38 chr15:50908911-50908933	AGG
<i>AP4E1</i>	GTGCCATACACACTTCTACT	hg38 -chr15:50925115-50925137	AGG
<i>ARF1</i>	GTGTTTCGCCAACAAGCAGGT	hg38 chr1:228097698-228097720	AGG
<i>ARF1</i>	GAAATGCGCATCCTCATGGT	hg38 chr1:228097163-228097185	GGG
<i>ARF1</i>	ATCCTCTACAAGCTTAAGCT	hg38 chr1:228097211-228097233	GGG
<i>ARF1</i>	CACCCAGCTTAAGCTTGTAG	hg38 -chr1:228097213-228097235	AGG
<i>ARF6</i>	CTCATCGATGCGGTTCGCGGT	hg38 -chr14:49894008-49894030	CGG
<i>ARF6</i>	ACCAGTTCCTGTCCCGAATC	hg38 -chr14:49894162-49894184	CGG
<i>ARF6</i>	GAAATGCGGATCCTCATGTT	hg38 chr14:49893773-49893795	GGG
<i>ARF6</i>	CATTACTACACTGGGACCCA	hg38 chr14:49893962-49893984	AGG
<i>ARFIP2</i>	CCATGACGGACGGGATCCTA	hg38 -chr11:6480401-6480423	GGG
<i>ARFIP2</i>	GGCATCAACACCTATAAGGT	hg38 -chr11:6479135-6479157	AGG
<i>ARFIP2</i>	TATGAGAGTGTCTGCAGCT	hg38 -chr11:6478835-6478857	GGG
<i>ARFIP2</i>	GTGCTTAAATCCTACCTTAT	hg38 chr11:6479125-6479147	AGG
<i>ARPC1B</i>	GGTCATCCTGCGGATCAACC	hg38 chr7:99388139-99388161	GGG
<i>ARPC1B</i>	GCCCTTCAGCGTCCACACGT	hg38 -chr7:99388096-99388118	AGG
<i>ARPC1B</i>	CTGTGCCGCAGGTCACAATA	hg38 -chr7:99388064-99388086	CGG
<i>ARPC1B</i>	ATGTGCTTGCAAACCCACCT	hg38 -chr7:99389900-99389922	GGG
<i>ARPC2</i>	GATGGTGTGTCTCGAGCAC	hg38 -chr2:218249388-218249410	TGG
<i>ARPC2</i>	AGTTATTAAGAGGGTGTAC	hg38 chr2:218234350-218234372	GGG
<i>ARPC2</i>	CACTGGCATTGGTGTGACGA	hg38 -chr2:218249371-218249393	GGG
<i>ARPC2</i>	CATGCCAGCTTGATGCACAA	hg38 -chr2:218238718-218238740	TGG
<i>ARPC3</i>	GATCCTGATACCAAACCTCAT	hg38 -chr12:110445508-110445530	CGG
<i>ARPC3</i>	ATTGGCCTTGAAGTAATAGA	hg38 chr12:110440339-110440361	TGG
<i>ARPC3</i>	AACCCTCACCGGCATCTTGG	hg38 chr12:110450246-110450268	CGG
<i>ARPC3</i>	TGCCATGTTTCCGATGAGTT	hg38 chr12:110445498-110445520	TGG
<i>ARPC4</i>	AGAACTTCTTTATCCTTCGA	hg38 chr3:9801722-9801744	AGG
<i>ARPC4</i>	GCCCGGCTCTCTACCATCG	hg38 -chr3:9793117-9793139	CGG
<i>ARPC4</i>	CCTCCACAGGCTTCCTTCGA	hg38 -chr3:9801735-9801757	AGG
<i>ARPC4</i>	TATCCTTCGAAGGAAGCCTG	hg38 chr3:9801732-9801754	TGG
<i>ARPC5</i>	CAGTGTCTCGCGCCCGCTTC	hg38 -chr1:183635624-183635646	CGG
<i>ARPC5</i>	TAGCACTGCTATTGTCAGAC	hg38 chr1:183630484-183630506	GGG
<i>ARPC5</i>	CCTGACTCTTGGTGTGATA	hg38 chr1:183633090-183633112	GGG
<i>ARPC5</i>	ACACCCTTAACCTCCATCAC	hg38 -chr1:183633152-183633174	AGG
<i>ARRB1</i>	TCCTACCTCCTTATCCAGAG	hg38 chr11:75278603-75278625	AGG
<i>ARRB1</i>	AGAAGCCTCTCTGGATAAGG	hg38 -chr11:75278608-75278630	AGG
<i>ARRB1</i>	ACGTGGACGTTGACGCTGAT	hg38 chr11:75277408-75277430	GGG
<i>ARRB1</i>	ATCTCAAAGAGCGGAGAGGT	hg38 -chr11:75284230-75284252	AGG
<i>ARRB2</i>	GACTACCTGAAGGACCGCAA	hg38 chr17:4716170-4716192	AGG
<i>ARRB2</i>	GTCCCGCTTGCCCAAGTACA	hg38 -chr17:4715977-4715999	CGG

<i>ARRB2</i>	CCAGGTCTTCACGGCCATAG	hg38 -chr17:4716437-4716459	CGG
<i>ARRB2</i>	GAGAAACCCGGGACCAGGTA	hg38 +chr17:4710728-4710750	AGG
<i>ASAP2</i>	GAACATGGGACCGAGCGGAA	hg38 +chr2:9344589-9344611	CGG
<i>ASAP2</i>	GGGAAGGCCTCCATCGAGAT	hg38 +chr2:9379038-9379060	AGG
<i>ASAP2</i>	GGCCCACTCACCTATCTCGA	hg38 -chr2:9379048-9379070	TGG
<i>ASAP2</i>	ATGATTCGGACTGAAATAAG	hg38 +chr2:9323167-9323189	CGG
<i>ATG12</i>	CCTCCAGCAGCAATTGAAGT	hg38 +chr5:115841497-115841519	AGG
<i>ATG12</i>	TCGAGTGTCTCCAAGCAAGA	hg38 -chr5:115841549-115841571	TGG
<i>ATG12</i>	GTCTCCAAGCAAGATGGCGG	hg38 -chr5:115841543-115841565	AGG
<i>ATG12</i>	AGAAGTTGGAACCTCTCTATG	hg38 -chr5:115832601-115832623	AGG
<i>ATM</i>	GACACAATGCAACTTCCGTA	hg38 -chr11:108250839-108250861	AGG
<i>ATM</i>	GTTAGTGATGCAAACGAACC	hg38 +chr11:108267300-108267322	TGG
<i>ATM</i>	GACCAATACTGTGTCCTTTA	hg38 +chr11:108268507-108268529	GGG
<i>ATM</i>	AATGGAGACAGCTCACAGTT	hg38 -chr11:108250747-108250769	AGG
<i>ATP6V0A1</i>	CTTGTGCACGTAGTCGCCCT	hg38 -chr17:42480662-42480684	AGG
<i>ATP6V0A1</i>	ATGTTTGGGAGACTTCGGTCA	hg38 +chr17:42494375-42494397	TGG
<i>ATP6V0A1</i>	GGTGGGCAACGGACCGACAG	hg38 +chr17:42507546-42507568	AGG
<i>ATP6V0A1</i>	CTGGGTTTCAGCTGTAGAACA	hg38 -chr17:42495647-42495669	GGG
<i>BECN1</i>	TTGCGCTATACTGACCTGTA	hg38 +chr17:42811640-42811662	GGG
<i>BECN1</i>	ATTGCGCTATACTGACCTGT	hg38 +chr17:42811639-42811661	AGG
<i>BECN1</i>	GGTTTCCGTAAGGAACAAGT	hg38 +chr17:42813983-42814005	CGG
<i>BECN1</i>	GAAGGTTGCATTAAAGACGT	hg38 +chr17:42815916-42815938	TGG
<i>BIN1</i>	CCGCCCTTCTGTAGCCGCGT	hg38 -chr2:127063638-127063660	AGG
<i>BIN1</i>	ACCTGGCCTCCGTCAAAGGT	hg38 -chr2:127070757-127070779	AGG
<i>BIN1</i>	TCATCCCTGCCGGGCCAATC	hg38 +chr2:127070572-127070594	GGG
<i>BIN1</i>	GTGTATGAGCCCGATTGGCC	hg38 -chr2:127070581-127070603	CGG
<i>CAMK1</i>	TGTGGAACCTCCGGGATACGT	hg38 -chr3:9761630-9761652	GGG
<i>CAMK1</i>	GGCATCATTCTCGTCATAGA	hg38 +chr3:9760729-9760751	AGG
<i>CAMK1</i>	CTGTGGAACCTCCGGGATACG	hg38 -chr3:9761631-9761653	TGG
<i>CAMK1</i>	GATGTAGGCGATGACACCTA	hg38 +chr3:9761463-9761485	TGG
<i>CAV1</i>	ACTAACCCTCCGACAGCTA	hg38 -chr7:116526372-116526394	CGG
<i>CAV1</i>	AGTGTACGACGCGCACACCA	hg38 +chr7:116526614-116526636	AGG
<i>CAV1</i>	ATGTTGCCCTGTTCCCGGAT	hg38 -chr7:116526543-116526565	GGG
<i>CAV1</i>	TGCCATCGGGATGCCAAAGA	hg38 -chr7:116559064-116559086	GGG
<i>CAV2</i>	GCTCCATTGTGTACGAGCGT	hg38 +chr7:116506056-116506078	AGG
<i>CAV2</i>	CGTCCTACGCTCGTACACAA	hg38 -chr7:116506059-116506081	TGG
<i>CAV2</i>	AATTCCTCCGAATGAAGGCCA	hg38 -chr7:116500393-116500415	GGG
<i>CAV2</i>	TGCCTTCAGTGACAGACAATA	hg38 +chr7:116506009-116506031	TGG
<i>CAV3</i>	GTGGATATCCTTGACGATCT	hg38 -chr3:8733908-8733930	GGG
<i>CAV3</i>	TGATGCACTGGATCTCGATC	hg38 -chr3:8745741-8745763	AGG
<i>CAV3</i>	CCACACGCCGTCAAAGCTGT	hg38 -chr3:8745563-8745585	AGG
<i>CAV3</i>	GTGGGCACCTACAGCTTTGA	hg38 +chr3:8745556-8745578	CGG
<i>CBL</i>	GAAGGCGGCCGTTCCACCTA	hg38 -chr11:119284963-119284985	GGG
<i>CBL</i>	TAAAGGTACTGAACCCATCG	hg38 +chr11:119278551-119278573	TGG
<i>CBL</i>	ATCAAACGGATCTACCACGA	hg38 -chr11:119278565-119278587	TGG
<i>CBL</i>	GTGCTGCTCTCGGTGATAGA	hg38 -chr11:119297454-119297476	TGG
<i>CBLB</i>	TTGTGGGATGTGACTCCTA	hg38 -chr3:105702220-105702242	GGG
<i>CBLB</i>	CCAATCGAGTGCAACTTAAC	hg38 +chr3:105740600-105740622	CGG

<i>CBLB</i>	TGTGACACATCCAGGTTACA	hg38 -chr3:105745978-105746000	TGG
<i>CBLB</i>	GCTGCTATAGATTTAGACGT	hg38 +chr3:105658966-105658988	GGG
<i>CBLC</i>	GAAGACGTCGAACTCGAAGA	hg38 -chr19:44781326-44781348	TGG
<i>CBLC</i>	TTCTGCCGCTGCGAGATCAA	hg38 +chr19:44793498-44793520	GGG
<i>CBLC</i>	GGTCGACGCATTGCTCTTCT	hg38 -chr19:44778012-44778034	AGG
<i>CBLC</i>	GGTTGTGGGTCTTTCCATCT	hg38 -chr19:44790013-44790035	GGG
<i>CDC42</i>	GGAGTGTTCTGCACTTACAC	hg38 +chr1:22086845-22086867	AGG
<i>CDC42</i>	GAAGCCTTTATACTTACAGT	hg38 -chr1:22078578-22078600	CGG
<i>CDC42</i>	AGAAAGGAGTCTTTGGACAG	hg38 -chr1:22086689-22086711	TGG
<i>CDC42</i>	TGAGTCCCAACAAGCAAGAA	hg38 -chr1:22086705-22086727	AGG
<i>CFL1</i>	GCATAGCGGCAGTCCTTATC	hg38 +chr11:65855998-65856020	TGG
<i>CFL1</i>	ATTGCAAGCAAAGTCTGACG	hg38 -chr11:65855413-65855435	AGG
<i>CFL1</i>	CTCATAGGTTGCATCATAGA	hg38 +chr11:65855976-65855998	GGG
<i>CFL1</i>	TTGCATCATAGAGGGCATAG	hg38 +chr11:65855984-65856006	CGG
<i>CIB1</i>	CTTCAAGGAGCGAATCTGCA	hg38 -chr15:90231477-90231499	GGG
<i>CIB1</i>	ATGGGACTTGATGTCTGGCG	hg38 +chr15:90231376-90231398	TGG
<i>CIB1</i>	CTGCAGATTCGCTCCTTGAA	hg38 +chr15:90231479-90231501	GGG
<i>CIB1</i>	AAAGATGCGGAAGGCATAAT	hg38 +chr15:90231358-90231380	GGG
<i>CIB2</i>	CGCCACGATCCTTTCTTTGA	hg38 +chr15:78109353-78109375	AGG
<i>CIB2</i>	CTTCAAAGAAAGGATCGTGG	hg38 -chr15:78109352-78109374	CGG
<i>CIB2</i>	CTGGTTACCATAGATCTTGA	hg38 +chr15:78109227-78109249	AGG
<i>CIB2</i>	AGAGCAGCTAGACAACCTACC	hg38 -chr15:78131164-78131186	AGG
<i>CIB3</i>	CGACGACTACATTTGTGCGT	hg38 -chr19:16164881-16164903	GGG
<i>CIB3</i>	GATTGCCAGGTATTCTCTG	hg38 -chr19:16168242-16168264	AGG
<i>CIB3</i>	CCCATCCTCAGAGAATACCT	hg38 +chr19:16168237-16168259	GGG
<i>CIB3</i>	ATACCTGGGCAATCCTCTGG	hg38 +chr19:16168251-16168273	CGG
<i>CLINT1</i>	GGATCAGCTGATTTATTCGG	hg38 -chr5:157794948-157794970	AGG
<i>CLINT1</i>	GGTTTGAAGGCTGCATACC	hg38 +chr5:157789401-157789423	AGG
<i>CLINT1</i>	ACTGCCAAAGAAGTCCGACC	hg38 +chr5:157791898-157791920	TGG
<i>CLINT1</i>	ACTCGCCACTGGAAGCAACA	hg38 +chr5:157791909-157791931	GGG
<i>CLTA</i>	CTGAGTGGGAACGGGTGGCC	hg38 +chr9:36211653-36211675	CGG
<i>CLTA</i>	GCGCCAAGAAGGCCGACGCC	hg38 -chr9:36191146-36191168	GGG
<i>CLTA</i>	GAACGGATCCAGCTCAGCCA	hg38 -chr9:36191055-36191077	TGG
<i>CLTA</i>	CCTTCAAAGATGCCAATTCT	hg38 +chr9:36204059-36204081	CGG
<i>CLTB</i>	GTAGCCATCAGCAGGACCGT	hg38 +chr5:176398021-176398043	TGG
<i>CLTB</i>	ATCCGAGGAGGCTTTCGTGA	hg38 -chr5:176392920-176392942	AGG
<i>CLTB</i>	GCAGGCATAGAGAACGACGA	hg38 -chr5:176416236-176416258	GGG
<i>CLTB</i>	GGTCCTAGATGCTGCATCTA	hg38 -chr5:176397704-176397726	AGG
<i>CLTC</i>	CTGGATCCTTTGACGTACC	hg38 -chr17:59679438-59679460	AGG
<i>CLTC</i>	TCAAGTAACCGCGTCTGTAA	hg38 -chr17:59666193-59666215	AGG
<i>CLTC</i>	CATGGCTCTGAGACATTCTA	hg38 -chr17:59666837-59666859	GGG
<i>CLTC</i>	CGATCACACACAATGATAAG	hg38 -chr17:59673671-59673693	TGG
<i>CLTCL1</i>	TCTGTAACAGAGCTCGACGT	hg38 +chr22:19191409-19191431	TGG
<i>CLTCL1</i>	GTCCGGCTAGGGTTGACCTA	hg38 +chr22:19222077-19222099	GGG
<i>CLTCL1</i>	CACCACGCTGCTGTCATAGT	hg38 +chr22:19221458-19221480	AGG
<i>CLTCL1</i>	AGTGCTCCTGAAAGCGAACA	hg38 +chr22:19291605-19291627	GGG
<i>COPA</i>	GCTTGGGCCCGAGTTCTAGT	hg38 +chr1:160291352-160291374	AGG
<i>COPA</i>	CATGTCATAATTGAGCTGGT	hg38 +chr1:160290621-160290643	AGG

<i>COPA</i>	GATTCTTCTCACAGGCAGAC	hg38 chr1:160290653-160290675	AGG
<i>COPA</i>	TAGTAGGCGCCGAGCAAAGG	hg38 chr1:160291368-160291390	TGG
<i>CYTH3</i>	GCGATGAACCGTTCTGCCGT	hg38 chr7:6170882-6170904	GGG
<i>CYTH3</i>	AATAGAGGCAGTTATCGGTC	hg38 chr7:6165751-6165773	AGG
<i>CYTH3</i>	CGACAATCTAACTTCCGTAG	hg38 -chr7:6187661-6187683	AGG
<i>CYTH3</i>	ATGAACCGCGGCATCAACGA	hg38 -chr7:6170858-6170880	GGG
<i>DAB2</i>	CGTCTACTCCGCTGAGTAAT	hg38 -chr5:39382957-39382979	GGG
<i>DAB2</i>	GCACCTACCTAGACCCACCA	hg38 chr5:39381446-39381468	GGG
<i>DAB2</i>	AATTTGACCAGATCTCTAAC	hg38 -chr5:39382900-39382922	CGG
<i>DAB2</i>	CTGCTTTACGCCATTCTGTA	hg38 chr5:39382717-39382739	TGG
<i>DIAPH1</i>	ATTGAGGCGAGGCCGCAGTC	hg38 chr5:141528906-141528928	GGG
<i>DIAPH1</i>	ACATGGTCTTGATTCCAAAC	hg38 chr5:141580865-141580887	TGG
<i>DIAPH1</i>	CTTGGTCCGAAATGACTATG	hg38 -chr5:141577479-141577501	AGG
<i>DIAPH1</i>	ATTGAGATTGAGGGATTAAT	hg38 -chr5:141576755-141576777	TGG
<i>DNM1</i>	ATCTGGAACCTCGATGTCGGG	hg38 -chr9:128219108-128219130	AGG
<i>DNM1</i>	CGCCACTTGGCTGACCGTAT	hg38 chr9:128220288-128220310	GGG
<i>DNM1</i>	GATCGAGGCCGAGACCGACA	hg38 chr9:128218646-128218668	GGG
<i>DNM1</i>	CTTGTTCTCCAGCACATCAC	hg38 -chr9:128220045-128220067	GGG
<i>DNM2</i>	G TTCAGGAATCGTCACCCGG	hg38 chr19:10759755-10759777	CGG
<i>DNM2</i>	TGATGACACCGATGGTCCGT	hg38 -chr19:10777119-10777141	AGG
<i>DNM2</i>	CGTGTGGCGAGTAGACTCGA	hg38 -chr19:10772606-10772628	AGG
<i>DNM2</i>	TCTGGTCTGCCGAGGAGTAT	hg38 -chr19:10829071-10829093	AGG
<i>DNM3</i>	TTACAATGCCCGACCCTCGA	hg38 -chr1:171921757-171921779	GGG
<i>DNM3</i>	TTGGTAGGGTATCCCGAATG	hg38 -chr1:172038330-172038352	TGG
<i>DNM3</i>	CGATATGTCTGTAAGCCGGG	hg38 -chr1:172033199-172033221	TGG
<i>DNM3</i>	TACCAGATCCACACTCTTCA	hg38 -chr1:172048686-172048708	AGG
<i>EEA1</i>	AATCTTGCTTTGAAGCGGTA	hg38 -chr12:92864854-92864876	CGG
<i>EEA1</i>	TTGACGTCCACTGTGTTTAT	hg38 chr12:92891648-92891670	AGG
<i>EEA1</i>	GTGGTGGTTAAACCATGTTA	hg38 -chr12:92929058-92929080	AGG
<i>EEA1</i>	CTGTAGATCCAATCTTGTAAC	hg38 chr12:92802707-92802729	TGG
<i>EFS</i>	GGCTGACGCTCGTTTCAGGT	hg38 chr14:23359794-23359816	TGG
<i>EFS</i>	GAATGCCCTCGTACTCATTG	hg38 chr14:23359352-23359374	TGG
<i>EFS</i>	GGACACCACAATGAGTACGA	hg38 -chr14:23359357-23359379	GGG
<i>EFS</i>	AGCCATGGCCATTGCCACGT	hg38 -chr14:23365007-23365029	CGG
<i>EPN1</i>	TGCCGTGCGGGTCCACGTAC	hg38 -chr19:55685494-55685516	TGG
<i>EPN1</i>	CAGCGAGTCCAGGTCGACGA	hg38 -chr19:55694900-55694922	GGG
<i>EPN1</i>	TTCAGGGTGAGCGTCGCGGG	hg38 -chr19:55695195-55695217	AGG
<i>EPN1</i>	CTTCCGCCCTGGATTATAGG	hg38 -chr19:55695347-55695369	AGG
<i>EPN2</i>	AGGTTACACAGGGCCGCGTT	hg38 -chr17:19331984-19332006	GGG
<i>EPN2</i>	CTTGCTTGAGGCGACAGTCA	hg38 -chr17:19331922-19331944	GGG
<i>EPN2</i>	GATTGTACGGTGGCTCCAGT	hg38 -chr17:19328749-19328771	GGG
<i>EPN2</i>	CAGTGAGTCCAGGTTACCA	hg38 -chr17:19331994-19332016	GGG
<i>EPN3</i>	TTCCAGTACATCGACCGCGA	hg38 chr17:50536881-50536903	CGG
<i>EPN3</i>	TCTCGGACATGAGCGAACTA	hg38 -chr17:50536661-50536683	GGG
<i>EPN3</i>	GATGTCAGCCAAGTCCAGGA	hg38 -chr17:50540251-50540273	TGG
<i>EPN3</i>	ACCCATGGGACATCCAGGT	hg38 chr17:50540317-50540339	GGG
<i>EPS15</i>	GTTGGAGTTCCGATCTTTGG	hg38 chr1:51363889-51363911	TGG
<i>EPS15</i>	TGCCAATTCTTCTTCGTAAG	hg38 chr1:51408264-51408286	TGG

<i>EPS15</i>	TATGATCGAATGGGCCAAGA	hg38 -chr1:51356807-51356829	GGG
<i>EPS15</i>	ACTGGAGATTCCCTGGTGTAT	hg38 +chr1:51405903-51405925	GGG
<i>EPS15L1</i>	TTGGAGGGTGGGATGAGGGA	hg38 +chr19:16425237-16425259	CGG
<i>EPS15L1</i>	CCTGGTGTGAACGCGCAAAG	hg38 +chr19:16402162-16402184	TGG
<i>EPS15L1</i>	CGATCCGGCATAACACAGGGA	hg38 -chr19:16441957-16441979	GGG
<i>EPS15L1</i>	GATGTTCTGCTGTCACACCA	hg38 +chr19:16402257-16402279	GGG
<i>ERC1</i>	GCTAATGGCCGACAACACTACG	hg38 +chr12:1408166-1408188	AGG
<i>ERC1</i>	GCAGTCATCCGAACACCGTA	hg38 -chr12:1028198-1028220	AGG
<i>ERC1</i>	GTCGAACCAACAGTACGGGA	hg38 +chr12:1028001-1028023	GGG
<i>ERC1</i>	GTGATGCTCTCCAAATGCTA	hg38 -chr12:1028268-1028290	TGG
<i>EZR</i>	GTAGCTCACCGGCTCGTACA	hg38 +chr6:158767408-158767430	CGG
<i>EZR</i>	TAGCTCACCGGCTCGTACAC	hg38 +chr6:158767409-158767431	GGG
<i>EZR</i>	GTCCTGGCCTGGCTGTTACA	hg38 +chr6:158766899-158766921	GGG
<i>EZR</i>	CAATGTCCGAGTTACCACCA	hg38 +chr6:158789347-158789369	TGG
<i>FYN</i>	GATTGTGAACCTCCCGTACA	hg38 +chr6:111674569-111674591	GGG
<i>FYN</i>	GTGAACTCTTCGTCTCATA	hg38 -chr6:111719831-111719853	GGG
<i>FYN</i>	TGGATACTACATTACCACCC	hg38 -chr6:111702927-111702949	GGG
<i>FYN</i>	TTGCTGATCGCAGATCTCTA	hg38 +chr6:111694465-111694487	TGG
<i>GIT1</i>	GCTGAGTATCCGGGTTAAC	hg38 +chr17:29577658-29577680	AGG
<i>GIT1</i>	TGTGTGTTCCGCCCGTTAC	hg38 +chr17:29576358-29576380	TGG
<i>GIT1</i>	GTTGGTCGTGAGGTCCTC	hg38 +chr17:29576949-29576971	TGG
<i>GIT1</i>	GTGTGCGGCCATTAACATCA	hg38 +chr17:29581943-29581965	GGG
<i>GORASP1</i>	GAGAAATCCCGACACGTCC	hg38 +chr3:39098867-39098889	AGG
<i>GORASP1</i>	TTCCAGGCAGAGTGA	hg38 -chr3:39100307-39100329	TGG
<i>GORASP1</i>	TTGGCTATGGGTATCTACAC	hg38 -chr3:39100467-39100489	CGG
<i>GORASP1</i>	CTGAGCTTCAAGCAGCTCGG	hg38 +chr3:39098329-39098351	CGG
<i>GRB2</i>	GGTCTGAGTTATCCATGACA	hg38 +chr17:75320451-75320473	TGG
<i>GRB2</i>	AGTACTTCCCGGCTCCATCT	hg38 +chr17:75321772-75321794	CGG
<i>GRB2</i>	GCACTGAGCAGCGCTCAGAA	hg38 -chr17:75393625-75393647	TGG
<i>GRB2</i>	AATTGAACTTACCACCCAG	hg38 +chr17:75321748-75321770	AGG
<i>HGS</i>	GTTACCTAGGAGACGCTCGA	hg38 -chr17:81684086-81684108	AGG
<i>HGS</i>	ACTCTTCATGCGGTTACGA	hg38 -chr17:81695859-81695881	AGG
<i>HGS</i>	TCTGCGACCTGATCCGCCAA	hg38 +chr17:81685659-81685681	GGG
<i>HGS</i>	GTATCTCAACCGGAACTACT	hg38 +chr17:81694932-81694954	GGG
<i>HIP1</i>	AATGGTTGAGGCCACAACGC	hg38 +chr7:75542879-75542901	CGG
<i>HIP1</i>	CGCTCAATTAAGTGGTCCCT	hg38 +chr7:75561384-75561406	GGG
<i>HIP1</i>	AATGGCGTCGCTGGTCAAGT	hg38 +chr7:75554162-75554184	GGG
<i>HIP1</i>	TGTCCAGGGAGTTGAATACT	hg38 +chr7:75573884-75573906	AGG
<i>HIP1R</i>	GGACCCACTTACGGTCGGCA	hg38 -chr12:122858935-122858957	GGG
<i>HIP1R</i>	CGTGCTGGCTGCGATCTCGT	hg38 -chr12:122860738-122860760	GGG
<i>HIP1R</i>	GATGGTATCCGCAGCCAGGT	hg38 -chr12:122858874-122858896	GGG
<i>HIP1R</i>	GAGCTGCTCATTATCCACCA	hg38 -chr12:122856065-122856087	GGG
<i>IP6K3</i>	ACCACCGGGAGAGCTACCGT	hg38 +chr6:33722876-33722898	GGG
<i>IP6K3</i>	AATGAGCACACCACCTACGA	hg38 -chr6:33722793-33722815	TGG
<i>IP6K3</i>	CGCATCTGCGGCATGCAGGT	hg38 -chr6:33725436-33725458	AGG
<i>IP6K3</i>	CTTGGGTGAGCGTGCCAGCT	hg38 +chr6:33728092-33728114	GGG
<i>ITSN1</i>	CTGTGGGAACAGAAGATACT	hg38 -chr21:33750231-33750253	AGG
<i>ITSN1</i>	TTCCAAGTGCCGGCCAGTTA	hg38 +chr21:33813987-33814009	AGG

<i>ITSN1</i>	GATGTCGATTGACCACCCAA	hg38 chr21:33775011-33775033	AGG
<i>ITSN1</i>	TTTGGCTCTCCAAGGATATA	hg38 -chr21:33818298-33818320	GGG
<i>ITSN2</i>	GGGCCGGCAGACCTGATTGT	hg38 chr2:24313479-24313501	AGG
<i>ITSN2</i>	GGAAAGCCAACTATGAGCGA	hg38 -chr2:24300131-24300153	GGG
<i>ITSN2</i>	TGTGCTAACAGAAGGCACTA	hg38 chr2:24310553-24310575	GGG
<i>ITSN2</i>	ACTGAATAGGCTGCCGAGGT	hg38 chr2:24254375-24254397	AGG
<i>LIMK1</i>	TGGCCGGCAGACTACGCGGA	hg38 -chr7:74107096-74107118	GGG
<i>LIMK1</i>	GATCCGGTCTCCGACGTGGA	hg38 -chr7:74105913-74105935	TGG
<i>LIMK1</i>	ATTCCATCCACGTCCGAGAC	hg38 chr7:74105910-74105932	CGG
<i>LIMK1</i>	GTGAAGAATCCATCCACGT	hg38 chr7:74105903-74105925	CGG
<i>MAP1LC3A</i>	GGTGATCATCGAGCGCTACA	hg38 chr20:34559346-34559368	AGG
<i>MAP1LC3A</i>	CTGCTCGTAGATGTCCGCGA	hg38 -chr20:34559813-34559835	TGG
<i>MAP1LC3A</i>	GTAGCGCTCGATGATCACCT	hg38 -chr20:34559342-34559364	GGG
<i>MAP1LC3A</i>	TCAGAAGCCGAAGTTTCCT	hg38 -chr20:34559876-34559898	GGG
<i>MAP4K2</i>	TATCTTCACGGCGGCCAGTT	hg38 chr11:64802901-64802923	CGG
<i>MAP4K2</i>	TAGCTTGACTATCTTCACGG	hg38 chr11:64802892-64802914	CGG
<i>MAP4K2</i>	CAGTGCCTCTCGGCAGACGT	hg38 chr11:64802069-64802091	AGG
<i>MAP4K2</i>	GAGGAAGAGTGGACACTACT	hg38 -chr11:64798812-64798834	GGG
<i>MAPK8IP1</i>	TCTCCGATGGCCGACTCATA	hg38 -chr11:45903031-45903053	GGG
<i>MAPK8IP1</i>	TCGAGACCGAATCCACTACC	hg38 chr11:45902556-45902578	AGG
<i>MAPK8IP1</i>	AGTGGCCTCTAGTCGCACAT	hg38 -chr11:45902579-45902601	CGG
<i>MAPK8IP1</i>	GGCACAGTTGTCATAGACGG	hg38 -chr11:45902996-45903018	TGG
<i>MAPK8IP2</i>	CTGAGAAGCCGCTCGAGCGG	hg38 chr22:50603993-50604015	CGG
<i>MAPK8IP2</i>	GTGAGCCGCATGATCTCCGA	hg38 chr22:50604362-50604384	GGG
<i>MAPK8IP2</i>	GGCCGTACCTGAACACAGCC	hg38 -chr22:50605429-50605451	CGG
<i>MAPK8IP2</i>	GGGTTGCTGAGGAATAGGCA	hg38 -chr22:50604599-50604621	GGG
<i>MAPK8IP3</i>	GCCTGGGCCATGGAGCAGTA	hg38 -chr16:1768300-1768322	GGG
<i>MAPK8IP3</i>	GAGCACGTGCGTAACGACGA	hg38 chr16:1763715-1763737	CGG
<i>MAPK8IP3</i>	GAAGCGCGACAGCCGCAACA	hg38 chr16:1747214-1747236	TGG
<i>MAPK8IP3</i>	GTTCCGCTCCATGAGCACAC	hg38 -chr16:1762400-1762422	GGG
<i>NEDD4</i>	CCACTTTATCCATTACCGGT	hg38 -chr15:55873953-55873975	TGG
<i>NEDD4</i>	AAGTCCGGCATGCACCAAAT	hg38 -chr15:55850584-55850606	GGG
<i>NEDD4</i>	ACATCCAAGTTACTTGACGG	hg38 chr15:55860489-55860511	TGG
<i>NEDD4</i>	CTGTTCTTGAAGACTCTTAC	hg38 -chr15:55842098-55842120	CGG
<i>NEDD4L</i>	ACCCGGCGTGGTATGTACAT	hg38 -chr18:58341048-58341070	AGG
<i>NEDD4L</i>	AAATTAGCATGGGTTACCGG	hg38 -chr18:58333887-58333909	TGG
<i>NEDD4L</i>	GTATAGGGTCGCTCCATGGT	hg38 -chr18:58322434-58322456	TGG
<i>NEDD4L</i>	ACATGAGGTCCAGCTCAGTA	hg38 -chr18:58373218-58373240	GGG
<i>NSF</i>	AACGAAGTACCTTACCTGTA	hg38 -chr17:46751609-46751631	GGG
<i>NSF</i>	TATGCAGGCCCTCCTCACAG	hg38 chr17:46713846-46713868	TGG
<i>NSF</i>	GAGAACAGATCTTGATGAAC	hg38 -chr17:46713911-46713933	GGG
<i>NSF</i>	TATGAACGGTATCATCAAT	hg38 chr17:46711001-46711023	GGG
<i>PACSN1</i>	GCCGTCATCGATGCGCTTCA	hg38 -chr6:34527351-34527373	CGG
<i>PACSN1</i>	TCAGGTCGTTGCATAGACGG	hg38 -chr6:34527373-34527395	TGG
<i>PACSN1</i>	AGTGGTCAGACGACGAGAGT	hg38 chr6:34531638-34531660	GGG
<i>PACSN1</i>	CCAAGATCGAGAAGGCGTAC	hg38 chr6:34527417-34527439	GGG
<i>PACSN3</i>	AGGTGCGGGAGAAGCTGCAA	hg38 -chr11:47180590-47180612	GGG
<i>PACSN3</i>	CTCCACCGTGACTIONGCACCA	hg38 -chr11:47179247-47179269	GGG

<i>PACSN3</i>	CTCCAGAAGAGGACGCTGGA	hg38 -chr11:47182701-47182723	GGG
<i>PACSN3</i>	TGAGAAGACCGCCAGACGA	hg38 -chr11:47180278-47180300	GGG
<i>PAK1</i>	GTGGGTTGTTATGGAATACT	hg38 -chr11:77340720-77340742	TGG
<i>PAK1</i>	GATGTAGCCACGTCCCGAGT	hg38 +chr11:77355781-77355803	TGG
<i>PAK1</i>	TATTCCTGCAGTTACCTCGT	hg38 -chr11:77340752-77340774	GGG
<i>PAK1</i>	GCAGAGCAAACGGAGCACCA	hg38 -chr11:77336226-77336248	TGG
<i>PDCD6IP</i>	CTTAAGTCGAGAGCCGACCG	hg38 +chr3:33825234-33825256	TGG
<i>PDCD6IP</i>	CGTCCGCTGGACAAGCACGA	hg38 +chr3:33798894-33798916	GGG
<i>PDCD6IP</i>	AATCGCTGCTAACATTACC	hg38 +chr3:33822061-33822083	AGG
<i>PDCD6IP</i>	GCTCGAGACGCTCCTGAGGT	hg38 +chr3:33798920-33798942	GGG
<i>PI4KA</i>	CGGGTCCAACCGAACGAGAC	hg38 +chr22:20727807-20727829	GGG
<i>PI4KA</i>	GAGACGACCGCGTCCATGTA	hg38 +chr22:20709974-20709996	GGG
<i>PI4KA</i>	CACCCTCTCACGGCGCAGTA	hg38 -chr22:20727258-20727280	CGG
<i>PI4KA</i>	ACAATGGCCTCAGGGTTGCT	hg38 +chr22:20714667-20714689	GGG
<i>PICALM</i>	GATGTAAATTGGAGTCAACC	hg38 -chr11:85981205-85981227	AGG
<i>PICALM</i>	TAGCAGGATAGGCCATTACA	hg38 +chr11:85976655-85976677	GGG
<i>PICALM</i>	GTGGGAGTTTGGCAACAGGA	hg38 +chr11:85981926-85981948	AGG
<i>PICALM</i>	ACCTGAGAAGCAGTTGACAT	hg38 +chr11:85996843-85996865	AGG
<i>PIK3C2G</i>	AGGAAGCCCGGGATTTAGAT	hg38 -chr12:18346755-18346777	AGG
<i>PIK3C2G</i>	GACCTAGGTCACTTACAGTA	hg38 -chr12:18391246-18391268	GGG
<i>PIK3C2G</i>	AGTAAAGACGATGGGCAACC	hg38 -chr12:18424016-18424038	TGG
<i>PIK3C2G</i>	TTGAAAGGCTCTCTTCAACC	hg38 +chr12:18282703-18282725	CGG
<i>PIK3CG</i>	GTGGGCAGCACGAACTCGAT	hg38 -chr7:106867676-106867698	GGG
<i>PIK3CG</i>	ACTGTGAGGTCGGTGTTCGG	hg38 -chr7:106868681-106868703	AGG
<i>PIK3CG</i>	ACAACCTGCCGAAGGCGCCGG	hg38 +chr7:106867605-106867627	AGG
<i>PIK3CG</i>	TCTGCTGTGAGAGGGTTAAG	hg38 -chr7:106869248-106869270	TGG
<i>PIP5K1A</i>	TATCCGGCCCGATGATTACT	hg38 +chr1:151232344-151232366	TGG
<i>PIP5K1A</i>	CTGGGAAGCCCGCCGTTTGT	hg38 -chr1:151234348-151234370	AGG
<i>PIP5K1A</i>	GCTGCTTCCAGGATACTACA	hg38 +chr1:151232682-151232704	TGG
<i>PIP5K1A</i>	CGTACTTCCGGGAGCTATT	hg38 +chr1:151232321-151232343	TGG
<i>RAB11A</i>	CATTTTCGAGTAAATCGAGAC	hg38 -chr15:65877372-65877394	AGG
<i>RAB11A</i>	GAGTACGACTACCTCTTTAA	hg38 +chr15:65869604-65869626	AGG
<i>RAB11A</i>	GTTTGCAACAAGAAGCATCC	hg38 +chr15:65877432-65877454	AGG
<i>RAB11A</i>	GAGTGATCTACGTCATCTCA	hg38 +chr15:65877900-65877922	GGG
<i>RAB11B</i>	CACCCGCAACGAGTTCAACC	hg38 +chr19:8399915-8399937	TGG
<i>RAB11B</i>	GGTGGCGAACTCCACGCCGA	hg38 -chr19:8399950-8399972	TGG
<i>RAB11B</i>	TGATGGCGCGGTAGCGCTCC	hg38 -chr19:8400029-8400051	TGG
<i>RAB11B</i>	CCAGCGCTCCACGTTCTCAT	hg38 -chr19:8402142-8402164	AGG
<i>RAB11FIP5</i>	ATCGGCGTCGACAAGTTCCT	hg38 -chr2:73112404-73112426	GGG
<i>RAB11FIP5</i>	GACCCAACCTCGCTCCGACTT	hg38 +chr2:73088183-73088205	AGG
<i>RAB11FIP5</i>	TCAGGTTGTTGCGCGTGAAC	hg38 +chr2:73089227-73089249	TGG
<i>RAB11FIP5</i>	GTGGCCCTGAAGGTCCAGAA	hg38 +chr2:73088637-73088659	GGG
<i>RAB1A</i>	GCTCTCCTGAACTCACTATT	hg38 +chr2:65129877-65129899	CGG
<i>RAB1A</i>	AGTAGACTACACAACAGCGA	hg38 -chr2:65088938-65088960	AGG
<i>RAB1A</i>	AGAACAGTCTTTCATGACGA	hg38 -chr2:65088606-65088628	TGG
<i>RAB1A</i>	ATTCGTTGCATTCTTAGCAC	hg38 +chr2:65088631-65088653	TGG
<i>RAB29</i>	TGAGCCGGGACCAGATTGAC	hg38 -chr1:205770810-205770832	CGG
<i>RAB29</i>	GACCGGTTTCAGTAAAGAGAA	hg38 -chr1:205770793-205770815	CGG

<i>RAB29</i>	AACCGTTCTCTTTACTGAAC	hg38 chr1:205770791-205770813	CGG
<i>RAB29</i>	AGATTGGCCACATACCTTGT	hg38 chr1:205771457-205771479	TGG
<i>RAB2A</i>	TACATCATAATCGGCGACAC	hg38 chr8:60517232-60517254	AGG
<i>RAB2A</i>	TCTGTAATACGACCTTGTGA	hg38 -chr8:60584230-60584252	TGG
<i>RAB2A</i>	CTGGCGGGCATCTTCTAACCC	hg38 -chr8:60584749-60584771	AGG
<i>RAB2A</i>	TACTAGTTTACGATATTACA	hg38 chr8:60584269-60584291	CGG
<i>RAB3A</i>	CCTCTTGTTCGTTGCGATAGA	hg38 chr19:18202531-18202553	TGG
<i>RAB3A</i>	TGCATTGAAGGATTCCTCGT	hg38 chr19:18200338-18200360	TGG
<i>RAB3A</i>	GACATCCACCAGGCGCTCAA	hg38 chr19:18197587-18197609	AGG
<i>RAB3A</i>	GATGCCACCGGTGCTGACGA	hg38 chr19:18202570-18202592	AGG
<i>RAB3B</i>	GACACAGACCCGTCGATGCT	hg38 -chr1:51919991-51920013	GGG
<i>RAB3B</i>	GATGCCACCGGTGCTAACGA	hg38 chr1:51976947-51976969	AGG
<i>RAB3B</i>	ACATACCAAGCTGCTCTGCA	hg38 chr1:51933312-51933334	AGG
<i>RAB3B</i>	TATGGGTCTCATACCAGTCT	hg38 chr1:51937280-51937302	TGG
<i>RAB3C</i>	ATCATCGGCAATAGCAGTGT	hg38 chr5:58617721-58617743	GGG
<i>RAB3C</i>	GCCCATGGCTCCACGATAAT	hg38 -chr5:58726042-58726064	AGG
<i>RAB3C</i>	CACGAAGCGCCCATGCAGGT	hg38 chr5:58583215-58583237	GGG
<i>RAB3C</i>	CTGCATTCGTCAGCACAGTT	hg38 chr5:58617788-58617810	GGG
<i>RAB3D</i>	AGTCGTCCGCGTATCGGAAC	hg38 chr19:11337264-11337286	AGG
<i>RAB3D</i>	TGAAGGAGTCGTCCGCGTAT	hg38 chr19:11337258-11337280	CGG
<i>RAB3D</i>	TTCCTTCCTGTTCCGATACG	hg38 -chr19:11337270-11337292	CGG
<i>RAB3D</i>	CTGATAGGCAACAGCAGTGT	hg38 -chr19:11337299-11337321	GGG
<i>RAB4A</i>	TAACTTCACGATCTGCATCC	hg38 chr1:229297578-229297600	AGG
<i>RAB4A</i>	GTGACGAGAAGTTATTACCG	hg38 chr1:229295852-229295874	AGG
<i>RAB4A</i>	TTGGAACAAGTGCGCTCAC	hg38 chr1:229298988-229299010	AGG
<i>RAB4A</i>	ATGGGCTCAGGTATTCAGTA	hg38 chr1:229302882-229302904	CGG
<i>RAB4B</i>	GTGACGCGGAGTTATTACCG	hg38 chr19:40783782-40783804	AGG
<i>RAB4B</i>	CCCGGGTGGTCAACGTGGGT	hg38 chr19:40780427-40780449	GGG
<i>RAB4B</i>	GGTGTACGACATCACCAGGT	hg38 chr19:40783823-40783845	GGG
<i>RAB4B</i>	GGTGATGTCGTACACCAGCA	hg38 -chr19:40783816-40783838	GGG
<i>RAB5A</i>	TTGGTTGTGTGGTTCCGGTA	hg38 -chr3:19983775-19983797	AGG
<i>RAB5A</i>	CTACAACACTGATTCCTGGT	hg38 -chr3:19983794-19983816	TGG
<i>RAB5A</i>	AGACCCAACGGGCCAAATAC	hg38 chr3:19950920-19950942	GGG
<i>RAB5A</i>	GATAAAGCTATTACAATGTT	hg38 -chr3:19976101-19976123	AGG
<i>RAB5B</i>	CGTAAACCACGATTGCAGCT	hg38 -chr12:55990062-55990084	TGG
<i>RAB5B</i>	TTGAGATCTGGGACACAGCT	hg38 chr12:55989995-55990017	GGG
<i>RAB5B</i>	TACCAGGAGAGCACCATTGG	hg38 chr12:55987102-55987124	AGG
<i>RAB5B</i>	GTTGTCATCTGCATATGCCT	hg38 -chr12:55991364-55991386	GGG
<i>RAB5C</i>	CATTGCACTCGCGGGTAACA	hg38 -chr17:42128296-42128318	AGG
<i>RAB5C</i>	GGTGATGTCATAGACCACGA	hg38 chr17:42128655-42128677	TGG
<i>RAB5C</i>	AGAGCCGTGGAATTCCAGGT	hg38 -chr17:42128256-42128278	GGG
<i>RAB5C</i>	CTGGACCACTACAGCTGGAC	hg38 -chr17:42130505-42130527	GGG
<i>RAB6A</i>	GAACAGCCTCCTTCACTGAC	hg38 chr11:73677905-73677927	TGG
<i>RAB6A</i>	TCACTGACTGGTTGCTCCTG	hg38 chr11:73677917-73677939	AGG
<i>RAB6A</i>	GCTACACGTCGAAAGAGCTG	hg38 chr11:73679704-73679726	TGG
<i>RAB6A</i>	GAGCAACCAGTCAGTGAAGG	hg38 -chr11:73677911-73677933	AGG
<i>RAB6B</i>	GACGTCGTGATCCACTTAG	hg38 chr3:133839574-133839596	AGG
<i>RAB6B</i>	GTTGTAGCCAGTCTTCGCAC	hg38 chr3:133838175-133838197	TGG

<i>RAB6B</i>	CGTGTGGCGTCGGCTCTACC	hg38 -chr3:133834610-133834632	CGG
<i>RAB6B</i>	AGACGGACCTGGCTGATAAG	hg38 -chr3:133839505-133839527	AGG
<i>RAB7B</i>	ATGGTGTCCACGTTCTACAA	hg38 -chr1:205992637-205992659	GGG
<i>RAB7B</i>	ACGTTCTACAAGGGCTCCGA	hg38 -chr1:205992628-205992650	TGG
<i>RAB7B</i>	ACAAGATCGATCTGGCAGAC	hg38 -chr1:205992483-205992505	CGG
<i>RAB7B</i>	CATGGTGTCCACGTTCTACA	hg38 -chr1:205992638-205992660	AGG
<i>RAB8A</i>	CGTCCGAAACCGTTCCTGAC	hg38 -chr19:16121758-16121780	CGG
<i>RAB8A</i>	ACGGTTTCGGACGATCACAA	hg38 +chr19:16121768-16121790	CGG
<i>RAB8A</i>	GTTGTGCGAAGGACTTCTCGT	hg38 -chr19:16125495-16125517	TGG
<i>RAB8A</i>	GATCACACGGCCTACTACA	hg38 +chr19:16121780-16121802	GGG
<i>RAB8B</i>	ATCACGACAGCGTACTACAG	hg38 +chr15:63249676-63249698	AGG
<i>RAB8B</i>	AGTACGCTGTCGTGATTGTT	hg38 -chr15:63249669-63249691	CGG
<i>RAB8B</i>	CAGGATCATTCTTTGACAT	hg38 -chr15:63256515-63256537	CGG
<i>RAB8B</i>	TACCTCTTCTACATTTGCAC	hg38 -chr15:63259673-63259695	TGG
<i>RAC1</i>	AATCCTTACTGTTTGCGGAT	hg38 -chr7:6392028-6392050	AGG
<i>RAC1</i>	TACTGTTTGCGGATAGGATA	hg38 -chr7:6392022-6392044	GGG
<i>RAC1</i>	TATCCTATCCGCAAACAGTA	hg38 +chr7:6392025-6392047	AGG
<i>RAC1</i>	CATGGCTAAGGAGATTGGTA	hg38 +chr7:6402011-6402033	TGG
<i>RHOA</i>	GGCCACTCACCTAACTATC	hg38 +chr3:49368418-49368440	AGG
<i>RHOA</i>	CTGCTCTGCAAGCTAGACGT	hg38 -chr3:49360239-49360261	GGG
<i>RHOA</i>	TATAACATCGGTATCTGGGT	hg38 +chr3:49368465-49368487	AGG
<i>RHOA</i>	AACCAGGATGATGGGCACGT	hg38 +chr3:49362559-49362581	TGG
<i>ROCK1</i>	ATCTTGTAGAAAGCGTTCTGA	hg38 +chr18:20953633-20953655	GGG
<i>ROCK1</i>	ATGGCATCTTCGACACTCTA	hg38 +chr18:20954841-20954863	GGG
<i>ROCK1</i>	CCTGCTGCGGGATCCCAAAT	hg38 -chr18:21110841-21110863	CGG
<i>ROCK1</i>	TATTCAGGGAAGTGAGGTTA	hg38 -chr18:21039548-21039570	GGG
<i>ROCK2</i>	TGTTTAGGGAGGTACGACTT	hg38 -chr2:11222159-11222181	GGG
<i>ROCK2</i>	CTGATACTGCAGCCCGGTTA	hg38 -chr2:11215030-11215052	AGG
<i>ROCK2</i>	TAGTAGGTAAATCCGATGAA	hg38 +chr2:11221210-11221232	AGG
<i>ROCK2</i>	CTTAGCTTGAGGAACTAAT	hg38 -chr2:11198757-11198779	AGG
<i>SAR1A</i>	TTCCAACACTACATCCGAGT	hg38 -chr10:70161614-70161636	AGG
<i>SAR1A</i>	GATCTTGGTGGGCACGAGCA	hg38 -chr10:70161003-70161025	AGG
<i>SAR1A</i>	AGACAATCCATTAATTGCT	hg38 +chr10:70157820-70157842	GGG
<i>SAR1A</i>	CAAGATAAGGATTGGCACAT	hg38 +chr10:70153922-70153944	TGG
<i>SEC13</i>	TCTTTGATGTGCGCAATGGA	hg38 -chr3:10315347-10315369	GGG
<i>SEC13</i>	ATGACCGGAAAGTCATTATC	hg38 -chr3:10312637-10312659	TGG
<i>SEC13</i>	CCTGGAGGCAACCATAGCTA	hg38 +chr3:10311683-10311705	AGG
<i>SEC13</i>	CTGCTTGGGAGCACACAACA	hg38 +chr3:10311742-10311764	AGG
<i>SH3GLB1</i>	CTGCACGGCGCGACTGAGGA	hg38 -chr1:86704949-86704971	AGG
<i>SH3GLB1</i>	TCTGGAGGTCCAACATATAC	hg38 -chr1:86735144-86735166	TGG
<i>SH3GLB1</i>	TTTGGCCCAGGAACAGCTTA	hg38 +chr1:86719614-86719636	TGG
<i>SH3GLB1</i>	TTGGACCTCCAGAAACAAC	hg38 +chr1:86735154-86735176	GGG
<i>SH3GLB2</i>	GCGGTAGCACTGTGCGTAGT	hg38 +chr9:129009803-129009825	AGG
<i>SH3GLB2</i>	GAGACTTGACGAACTCGTGG	hg38 +chr9:129009832-129009854	AGG
<i>SH3GLB2</i>	AGATTTCCCGGCACCTTCGT	hg38 -chr9:129009326-129009348	GGG
<i>SH3GLB2</i>	GGAGCTGCTGGCTCAGTACA	hg38 -chr9:129021130-129021152	TGG
<i>SNAP91</i>	GTTGCAAATAAATCAACCGG	hg38 +chr6:83607723-83607745	TGG
<i>SNAP91</i>	GATGTGCGGGCCAAACGCTCA	hg38 -chr6:83707906-83707928	CGG

<i>SNAP91</i>	TTGCAAATAAATCAACCGGT	hg38 chr6:83607724-83607746	GGG
<i>SNAP91</i>	TCATCTCTTGCCAGCTTAGT	hg38 chr6:83580452-83580474	AGG
<i>SNX1</i>	ACAGAAGCTTACGCGGACTA	hg38 chr15:64131882-64131904	TGG
<i>SNX1</i>	GTGCAAACCTCACGACCACCG	hg38 chr15:64096162-64096184	CGG
<i>SNX1</i>	TCAGGGTCCTGTAACATGGT	hg38 chr15:64127756-64127778	AGG
<i>SNX1</i>	CACCTGTGTTGTAACCTTTGT	hg38 chr15:64123527-64123549	AGG
<i>SNX2</i>	GTGCCGACCTAATCCTCAGA	hg38 chr5:122775422-122775444	GGG
<i>SNX2</i>	TCTGCCAGCACTTCATTCGA	hg38 chr5:122826061-122826083	TGG
<i>SNX2</i>	CGTGATCTTTGATAGATCCA	hg38 chr5:122799828-122799850	GGG
<i>SNX2</i>	TGATGGCATGAATGCCTATA	hg38 chr5:122802082-122802104	TGG
<i>STAU1</i>	CTGCAGGATCCTCAACGCTT	hg38 chr20:49151609-49151631	TGG
<i>STAU1</i>	GATCAATCCGATTAGCCGAC	hg38 chr20:49123184-49123206	TGG
<i>STAU1</i>	CAAACCTCCCTGCGGCGCGGG	hg38 chr20:49123100-49123122	AGG
<i>STAU1</i>	TTGACTAACTCCTACAGCCT	hg38 chr20:49117990-49118012	GGG
<i>SYNJ1</i>	GTTGCTGGCTGCGCGTCAAT	hg38 chr21:32645762-32645784	AGG
<i>SYNJ1</i>	CGCCATTCTCCTTTCTTCGG	hg38 chr21:32726890-32726912	AGG
<i>SYNJ1</i>	GATTAAGCTGTGAACGAGCT	hg38 chr21:32695123-32695145	GGG
<i>SYNJ1</i>	ACAGGACCCTCTGATATTGT	hg38 chr21:32646458-32646480	AGG
<i>SYNJ2</i>	TTGATCTGCTTGACATTATA	hg38 chr6:158089866-158089888	AGG
<i>SYNJ2</i>	ACCCGTGGCGTGAACGACGA	hg38 chr6:158033627-158033649	CGG
<i>SYNJ2</i>	GCATTTGTGCTTGTATCGT	hg38 chr6:158076696-158076718	AGG
<i>SYNJ2</i>	GTGCTTCTGAAGGAGCAGTA	hg38 chr6:158059264-158059286	CGG
<i>SYT1</i>	TTGCCACCCAATTCCGAGTA	hg38 chr12:79299387-79299409	TGG
<i>SYT1</i>	GTACCATACTCGGAATTGGG	hg38 chr12:79299384-79299406	TGG
<i>SYT1</i>	ATTGCAATTAAGGCCACCG	hg38 chr12:79285789-79285811	TGG
<i>SYT1</i>	ATCATATACAGCCATCACTA	hg38 chr12:79299412-79299434	GGG
<i>SYT2</i>	TCAGGTGGATCTTCACGTAC	hg38 chr1:202599328-202599350	GGG
<i>SYT2</i>	GCCATAGGCAAGATCTTCGT	hg38 chr1:202596887-202596909	GGG
<i>SYT2</i>	GGCCGTGGGCACATAGCGCA	hg38 chr1:202600424-202600446	GGG
<i>SYT2</i>	GATGCAGACAGTGAGCTTCC	hg38 chr1:202600403-202600425	CGG
<i>TNIK</i>	AGCAGCTGGAGCAGCAGCAG	hg38 chr3:171157547-171157569	CGG
<i>TNIK</i>	GCGTGGCATCTCCACGCGGT	hg38 chr3:171126014-171126036	GGG
<i>TNIK</i>	GTTAACCTACCCACAGACGT	hg38 chr3:171066566-171066588	GGG
<i>TNIK</i>	GCTCAGTTCTCCGAGATCA	hg38 chr3:171110852-171110874	GGG
<i>TSG101</i>	GGCGGATAGGATGCCGAAAT	hg38 chr11:18509568-18509590	AGG
<i>TSG101</i>	GATTGGGAGGGTATCCGAT	hg38 chr11:18506861-18506883	GGG
<i>TSG101</i>	TAGGGATGGCACAATCAGCG	hg38 chr11:18484043-18484065	AGG
<i>TSG101</i>	CTGATTGTGCCATCCCTACT	hg38 chr11:18484048-18484070	GGG
<i>VAMP1</i>	TCTTCCTGTTTCGTGGACCGA	hg38 chr12:6462965-6462987	GGG
<i>VAMP1</i>	TACAATAACTACCACGATGA	hg38 chr12:6464891-6464913	TGG
<i>VAMP1</i>	TATTAATGTGGGATAAGCCC	hg38 chr12:6463052-6463074	AGG
<i>VAMP1</i>	TACCTCCTCCACTTGTGCCT	hg38 chr12:6466222-6466244	GGG
<i>VAMP2</i>	GGCTGCGCTTGTTCAAACT	hg38 chr17:8161644-8161666	GGG
<i>VAMP2</i>	TGGCTGCGCTTGTTCAAAC	hg38 chr17:8161643-8161665	TGG
<i>VAMP2</i>	CTCCAAACCTCACCAGTAAC	hg38 chr17:8162282-8162304	AGG
<i>VAMP2</i>	CACACTCACCTCATCCACCT	hg38 chr17:8162240-8162262	GGG
<i>VAPA</i>	CAGACCTCAAATTCAAAGGT	hg38 chr18:9914318-9914340	AGG
<i>VAPA</i>	TACCGAAACAAGGAACTAA	hg38 chr18:9950484-9950506	TGG

VAPA	CCCACAGACCTCAAATTCAA	hg38 +chr18:9914314-9914336	AGG
VAPA	TTCAGTGGAACAGCTTTGCT	hg38 -chr18:9950407-9950429	AGG
VAPB	GCATCGATGATTCCGCTGTT	hg38 -chr20:58418318-58418340	GGG
VAPB	CGGGTTGCCAAGCTTTAGGT	hg38 -chr20:58418235-58418257	TGG
VAPB	TGAAGACTACAGCACACAGT	hg38 +chr20:58418283-58418305	AGG
VAPB	GGCCTCACACAGTACCTACG	hg38 -chr20:58418297-58418319	TGG
VAV2	TCGGGCGGCAAAGTTATACC	hg38 +chr9:133768541-133768563	TGG
VAV2	CGAACGTTCCCGGGACTTGT	hg38 +chr9:133770406-133770428	AGG
VAV2	GGCCATCGACGTGTCCGTGA	hg38 -chr9:133806127-133806149	TGG
VAV2	TACTCACTGAACTTGCAGGG	hg38 +chr9:133783496-133783518	AGG
VCP	TACCAAATCGCCGTAGAGCT	hg38 +chr9:35062000-35062022	GGG
VCP	CGATACGCTTCCAGGAAGTA	hg38 +chr9:35066689-35066711	CGG
VCP	GCTGCCATTGATGACACAG	hg38 -chr9:35066750-35066772	TGG
VCP	TGGGTGCTCCACAGGATACT	hg38 +chr9:35060508-35060530	AGG
VPS36	TTGGACCTTATGCAGTCGGA	hg38 -chr13:52449987-52450009	GGG
VPS36	GGGAATAATGTCACTCACGG	hg38 -chr13:52423609-52423631	AGG
VPS36	TATTTCCATGCTCAGCAAGT	hg38 +chr13:52426028-52426050	AGG
VPS36	TCATATTTGAACAGGAACGA	hg38 -chr13:52423631-52423653	GGG
VPS4A	GAGTGCTCCCGAGATGCAAC	hg38 -chr16:69321108-69321130	CGG
VPS4A	GGCCGCACGAAGTACCTGGA	hg38 -chr16:69311525-69311547	GGG
VPS4A	TGCCACGGCTTTGGCCAGGT	hg38 -chr16:69319444-69319466	AGG
VPS4A	GTTGGGCTTCTCCATCACGA	hg38 -chr16:69318826-69318848	CGG
WAS	TCACGAGTTCACGATACCGT	hg38 +chrX:48686841-48686863	GGG
WAS	GCCGTAAAGGCGGATGAAGT	hg38 -chrX:48684395-48684417	AGG
WAS	ATCGTGAACCTCGTGATGTCA	hg38 -chrX:48686833-48686855	GGG
WAS	TTGTATCTTCTCCTGCACGA	hg38 -chrX:48685789-48685811	GGG
WASF1	ACATCGTACGTCTCCTGTAA	hg38 +chr6:110108570-110108592	TGG
WASF1	CTCATGACAGGCGGCGAGAA	hg38 -chr6:110105508-110105530	TGG
WASF1	TATACTCACTCCTTATAGGT	hg38 -chr6:110108523-110108545	AGG
WASF1	TCAATATACTCACTCCTTAT	hg38 -chr6:110108527-110108549	AGG
WASF2	TCGGTGCACCCTCTCAGCAA	hg38 +chr1:27418997-27419019	GGG
WASF2	TTGAATGGTGGAACTTCTGA	hg38 +chr1:27418370-27418392	AGG
WASF2	CTAGCCAGCCATTACCTGTA	hg38 +chr1:27418254-27418276	AGG
WASF2	GTCGGTGCACCCTCTCAGCA	hg38 +chr1:27418996-27419018	AGG
WASF3	CGTTACGGATTACTCTTACC	hg38 +chr13:26681069-26681091	CGG
WASF3	GTCACATGCATCGGACGTTA	hg38 +chr13:26681054-26681076	CGG
WASF3	TACCCATTTCGAATAGCAGCG	hg38 -chr13:26682955-26682977	AGG
WASF3	TATGGTGTCAGGATGTTTACG	hg38 -chr13:26667645-26667667	AGG